2016

CENTRAL NEURAL MECHANISMS OF SALT-SENSITIVE HYPERTENSION

Robert Larson
Michigan Technological University, ralarson@mtu.edu

CENTRAL NEURAL MECHANISMS OF SALT-SENSITIVE HYPERTENSION

By

Robert A. Larson

A DISSERTATION

Submitted in partial fulfillment of the requirements for the degree of

DOCTOR OF PHILOSOPHY

In Biological Sciences

MICHIGAN TECHNOLOGICAL UNIVERSITY

2016

This dissertation has been approved in partial fulfillment of the requirements for the Degree of DOCTOR OF PHILOSOPHY in Biological Sciences

Department of Biological Sciences

Dissertation Advisor: *Dr. Qing-Hui Chen*

Committee Member: *Dr. Jason R. Carter*

Committee Member: *Dr. Tarun K. Dam*

Committee Member: *Dr. Zhiying Shan*

Department Chair: *Dr. Chandrashekhar P. Joshi*

Table of Contents

List of Figures

List of Tables

Preface

Chapter 2 presents the original research article “Sympathoexcition in AngII-salt hypertension reduces SK channel function in the hypothalamic paraventricular nucleus.” The article is used with the permission of the American Physiological Society, as a collaborative work with co-authors Dr. Le Gui (L.G.), Michael J. Huber (M.J.H.), Andrew D. Chapp (A.D.C.), Dr. Jianhua Zhu (J.Z.), Dr. Lila P. Lagrange (L.P.L), Dr. Zhiying Shan (Z.S.), and Dr. Qing-Hui Chen (Q.H.C). Author Contributions: Robert A. Larson (R.A.L.), L.G., M.J.H., and J.Z. performed experiments; R.A.L., L.G., M.J.H, and Q.H.C. analyzed data; R.A.L., L.G., J.Z., and Q.H.C., prepared figures. R.A.L., and L.G. drafted manuscript; R.A.L., L.P.L, and Q.H.C. edited and revised manuscript. R.A.L., L.G., M.J.H, A.D.C., J.Z., L.P.L., Z.S., and Q.H.C. approved final version of manuscript; Z.S. and Q.H.C. conceptualized and designed the research.

Chapter 3 presents the original research article “High salt intake augments excitability of pre-sympathetic PVN neurons through dysfunction of the endoplasmic reticulum Ca^{2+} store.” This article is under review by the American Heart Association, as a collaborative work with co-authors Andrew D. Chapp (A.D.C), Michael J. Huber (M.J.H.), Dr. Le Gui (L.G.), Dr. Zixi (Jack) Cheng (Z.J.C.), Dr. Zhiying Shan (Z.S.), and Dr. Qing-Hui Chen (Q.H.C). Author Contributions: Robert A. Larson (R.A.L.), A.D.C., L.G., M.J.H., performed experiments; R.A.L., A.D.C., M.J.H., L.G., and Q.H.C. analyzed data; R.A.L., A.D.C., L.G., and Q.H.C. prepared figures. R.A.L. and A.D.C. drafted manuscript; R.A.L. and Q.H.C. edited and revised manuscript; R.A.L., A.D.C., M.J.H., L.G., Z.J.C., Z.S., and Q.H.C. approved the final version of manuscript; R.A.L., A.D.C, Z.J.C., Z.S., and Q.H.C. conceptualized and designed the research.

Acknowledgments

This degree would not be possible without the support and guidance of many individuals. I would like to express my sincere appreciation to my advisor, Dr. Qing-Hui Chen for his patience, guidance, instruction, and encouragement. The experience I have gained in his lab will serve me well in the future. He always provided me with opportunities to push the boundaries, and explore as much as I could in the lab, while keeping me on track for success. I will take the knowledge I have gained in his lab with me for all future endeavors.

I would like to express my appreciation to all of my committee members for providing me with knowledge and support throughout my time here at Michigan Tech. Dr. Jason Carter introduced me to research, and has been instrumental in my pursuit of a career in academia. His guidance throughout my early career is a major reason for my success thus far, and into the future. I would like to thank Dr. Tarun Dam for always being supportive of my work in the lab and in the classroom. He is one of the best instructors I have encountered in my many years in school, and his passion for his students is incredible and matched by very few. I would also like to thank Dr. Jenny Shan for answering my many questions, including me in her research, and teaching me many valuable lab techniques.

I would like to thank all of the members of our lab for their help and support. My office and lab-mate Andrew Chapp and I have been partners in many pursuits over the years and he was always a great sounding board for ideas. I would like to thank Michael Huber for sharing a work station with me and always being so helpful with everything. Mingjun Gu was so helpful in keeping everything in the lab going and doing whatever it takes to make life easier for the graduate students.

I would like to thank many friends and fellow graduate students for their help along the way. Dr. Huan Yang and Dr. Christopher Schwartz were

instrumental in my early success in Dr. Carter's lab. Dr. Aparupa Sengupta, Dr. Emily Geiger, Ida Fonkue, Stephanie Hamilton, Sarah Stream and Jennifer Witting also provided support and contributed to my success over the years. I would like to thank Dr. John Durocher for his friendship and guidance since the day I started graduate school. His friendship has made my experience as a graduate student significantly more successful and enjoyable. Jeff Lewin was always extremely helpful in solving any issues in the lab, and he always provided excellent support and guidance throughout my time at Michigan Tech. I also greatly appreciate everything Terry Anderson has done for me over the years. She solves a lot of problems before they even arise and was always extremely helpful and friendly to all of the KIP graduate students. I would also like to thank the late Dr. Thomas Drummer. His helpfulness and encouragement provided me with a lot of confidence early in my career, and his guidance played a significant role in my success. I would also like to thank all of my co-workers in the lab at Aspirus Keweenaw Hospital. Their kindness, friendship, and professionalism shaped my early career, and their flexibility and willingness to help me in any way possible was a large contributor to my almost 12 year career in the lab.

Finally, I would like to thank my family for always providing me with love support in all of my academic endeavors. My parents have always been instrumental in my success through their love and guidance. They taught me the importance of hard work at a young age, and I have carried that work ethic throughout my career. My sister and brothers have always been very supportive during the last many years, and always lent an ear to talk to when things were tough. I'm very grateful to everyone who has contributed to my success during my time as a graduate student.

List of Abbreviations

HTN Hypertension

PVN Paraventricular Nucleus

SK Small conductance Ca^{2+}-activated K^{+}

HS High Salt

NS Normal Salt

AngII Angiotensin II

ER Endoplasmic Reticulum

CVD Cardiovascular Disease

ABP Arterial Blood Pressure

SNS Sympathetic Nervous System

SNA Sympathetic Nerve Activity

NTS Nucleus Tractus Solitarii

RVLM Rostral Ventrolateral Medulla

IML Intermediolateral Cell Column

CO Cardiac Output

TPR Total Peripheral Resistance

MAP Mean Arterial Blood Pressure

HR Heart Rate

ECF Extracellular Fluid

ICF Intracellular Fluid

ADH Anti-Diuretic Hormone

ACE Angiotensin Converting Enzyme

EO Endogenous Ouabain

NO Nitric Oxide

RSNA Renal Sympathetic Nerve Activity

MSNA Muscle Sympathetic Nerve Activity

SSNA Splanchnic Sympathetic Nerve Activity

LSNA Lumber Sympathetic Nerve Activity

AngII-salt Angiotensin II-High Salt

MCFP Mean Circulatory Filling Pressure

CGx Celic Ganglionectomy

GABA Gamma Aminobutyric Acid

$GABA_A$ Gamma Aminobutyric Acid Type A Receptor

BBB Blood Brain Barrier

AVP Arginine Vasopressin

CVO Circumventricular Organ

SFO Subfornical Organ

MnPO Median Preoptic Nucleus

OVLT Organum Vasculosum Lamina Tarminalis

AT1R Angiotensin II Type 1 Receptor

SHR Spontaneously Hypertensive Rat

WKY Wistar-Kyoto Rat

AHP After Hyperpolarization Potential

mAHP Medium After Hyperpolarization Potential

ATP Adenosine Triphosphate

UPR Unfolded Protein Response

CICR Ca^{2+} induced Ca^{2+} Release

IP3R Inositol-1,4,5-triphosphate Receptor

RYR Ryanodine Receptor

VDCC Voltage Dependent Ca^{2+} Channel

$[Ca2+]_i$ Intracellular Ca^{2+} Concentration

$[Ca2+]_{er}$ Endoplasmic Reticulum Ca^{2+} Concentration

GPLC G-Protein Linked Receptor

CaM Calmodulin

ADP After Depolarization Potential

CK2 Casein Kinase II

CSF Cerebrospinal Fluid

Abstract

Hypertension (HTN) is a major risk factor for the development of cardiovascular disease, and it's estimated that over 80 million adults in the United States have HTN. Essential HTN often demonstrates sensitivity to salt, and reductions in dietary salt attenuate high blood pressure in this population. Evidence indicates that the paraventricular nucleus (PVN) of the hypothalamus is a key driver of HTN due to excess salt intake. The cellular mechanisms whereby PVN neuronal activity is augmented in response to salt are largely unknown. Previous work from our lab has demonstrated that small conductance calcium activated potassium (SK) channel function is diminished in the PVN in HTN induced by a 2% high salt (HS) combined with chronic infusion of angiotensin II (AngII) (AngII-salt HTN). In **study 1** we demonstrate SK channel dysfunction in AngII-salt HTN. Furthermore, SK channel dysfunction was present in rats fed a HS diet alone indicating that dietary salt likely plays a dominant role in reducing SK channel function. In **study 2** we examined the contribution of the endoplasmic reticulum (ER), and intracellular organ largely responsible for intracellular Ca^{2+} homeostasis, in regulating sympathoexcitatory response *in vivo*, and neuronal excitability *in vitro*. We demonstrate that inhibiting ER function in the PVN augments sympathetic nerve activity and blood pressure *in vivo*, and neuronal excitability *in vitro*. We further demonstrate that HS diet augments excitability of PVN neurons through altered ER Ca^{2+} store function. Collectively, we demonstrate that HS diet diminishes SK channel function in the PVN and altered ER Ca^{2+} regulation may contribute to the augmented neuronal excitability in the PVN due to HS intake. Together, these mechanisms providing new and exciting targets for the treatment of salt-sensitive HTN.

Chapter 1. Literature Review

1.1 Introduction

Cardiovascular disease (CVD) is the leading cause of death in the U.S., and approximately 86 million Americans are living with some form of CVD.[1] Hypertension (HTN) is a major risk factor for the development of CVD including coronary heart disease, stroke, congestive heart failure and fatal arrhythmias. It is estimated that over 80 million Americans either have HTN, or are taking anti-hypertensive medications.[1] The development of new treatment strategies for HTN has the potential to significantly reduce the number of deaths each year due to CVD.

1.1.1 Blood Pressure

Blood is contained within the vasculature, and the hydrostatic pressure it exerts upon the walls of the blood vessels is known as blood pressure.[2] Contraction of the ventricles within the heart provides continuous circulation of blood from areas of high pressure to areas of low pressure within the body. In healthy individuals, the highest arterial blood pressure (ABP) is generated during the systolic phase of the cardiac cycle (ventricular contraction), and the lowest ABP occurs during the diastolic phase (ventricular relaxation) of the cardiac cycle. ABP in a healthy young individual is typically less than 120mmHg for systolic arterial pressure, and less than 80mmHg for diastolic arterial pressure. HTN is defined as having a systolic arterial blood pressure of ≥ 140mmHg and/or a diastolic arterial blood pressure of ≥ 90mmHg.[3]

1.1.2 Blood Pressure Regulation

Blood pressure levels are influence by a variety of systems including neural, hormonal and local control mechanisms. Short-term control of ABP (minutes to hours) is regulated largely by the sympathetic nervous system (SNS) through the baroreflex.[4] Stretch receptors in the aortic arch and carotid sinus sense ABP and send afferent signals to the nucleus tractus solatarii (NTS) in the brainstem.[5] The baroreflex circuitry extends from the NTS to the caudal

ventrolateral medulla that further has axon projections to the rostral ventrolateral medulla (RVLM).[6] The RVLM is a key excitatory site for sympathetic nerve activity (SNA),[7, 8] and RVLM neurons have axon projections to the pre-ganglionic sympathetic neurons in the spinal intermediolateral (IML) cell column.[9] When baroreceptors sense that blood pressure is elevated, the RVLM is inhibited, resulting in a decrease in SNA, whereas a decrease in ABP will result in less inhibition of the RVLM, and an increase in SNA to restore ABP back to normal levels. SNA targeting the heart can augment heart rate and stroke volume to increase cardiac output (CO). SNA targeting the vasculature also increases ABP by reducing blood vessel diameter; therefore, increasing total peripheral resistance (TPR). Finally, SNA targeting the kidneys promotes fluid and Na^+ retention through increased release of renin and production of angiotensin II (AngII).[10]

Long-term control of ABP is heavily influence by the pressure-natriuresis mechanism within the kidneys.[11, 12] Pressure-natriuresis alters ABP through alterations in renal excretion of water and salt. When ABP increases, excretion of sodium (natriuresis) and water (diuresis) diminish total blood volume thereby reducing CO and returning ABP to a normal level. Conversely, a decrease in ABP will cause retention of sodium and water to increase blood volume and cardiac output in order to return ABP to normal levels.

1.1.3 Sodium Homeostasis

Salt in the form of Sodium Chloride (NaCl) is an essential component of life and the body has multiple homeostatic pathways to ensure proper sodium balance. Salt levels are high in the extracellular fluids whereas the intracellular fluids have a relatively low level of sodium. Sodium depletion results in complex physiological and behavioral adjustments that work in concert to both conserve sodium and increase salt intake.[13] The body is composed largely of water that is distributed into two main compartments, the extracellular fluid (ECF) and the intracellular fluid (ICF).[14] Na^+ levels are high in the ECF and low in the ICF whereas potassium (K^+) levels are high in the ICF and low in the ECF.

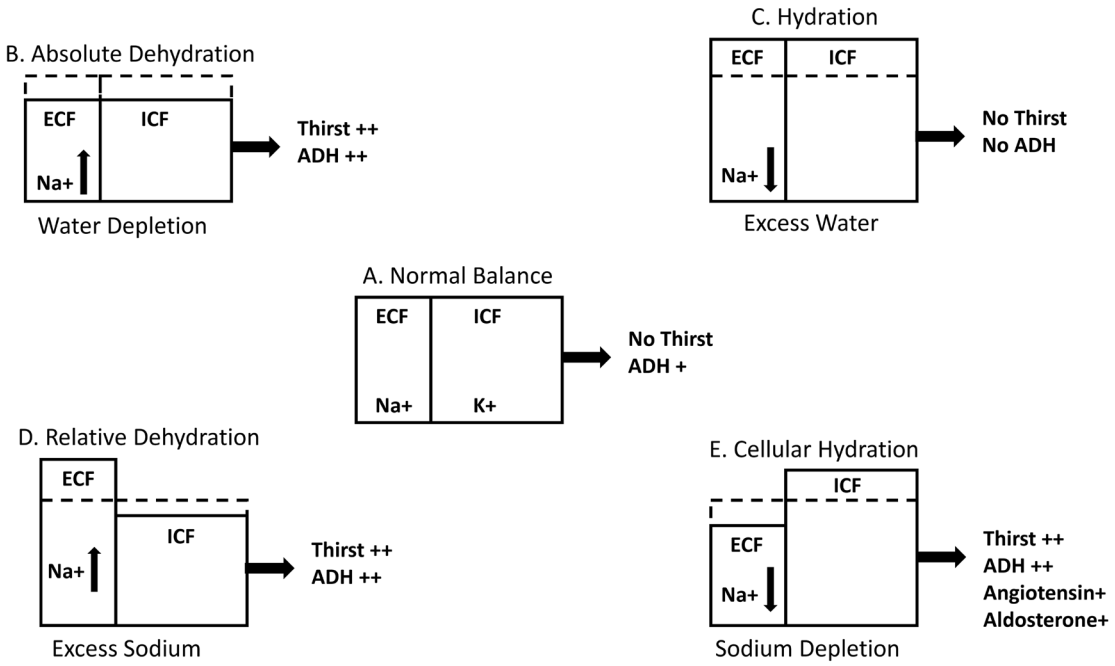

Figure 1.1 Diagram of changes in body fluid distribution during negative and positive water balance. Adapted from Anderson.[14]

Cell membranes are highly permeable to water, but relatively impermeable to Na^+. The relationship between these two properties forms the basis for water balance between the ECF and ICF being dependent on sodium levels in the ECF, as approximately two thirds of total water in the mammalian body resides within the cells.

Normal water balance and the relative distribution of water between the ICF and ECF is illustrated in Fig. 1.1A. A state in which body water is lost is known as absolute dehydration. As illustrated in Fig. 1.1B, the water volume of both the ICF and ECF is diminished triggering thirst behavior and release of anti-diuretic hormone (ADH) from the pituitary gland. ADH stimulates reabsorption of water in the kidneys to conserve total body water volume. Conversely, an excess of total body water results in expanded volume of the ICF and ECF and dilution of solutes as depicted in Fig. 1.1C. In this state, there is no thirst mechanism and ADH release is inhibited to diminish reabsorption of water in the kidneys. Excess consumption of sodium results in a state termed relative dehydration. In this state, increasing levels of Na^+ in the ECF draws

water from the ICF into the ECF as shown in Fig. 1.1D. In order to compensate for relative dehydration, the thirst response is activated, and ADH is released to conserve water in order to dilute the ECF. Additionally, Na^+ excretion by the kidneys is increased. Fig. 1.1E illustrates a state of Na^+ depletion, known as cellular hydration, where diminished Na^+ concentration in the ECF results in expansion of the ICF and diminished total blood volume. Several strategies are employed to conserve Na^+ in this state. Augmented levels of AngII act directly on the vasculature to produce vasoconstriction as well as stimulate release of aldosterone from the adrenal gland. Aldosterone acts directly on the kidneys to facilitate reabsorption of Na^+ and preserve the prevailing level of sodium.

1.2 Salt-Sensitive Hypertension

HTN is a multi-system disorder with multiple contributing mechanisms. Figure 1.2 demonstrates the three prominent mechanisms that contribute to HTN including renal mechanisms, vascular mechanisms, and central neural mechanisms. Mean arterial blood pressure (MAP) is directly proportional to CO and TPR and alterations in these three systems increase CO, TPR, or both, contributing to chronic increases in MAP.

1.2.1 Renal Mechanism

Strong evidence suggests that the kidneys play a significant role in HTN through the pressure natriuresis mechanism. Tigerstedt and Bergman were the first to demonstrate that the kidneys influence ABP[15, 16] They injected supernatant from homogenized rabbit kidneys into other rabbits and observed a significant increase in ABP. They termed the substance “renin” and further demonstrated its presence in renal venous but not arterial blood. Renin is liberated in the kidney and enters the blood where it converts Angiotensinogen to Angiotensin I. Angiotensin I is converted to AngII by angiotensin converting enzyme (ACE). Evidence indicates that chronic infusion of AngII increases intake of water and sodium,[17, 18] and this response is augmented by addition of aldosterone.[19, 20]

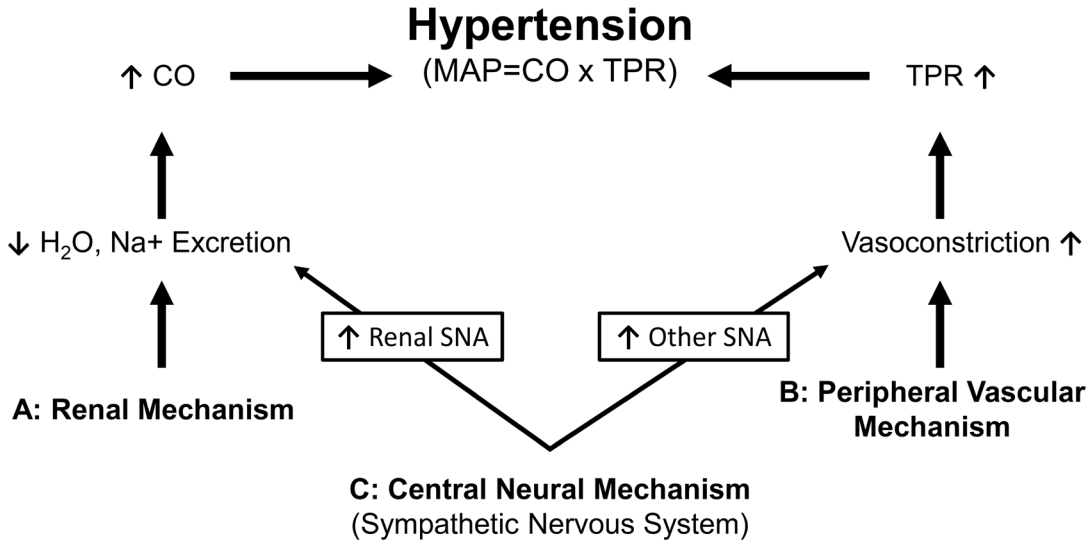

Figure 1.2 Mechanisms contributing to salt-sensitive hypertension. **A:** Altered renal function in HTN results in diminished H_2O and Na^+ excretion contributing to increased CO. **B:** The peripheral vascular mechanism contributes to HTN through vasoconstriction and increased TPR. **C:** The central neural mechanism contributes to elevated CO through enhanced renal SNA, and increased TPR through vasoconstriction in other vascular beds.

Pressure natriuresis is maintained through a relationship governed by ABP and renal Na^+ and fluid excretion, termed the renal function curve. Studies have demonstrated that the renal function curve is very steep in normotensive animals whereby small increases in ABP from the normal "set point" result in significant urinary Na^+ and fluid excretion. Conversely, a decrease in ABP will result in a significant drop in urinary Na^+ excretion in order to maintain proper fluid volume and ABP.[12, 21] In many forms of human and experimental HTN, the renal function curve is shifted to a higher ABP while Na^+ excretion remains at normal levels allowing for chronic elevations of ABP that are not lowered through Na^+ and fluid excretion.[22, 23] Elevations in AngII have been shown to flatten the renal function curve resulting in less Na^+ excretion at higher ABP, contributing to HTN.[21] AngII, in combination with aldosterone, decreases excretion of fluid and Na^+ in the kidneys resulting in an expansion of blood volume; therefore, increasing cardiac output and augmenting MAP (Fig 1.2).[24-27] The strongest evidence for the kidney being a major contributor to hypertension comes from studies involving kidney transplants. Evidence

demonstrates that normotensive rats develop HTN when they received kidney transplants from hypertensive rats, thus leading to the hypothesis that HTN follows the kidney.[28-30]

1.2.2 Vascular Mechanism

The vascular system is a key contributor to hypertension through changes in TPR. Increases in TPR in salt-sensitive HTN occur through a variety of mechanisms that result in a narrowing of blood vessel diameter. Numerous reports indicate that increases in vascular tone contribute to salt sensitive hypertension. Endogenous ouabain (EO) is a substance secreted by the adrenal gland that has been reported to increase Ca^{2+} signaling and augment vascular myogenic tone through inhibition of Na^{+} pumps and enhanced contractility in vascular cells.[31, 32] Reports indicate that EO levels are elevated by high salt diet,[33] and correlate with ABP levels in human essential HTN,[34, 35] as well as animal models of HTN.[36-38]

Impairment of endothelial vascular relaxation is a prominent mechanism contributing to augmented TPR in essential and salt-sensitive HTN in humans,[39-42] and animal models of salt-sensitive HTN.[43-45] Nitric oxide (NO) is produced by endothelial cells and is a primary mediator of vascular relaxation.[46] Diminished NO signaling is a major factor in the augmented TPR observed in HTN. Alterations in a number of pathways significantly diminish NO signaling in the vasculature with increased oxidative stress being the most prominent contributor to impaired endothelial vascular relaxation.[40, 47, 48] Studies have consistently demonstrated that reducing oxidative stress in the vasculature reverses endothelial dysfunction, and increases vasculature relaxation in a variety of pathological conditions including HTN.[49-52]

1.2.3 Central Neural Mechanism

The central nervous system is a key contributor to hypertension through targeted increases in SNA (Fig 1.2). Increases of renal SNA (RSNA) stimulate secretion of renin from the kidneys resulting in AngII production and aldosterone secretion. These mechanisms diminish excretion of H_2O and Na^{+} to increase

CO. SNA targeting vascular beds results in vasoconstriction and increased TPR.

Early evidence demonstrating over-activity of the SNS contributes to HTN involved examinations of plasma catecholamine levels in hypertensive human subjects. The majority of studies reported that plasma norepinephrine levels were consistently increased in young, hypertensive individuals.[53] It should be noted that circulating norepinephrine represents a relative small amount of total norepinephrine within the body, and cannot account for regional differences in release and uptake. Studies examining direct multifiber recordings of muscle sympathetic nerve activity (MSNA) have reported that burst frequency of MSNA is augmented in pre-hypertensive[54-56] and hypertensive subjects.[55, 57-61] Measurement of MSNA is limited in that it cannot provide information on sympathetic traffic to internal organs such as the heart and kidneys. Studies utilizing measurement of total norepinephrine spillover indicate that neuronal re-uptake of norepinephrine is impaired in subjects with essential HTN.[62, 63] Studies further indicate that norepinephrine spillover from the heart and kidneys is augmented in hypertensive subjects.[64, 65] Evidence indicates that the SNS plays a role in the pathogenesis of HTN, with the strongest evidence in young pre-hypertensive and hypertensive individuals.

Strong evidence for a contribution of the SNS to salt-sensitive HTN in animal models comes from studies demonstrating that chemical sympathectomy or ganglionic blockade prevent HTN in Dahl salt-sensitive rats.[66, 67] Evidence suggests that alterations in compensatory mechanisms likely contributes to augmented SNS activity in response to HS intake. Studies suggests that sympathetic activity is inhibited in Dahl salt-resistant rats in response to HS diet, but this response is not demonstrated in Dahl salt-sensitive rats.[68] Furthermore, human studies employing salt loading indicate that salt-resistant subjects have attenuated sympathetic activity in response to salt intake.[69, 70] It has been further demonstrated that salt loading results in a reflex decrease in renin and AngII levels.[13, 21] Additional evidence indicates that a HS diet in normal dogs resulted in an increased in cardiac output, but a decrease

in total peripheral resistance in order to maintain normal ABP.[71] When AngII levels were clamped, the vasodilatory response was lost and the dogs became hypertensive in response to high salt diet. These results indicate that a loss of reflex attenuation of the renin-angiotensin system in response to salt intake is a key contributor to high salt diet induced HTN.[72]

1.2.4 Angiotensin II-High Salt Model

The angiotensin II-high salt model (AngII-salt) is a physiological model of salt-sensitive hypertension. HTN is induced through the interaction of circulating AngII and dietary salt, which together increase activity of the SNS resulting in "neurogenic" hypertension. Sprague Dawley rats are fed a 2% HS diet for 4 weeks. After the second week of HS diet an osmotic minipump is implanted subcutaneously to deliver AngII at a rate of 150 ng/kg/min. Figure 1.3 demonstrates heart rate (HR) and MAP responses to AngII and vehicle infusion in rats fed a 0.4% normal salt (NS) diet, and rats fed a 2% high salt (HS) diet. HR was significantly attenuated in HS rats during days 3-6 of AngII infusion, but did not otherwise differ from NS rats. AngII infusion alone significantly increased MAP for the entire 14 day infusion period in NS rats, but the response was significantly augmented by HS diet.[73]

Evidence demonstrates that plasma norepinephrine and whole-body norepinephrine spillover are substantially augmented in HS compared to NS rats following 7 and 14-day infusions of AngII (Fig 1.4).[74] In addition, ICV administration of the sodium channel/transporter blocker benzamil significantly attenuated MAP in AngII-salt HTN compared to vehicle control.[75] AngII infusion alone is sufficient to generate HTN, but the combination of AngII and HS diet produces neurogenic hypertension driven primarily by the SNS.

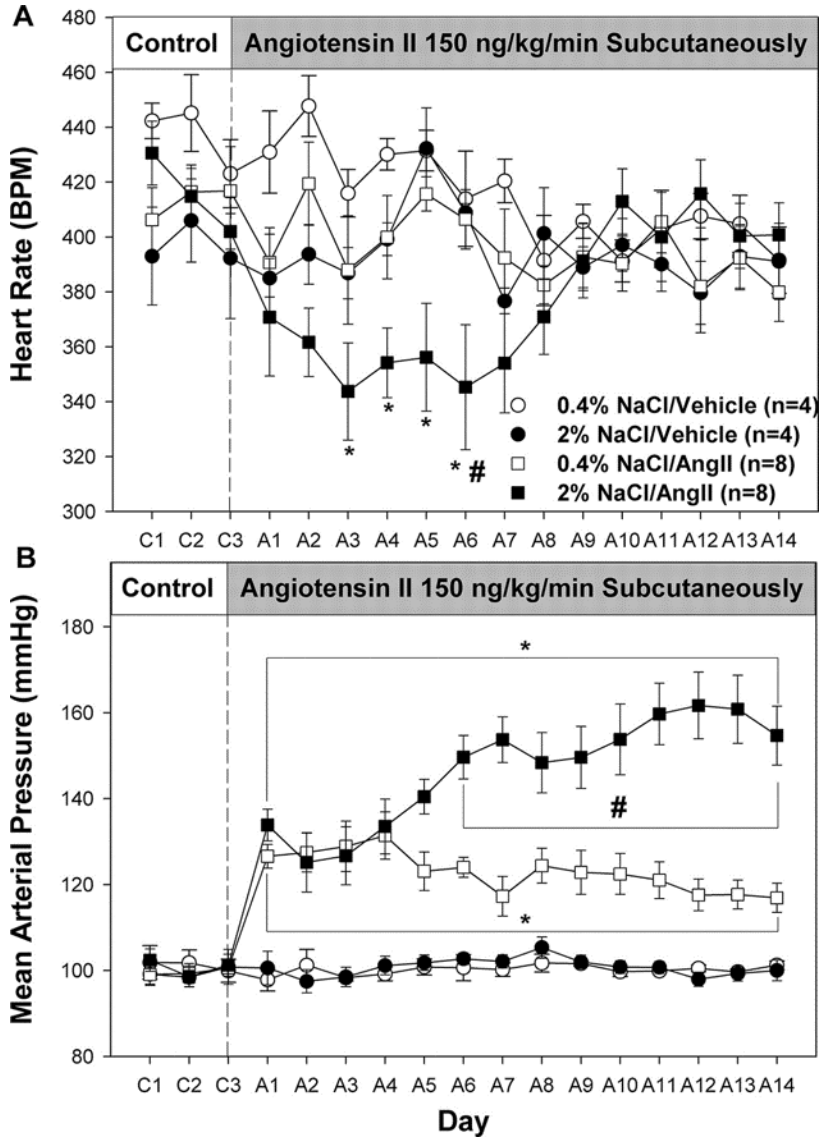

Figure 1.3 Mean arterial blood pressure is augmented in AngII-salt HTN. Heart rate (**A**) and MAP (**B**) response to chronic subcutaneous infusion of AngII (150 ng/kg per minute) or saline vehicle in rats fed either a 2% or 0.4% NaCl diet. C, control day; A, AngII or vehicle infusion day. *Significant difference ($P<0.01$) between specific AngII infusion day and control. #Significant difference ($P<0.01$) between specific AngII infusion day of rats fed 2% NaCl vs rats fed 0.4% NaCl.[73] (Reprinted with permission from *Hypertension*. 2006; 48:927-33. Copyright 2006, Wolters Kluwer Health, Inc.)

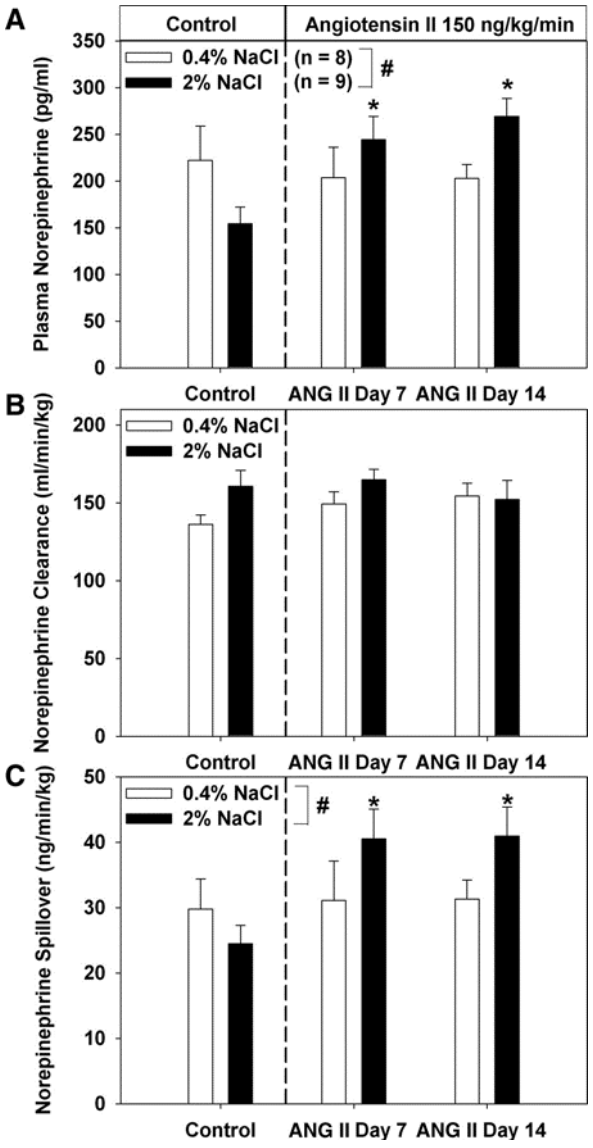

Figure 1.4 Norepinephrine Spillover is augmented in AngII-salt HTN. Plasma norepinephrine (**A**), whole body norepinephrine clearance (**B**), and whole body norepinephrine spillover (**C**) during control and on AngII infusion days 7 and 14 in rats fed 0.4% or 2% NaCl. *P<0.05 vs. control period. #Interaction P<0.05 two-way ANOVA.[74] (Reprinted with permission from *Am J Physiol Regul Integr Comp Physiol*. 2008; 294:R1262-7. Copyright 2008, The American Physiological Society).

Previous studies have established that the splanchnic vasculature is a key target for the elevated SNA in this model of HTN. One early study

demonstrated that MAP and mean circulatory filling pressure (MCFP), an index of venous smooth muscle tone, was significantly increased in AngII-salt rats compared to control. Additionally, they further demonstrated that the response was abolished by ganglionic blockade with hexamethonium demonstrating the contribution of the SNS in generating AngII-salt HTN.[73] Further studies revealed that celiac ganglionectomy (CGx) attenuated MAP and MCFP in AngII-salt HTN whereas renal denervation had no protective effect.[76] Interestingly, chronic sympathetic nerve recording in AngII-salt HTN revealed no change in lumbar sympathetic nerve activity (LSNA) and an initial decrease in RSNA that returned to baseline levels 10 days after the start of AngII infusion, despite a significant increase of MAP.[77] Collectively, these studies indicate that augmented splanchnic sympathetic nerve activity (SSNA) is likely an important contributor to the augmented MAP in this model of hypertension. Only one study has previously measured SSNA in response to AngII infusion. This study infused AngII and reported that SSNA was augmented on day 14 of the infusion.[78] It is important to note that level of dietary salt was not reported in this study. Chronic recording of SSNA in AngII-salt HTN remain to be reported, but indirect evidence indicates the importance of augmented SSNA in this model of HTN. The splanchnic vasculature is an important contributor to total peripheral resistance. It is hypothesized that elevations in SSNA shifts blood from the venous system to arteries. Veins are substantially more compliant than arteries and the shift of blood volume is an important mechanism to augment total peripheral resistance and ABP in this model.[72]

To date, the majority of studies exploring mechanisms in AngII-salt HTN have examined disease progression in the chronic model and noted the contribution of the SNS in the development of HTN. Recently, studies have been performed to examine alterations in neuronal activity/properties in AngII-salt hypertension to further elucidate mechanisms that contribute to the augmented SNA. Bardgett et al. sought to determine the contribution of neuronal activity in the PVN in the maintenance of ABP in AngII-salt HTN. They reported that bilateral microinjection of the gamma aminobutyric acid type A

($GABA_A$) receptor agonist muscimol elicited significantly greater decreases in SSNA, RSNA and MAP in AngII-salt rats compared to normotensive controls.[79] These results indicate that neuronal activity in the PVN is indeed required to maintain high SNA and ABP in this model of hypertension. The cellular mechanisms responsible for sympathoexcitation in AngII-salt hypertension remain to be fully elucidated.

1.3 Central Autonomic Regulation

1.3.1 Circumventricular Organs

Early studies demonstrated that infusion of solutes that are relatively impermeable to the cell membrane including NaCl and sucrose stimulate drinking and antidiuresis.[80-83] Further studies demonstrated that central osmoreceptors located outside of the blood brain barrier (BBB) are responsible for stimulating thirst and release of arginine vasopressin (AVP) in response to cell membrane impermeable hyperosmotic stimuli.[84] Additionally, the central sites governing osmotic regulation were suggested to lie in the anteroventral third ventricle and electrolytic lesions of the surrounding periventricular tissue significantly attenuated the drinking response to stimulation with hypertonic saline and AngII.[85-88] Specialized structures labeled the circumventricular organs (CVO) lack a complete BBB and have access to circulating blood allowing the ability to sense osmolality and circulating AngII levels (Fig 1.3). The subfornical organ (SFO) is a CVO that protrudes into the third ventricle of the brain. The SFO is dense in angII type 1 receptors (AT1R)[89] and microinjection of AngII into the SFO augments ABP.[90] SFO neurons have excitatory axon projections either directly to the paraventricular nucleus, or indirectly through the median preoptic nucleus (MnPO).[91, 92] The organum vasculosum lamina terminalis (OVLT) is a CVO located on the ventral-anterior wall of the third ventricle.[93] OVLT neurons have the ability to sense plasma osmolality and sodium levels.[94-96] Similar to the SFO, OVLT neurons have direct and indirect excitatory axon projections to the paraventricular nucleus[97] that play a critical

role in augmenting sympathetic nerve activity in response to hyperosmolality.[98, 99] Collectively, the CVOs sense circulating AngII and plasma osmolality and transmit excitatory neural activity to the PVN (Fig 1.5).

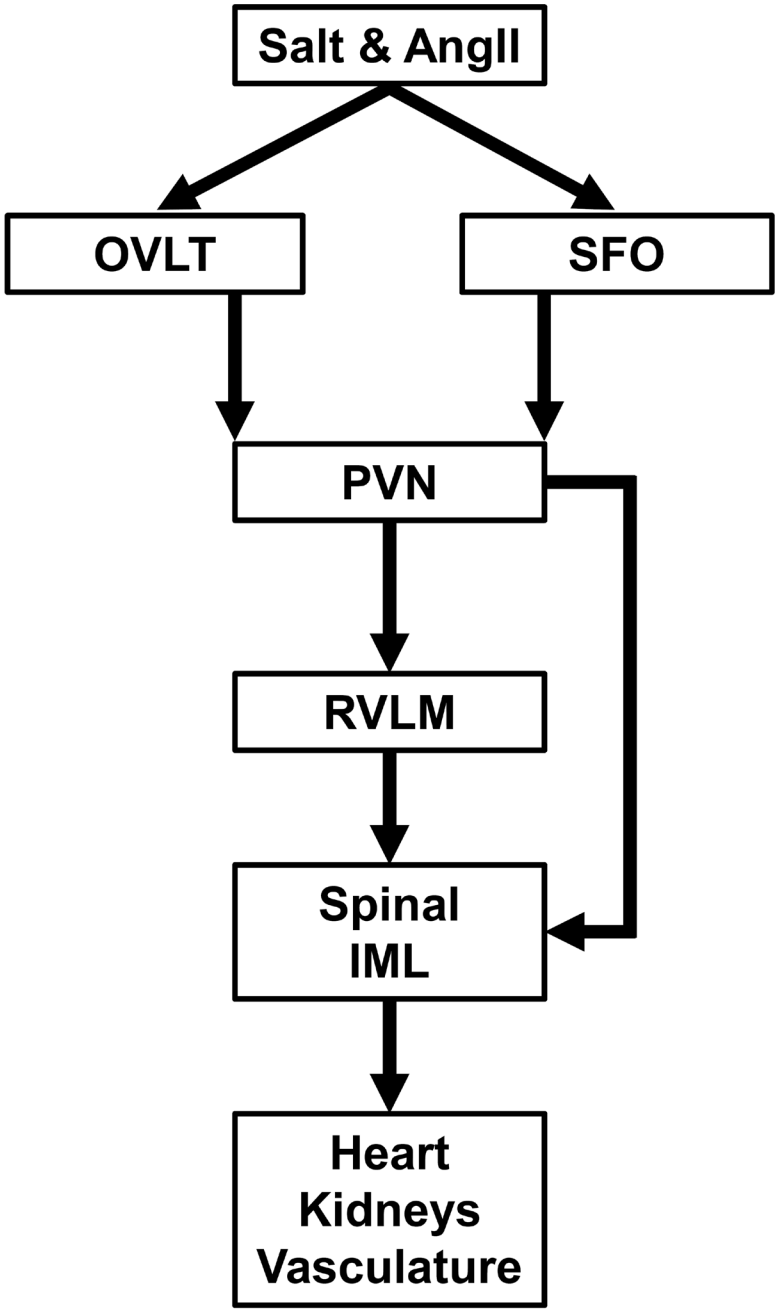

Figure 1.5 Central neural circuitry contributing to sympathetic activation in AngII-salt HTN.

1.3.2 Paraventricular Nucleus

The hypothalamic PVN is situated between the central sensory and effector centers for the SNS (Fig 1.5). The PVN consists of two distinct cell types including vasopressinergic or oxytocinergic magnocellular neurons,[100-102] and parvocellular pre-sympathetic neurons that project to the prominent excitatory centers for the SNS including the RVLM and spinal IML cell column (Fig 1.3).[103-105] The PVN is strongly inhibited by the inhibitory neurotransmitter gamma-aminobutyric acid (GABA) in normotensive rats demonstrated in conscious,[106, 107] and anesthetized conditions.[108-110] Additionally, small conductance Ca^{2+} activated K^{+} channels likely play a role in limiting PVN neuronal excitability in normotensive rats.[111] Interestingly, inhibition of the PVN is lost in multiple diseases involving fluid retention and the PVN becomes a driver of the augmented SNA in these disease states. Studies have demonstrated both augmented excitatory and diminished inhibitory neurotransmitter signaling in the PVN in heart failure.[110, 112-115] Additionally, studies have indicate that augmented neuronal activity in the PVN contributes to sympathoexcitation due to water deprivation.[116-119] Finally, the PVN plays an important role in the pathogenesis of salt-sensitive hypertension. Multiple reports indicate that lesions of the PVN attenuate ABP in Dahl salt-sensitive rats,[120] spontaneously hypertensive rats,[121, 122] and renal wrap HTN.[123] Recently is has been reported that inhibition of the PVN in AngII-salt HTN diminishes SNA and ABP demonstrating the contribution of PVN neuronal activity in maintaining the enhanced SNA and ABP in salt-sensitive HTN.[79]

1.3.3 Mechanisms Contributing to Augmented PVN Activity

Neuronal activity is governed by the confluence of intrinsic membrane properties with local synaptic activity. Alterations in either of these two distinct mechanisms can directly influence the excitability and firing rate of a neuron. Ion channels on the membrane surface largely determine intrinsic membrane properties whereas overall synaptic activity is determined through the balance of excitatory and inhibitor neurotransmitters binding to receptors on the neuron.

Numerous studies have demonstrated that neuronal activity in the PVN contributes to the augmented SNA and ABP in neurogenic hypertension through both synaptic and intrinsic mechanisms.

1.3.4 Synaptic Mechanisms

There are complex interactions among excitatory and inhibitory neurotransmitters with the PVN. Evidence indicates that blocking $GABA_A$ receptors in the PVN augments local glutamate levels.[124] In addition, sympathoexcitatory responses to GABA blockade in the PVN are attenuated by glutamate and AT1R receptor blockade.[108, 109, 124] The Dahl salt-sensitive rat is a well-characterized model of neurogenic HTN. Dahl salt-sensitive rats develop HTN in response to a high salt diet that is mediated in part through activation of the SNS.[120] Studies in Dahl salt-sensitive rats have demonstrated augmented activity of the excitatory neurotransmitters AngII and glutamate in the PVN.[125-127] Furthermore, loss of GABA inhibition also contributes to sympathoexcitation in Dahl salt-sensitive rats.[128] Similarly, HTN in spontaneously hypertensive rats is partially due to sympathoexcitaion and numerous studies have demonstrated augmented glutamatergic and diminished GABAergic signaling with the PVN of spontaneously hypertensive rats.[129-133] To date, only one study has examined altered neurotransmitter signaling in the PVN in AngII-salt hypertension and reported that loss of PVN GABA inhibition contributes to sympathoexcitation.[79] Interestingly, they also reported that the high PVN neuronal activity was not due to the actions of local tumor necrosis factor alpha or microglia activation. Augmented synaptic activity has been consistently demonstrated in HTN and likely plays a significant role in augmenting PVN neuronal activity.

1.3.5 Intrinsic Mechanisms

Less is known regarding alterations of intrinsic membrane properties that contribute to augmented PVN neuronal activity in salt-sensitive hypertension. Intrinsic mechanisms are particularly important due to their potential for increased post-synaptic excitability contributing to significantly augmented neurotransmitter release. The A-type K^+ current has previously been

demonstrated to modulate action potential waveform and firing frequency of PVN neurons with axon projections to the RVLM (PVN-RVLM).[134] One study has previously reported that diminished A-type K^+ current contributes to action potential broadening and augmented Ca^{2+} entry into the cell that could play a role in augmented neurotransmitter release in renovascular hypertension.[135]

SK channels serve as negative-feedback regulators of neuronal excitability. SK channels open in response to a rise in intracellular Ca^{2+} during action potentials and generate the medium afterhyperpolarization potential (mAHP) immediately following decay of an action potential (Fig 1.6).[136-141] Evidence indicates that SK channels are key regulators of excitability in PVN-RVLM neurons and SK channel blockade significantly augments neuronal excitability.[142] Blockade of SK channels via PVN microinjection of the selective SK channel blocker apamin in normotensive rats dramatically augments SNA (~300%) and ABP (~30mmHg) demonstrating their powerful inhibitory control in the PVN.[111]

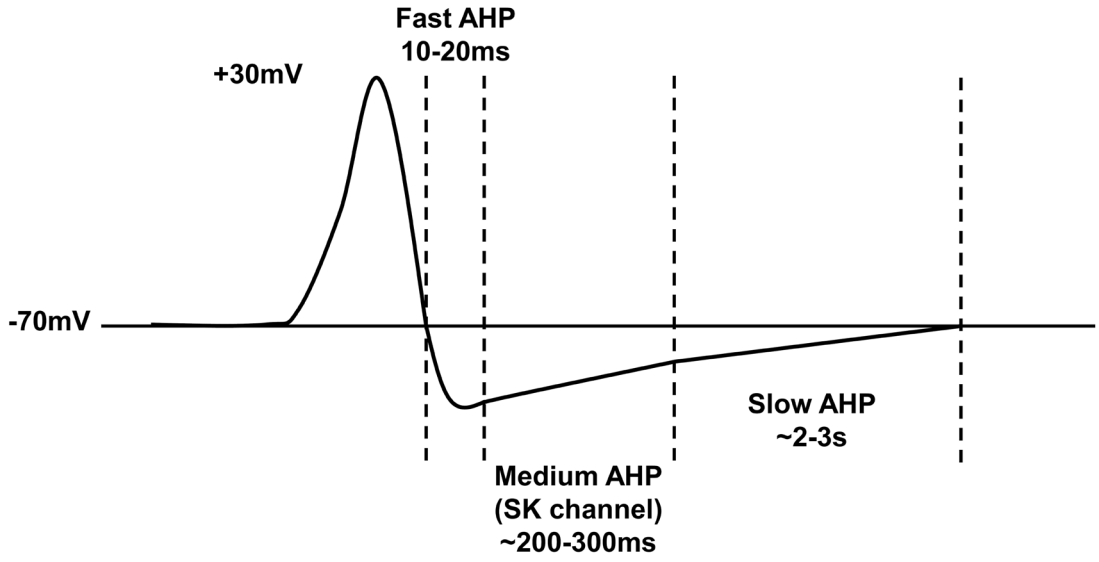

Figure 1.6 Representative drawing of an action potential with after-hyperpolarization potential (AHP). SK channels mediate the medium AHP to limit neuronal excitability.

Several studies have demonstrated that SK channel dysfunction contributes to the augmented neuronal excitability in neurogenic hypertension. Pachauau *et al.* demonstrated that spontaneous firing frequency was augmented in IML projecting PVN neurons of spontaneously hypertensive rats (SHR) compared to Wistar-Kyoto (WKY) control rats.[143] In addition, blockade of SK channels with apamin augmented excitability neurons from WKY but not SHR indicating SK channel dysfunction in PVN-IML neurons in SHR rats. They further demonstrated that the amplitude of the apamin-sensitive mAHP was significantly greater in WKY compared to SHR. To date, one study has probed for intrinsic mechanisms contribution to augmented excitability/activity of PVN neurons in AngII-salt hypertension. Chen et al. examined the contribution of SK channel in limiting neuronal excitability of PVN-RVLM neurons in AngII-salt hypertension.[144] They reported that SK channel current amplitude and density was decreased in AngII-salt hypertension. Additionally, the intrinsic excitability of PVN-RVLM neurons as measured by firing frequency in response to a ramp current protocol significantly augmented (Fig 1.7). Subthreshold depolarizing input resistance was also augmented in AngII-salt hypertension compared to control. Bath application of the SK channel blocker apamin significantly augmented neuronal excitability of neurons in the normotensive group, yet had no effect on neurons from AngII-salt indicating significant SK channel dysfunction (Fig 1.7). Additionally spike-frequency adaptation (SFA) was diminished in AngII-salt neurons (Fig 1.7). In normotensive neurons, termination of current pulses revealed an AHP whereas neurons in the AngII-salt group demonstrated a revealed after depolarization potential (ADP). Collectively, these results indicate that diminished SK current in PVN-RVLM neurons likely augments neuronal excitability in AngII-salt HTN and could play a large role in the sympathoexcitation in this model of hypertension.

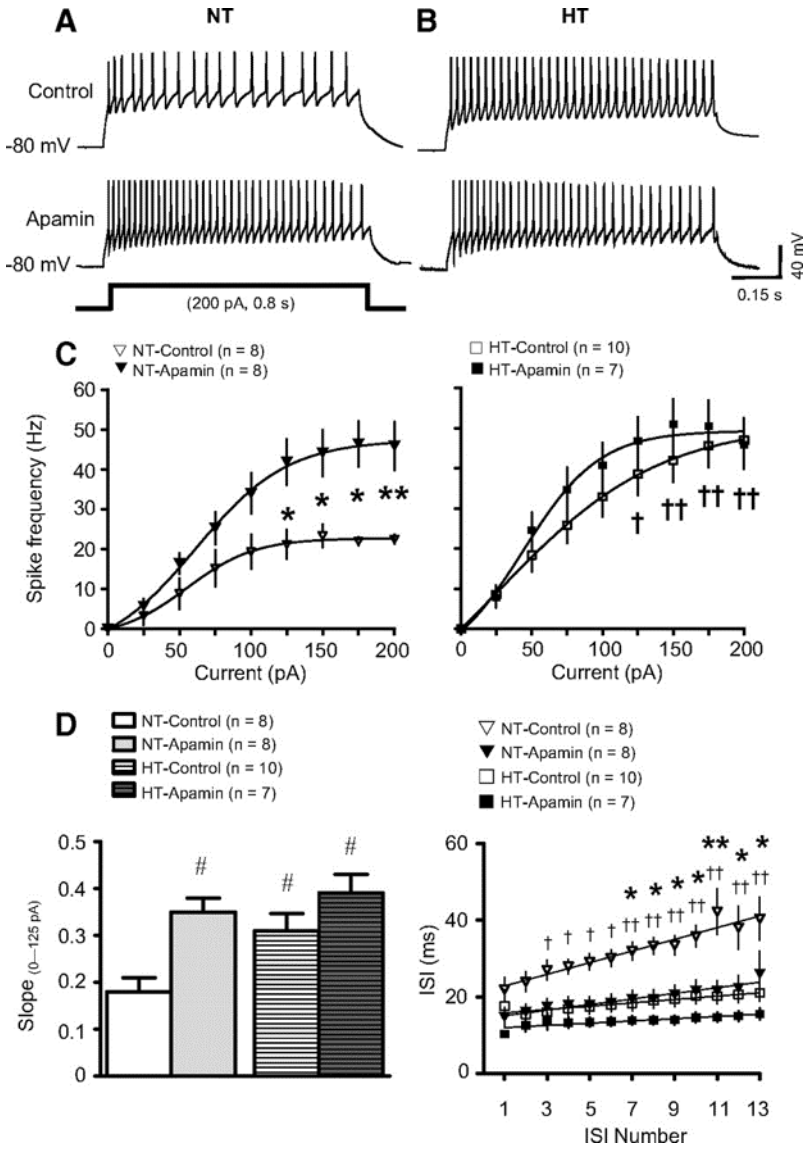

Figure 1.7 Excitability of PVN-RVLM neurons is augmented in AngII-salt HTN. **A:** Tracings from NT rats to a 200pA depolarizing current injection. **B:** Tracings from 2 different PVN-RVLM neurons from HT rats to depolarizing current injections. **C:** Stimulus response curve from NT (left) and HT (right) rats in the absence and presence of apamin. Note that excitability was greater in HT than NT rats under control conditions and apamin only increased discharge in the NT group. **D:** Slope of the stimulus-response curve was greater in HT compared to NT. Apamin significantly increased the slope in the NT group but not the HT group. Interspike intervals (ISIs) plotted for trains action potentials revealed that average ISI and spike-frequency adaptation (ISI prolongation) were greater (right) among neurons from the NT than HT rats. *P,0.01, **P<0.001 apamin vs. control groups from NT rats. #P<0.05 vs. NT groups in the absence of apamin.[144] (Reprinted with permission from *J Neurophysiol*. 2010; 104:2329-37. Copyright 2010, The American Physiological Society).

1.4 Endoplasmic Reticulum

The endoplasmic reticulum (ER) is an intracellular organelle that plays a significant role in protein folding, and intracellular Ca^{2+} homeostasis. The ER also plays a diverse role in cell regulation and helps provide a mechanism to deal with homeostatic perturbations in order to ensure viability of the cell.[145] Proteins ultimately destined for secretion or trans-membrane residence are folded and mature within the lumen of the ER.[145, 146] Proper protein folding is essential for cell viability and is dependent on aspects of the ER environment; therefore, alterations in the ER environment can have a large impact on protein folding and cell viability [147].

1.4.1 ER Stress

Protein synthesis is a very delicate process that requires strict quality control to ensure aberrant proteins are not released for functional use [148]. The ER requires specific properties in order to optimally process and release functional proteins including high levels of Ca^{2+} and adenosine triphosphate (ATP) compared to the cytosol, along with an oxidizing environment in order to ensure the formation of disulfide bonds.[149] Changes in energy availability or perturbations in intracellular Ca^{2+}, and/or an oxidative insult are just a few examples of how the ER of a cell can be altered to improperly synthesize or produce mis-folded proteins. Mutations in transcription or translation of proteins can also result in mis-folded proteins.[150] Studies indicate that close to 30% of new proteins are mis-folded and require corrections to the structure before being released from the ER.[151] The accumulation of a large number of mis-folded proteins within the ER triggers adaptive cellular strategies to return the cell to the homeostatic norm in a process called the unfolded protein response (UPR) triggering a pathological condition known as ER Stress.[152] Recently, evidence has emerged that ER stress may play a role in the enhanced sympathetic outflow in hypertension, however, the mechanism(s) remain to be determined.[153, 154]

1.4.2 Intracellular and ER Ca^{2+} Regulation

The ER is a key regulator of intracellular Ca^{2+} through the ER Ca^{2+} store. Ca^{2+} is an important second messenger that regulates many processes within a large variety of cell types. Neuronal Ca^{2+} signaling plays an important role in regulating excitability, synaptic activity, and gene expression.[155] Therefore, neuronal Ca^{2+} signaling is a highly regulated process involving voltage-gated membrane Ca^{2+} channels, metabotropic receptors including AT1, and Ca^{2+}-induced Ca^{2+} release (CICR) from Ca^{2+} stores in the ER. The ER Ca^{2+}-ATPase actively pumps Ca^{2+} across the ER lumen resulting in Ca^{2+} levels that are significantly higher (~1mM) compared to the cytoplasm (100nM) (Fig 1.8).[149] Release of Ca^{2+} from the ER is mediated through two types of ligand gated Ca^{2+} channels including inositol-1,4,5-triphosphate receptors (IP3R), and ryanodine receptors (RyR).[155, 156] IP3R activation occurs through rising levels of inositol-1,4,5-triphosphate due to synaptic activation of metabotropic neurotransmitter receptors including, AT1 receptors, prominently located in the PVN (Fig. 1.8).[157] RyR activation occurs through rising levels of intracellular Ca^{2+} during action potentials (Fig 1.8).[156] SK channels are activated by a swift rise in intracellular Ca^{2+} primarily mediated through voltage-gated Ca^{2+} channels and CICR from the ER stores.[136] Studies report that inhibition of ER Ca^{2+} release diminishes the mAHP primarily mediated by SK channels in sympathetic neurons demonstrating the role of ER Ca^{2+} in SK channel activation.[158, 159] Altered ER Ca^{2+} regulation could play an important role in SK channel dysfunction and augmented neuronal excitability in the PVN.

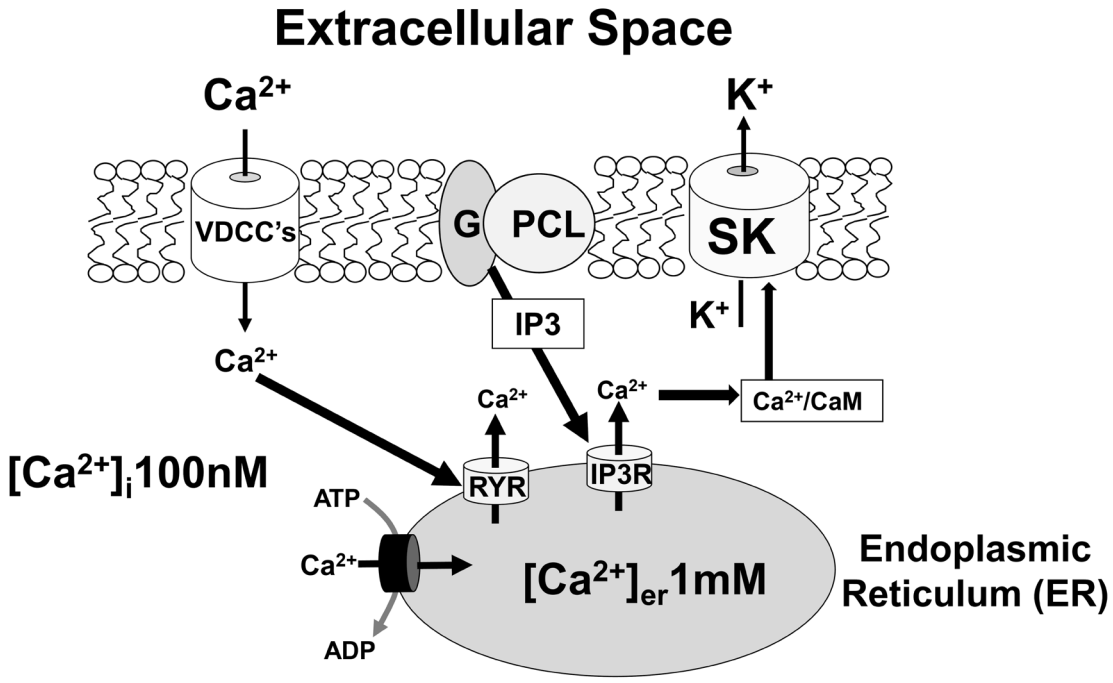

Figure 1.8 Representative diagram of intracellular Ca^{2+} regulation. High ER Ca^{2+} levels ($[Ca^{2+}]_{er}$) are maintained through the ER Ca^{2+} ATPase. Ca^{2+} entry from voltage dependent Ca^{2+} channels (VDCC's) stimulates Ca^{2+} release from ryanodine receptors (RYR) on the ER membrane. Inositol triphosphate (IP3) from g-protein coupled receptors (GPCL) stimulates Ca^{2+} release from IP3 receptors (IP3R) on the ER membrane. Intracellular Ca^{2+} ($[Ca^{2+}]_i$) binds with calmodulin (CaM) and together the complex activates SK channels. Adapted from Paschen.[149]

1.5 Summary and Hypothesis

Salt-sensitive hypertension is a complex disorder involving the interactions of multiple systems within the body. Evidence indicates that disruption of compensatory mechanisms normally responsible for excretion of excess salt from the body play a substantial role in HTN due to HS diet. Numerous studies have demonstrated that the central nervous plays a dominant role in AngII-salt HTN through sustained activation of the SNS. The hypothalamic PVN is an important regulator center due to its position between the sensory and effector centers for the SNS. Evidence indicates that PVN neuronal activity is augmented in AngII-salt hypertension and is a driver of the high level of SNA and ABP. To date little is known regarding cellular mechanisms in the PVN that contribute to the augmented neuronal excitability/activity in AngII-salt HTN. Additionally, while numerous studies have examined synaptic mechanisms that contribute to augmented PVN neuronal activity in various models of neurogenic hypertension, less is known regarding intrinsic cellular mechanisms.

Hypothesis 1: Our laboratory has previously reported that SK channel dysfunction augments excitability of PVN-RVLM neurons in AngII-salt HTN. Additionally, we have demonstrated that SK channel blockade in the PVN significantly augments SNA and ABP in normotensive anesthetized rats. Therefore, in **study 1, we hypothesized that SNA and ABP responses to PVN SK channel blockade would be attenuated in AngII-salt HTN due to SK channel dysfunction.** Furthermore, we sought to examine the individual contributions of HS and AngII to PVN SK channel dysfunction.

Hypothesis 2: The ER is a prominent regulator of intracellular Ca^{2+} and CICR from the ER during action potentials is a prominent activator of SK channels. To date, studies have not examined the contribution of the ER in regulating neuronal excitability in the PVN, or its contribution to SNA and ABP. **We**

hypothesized that inhibition of ER Ca^{2+} function in the PVN would augment SNA and ABP. In study 1, we demonstrate dysfunction of SK channels in rats fed a 2% HS diet; therefore, **we further hypothesized that dysfunction of the ER Ca^{2+} store may be an underlying mechanism contributing to SK channel dysfunction and sympathoexcitation due to HS diet.**

Chapter 2.

Sympathoexcitation in ANG II-salt Hypertension involves Reduced SK Channel Function in the Hypothalamic Paraventricular Nucleus.[1]

2.1 Introduction

Studies suggest that the central nervous system substantially contributes to AngII-salt hypertension (AngII-salt HTN) through elevations in sympathetic nervous system (SNS) activity.[74, 76, 77, 79] Prominent forebrain circumventricular organs including the organum vasculosum lamina terminalis (OVLT) and subfornical organ (SFO) lack a complete blood brain barrier and therefore have the ability to detect alterations in plasma osmolality and AngII levels,[99, 160-163] and transmit efferent activity to the hypothalamic paraventricular nucleus (PVN).[98, 164] PVN neurons, in turn, have axon projections to the spinal intermediolateral (IML) cell column and the rostral ventrolateral medulla (RVLM),[104, 105] the main excitatory centers that play an important role in regulating sympathetic nerve activity (SNA).[7]

The PVN is a key regulator of SNA given its prominent position between the sensory and effector components of the SNS, and enhanced PVN activity has been demonstrated in a variety of cardiovascular diseases.[72, 121, 165] Evidence demonstrates that enhanced neuronal activity within the PVN is required for the maintenance of several models of neurogenic HTN including AngII-salt.[79, 121, 166, 167] A number of studies have demonstrated an up-regulation

[1] The material contained in this chapter was previously published in *American Journal of Physiology- Heart & Circulatory Physiology*. Reprinted with permission from Larson RA, Gui L, Huber MJ, Chapp AD, Zhu J, LaGrange LP, Shan Z and Chen QH. American Journal of Physioliology- Heart and Circulatory Physiology. 2015; 308:H1547-55.

of excitatory glutamatergic and angiotensinergic signaling within the PVN in hypertensive rats.[168-171] Furthermore, evidence demonstrates the role of GABA inhibition on PVN neurons,[172, 173] and that GABA dis-inhibition contributes to the augmented SNA in HTN.[174, 175] To date, little information is available regarding alterations of intrinsic membrane properties of PVN neurons in HTN. One previous study by Sonner *et al* demonstrated a reduction in potassium A-current in PVN-RVLM neurons in renal-vascular HTN that contributed to augmented *in vitro* spontaneous neuronal discharge.[176]

Small conductance calcium activated potassium (SK) channels act as negative feedback regulators of neuronal excitability through their influence on the medium after-hyperpolarization potential (mAHP).[136-141] Previous studies have demonstrated that SK channels greatly influence excitability in PVN neurons with axon projections to the rostral ventrolateral medulla (PVN-RVLM),[142] and reduced SK channel current significantly enhanced the excitability of PVN-RVLM neurons in rats with AngII-salt HTN.[144] Very recently, Pachuau *et al* has reported that diminished SK current contributed to the increased excitability of spinal IML projecting PVN (PVN-IML) neurons in spontaneous hypertensive rats (SHR).[143] Furthermore, our lab has recently reported that blockade of SK channels in the PVN in normotensive rats substantially augments SNA and ABP *in vivo.*[111] The present study was performed to determine if SK channel dysfunction is present in the PVN of anesthetized rats with AngII-salt HTN. In addition, recent evidence suggests that the neurogenic phase of AngII-salt HTN is more dependent on the level of dietary salt.[75] Therefore, we examined the individual contributions of high salt (HS) diet and AngII alone to PVN SK channel dysfunction.

2.2 Materials and Methods

2.2.1 Animals

Male Sprague-Dawley rats (n=48, 200-300 g) purchased from Charles River Labs (Wilmington, MA, USA) were housed in a temperature controlled

room (22-23°C) with a 12:12 hour light-dark cycle. Chow and tap water were available ad libitum unless otherwise noted. All experimental and surgical procedures were carried out under the guidelines of the National Institutes of Health Guide for the Care and Use of Laboratory Animals with the approval of the Institutional Animal Care and Use Committee at Michigan Technological University.

2.2.2 Protocols of Animal Experimental Model

Rats in the control group consumed a normal salt (NS, 0.4% NaCl) diet whereas rats in the high salt (HS) group were placed on a high salt (2% NaCl) diet for 4 weeks. The AngII-salt hypertension group (AngII-salt HTN) was fed a HS diet for 4 weeks and received a systemic infusion of Ang II (150 ng/kg/min) subcutaneously during the last 2 weeks on the HS diet. The AngII administration only (AngII) group was fed a NS diet for 4 weeks and AngII was infused subcutaneously for the last 2 weeks. For AngII-salt HTN and AngII groups, animals were anesthetized with isoflurane (3% in O_2) and an osmotic mini pump (2ML2, Alzet) was implanted subcutaneously to deliver AngII (150 ng/kg/min) for two weeks prior to experimentation.

2.2.3 Experiment Preparation

Rats were anesthetized with an intraperitoneal injection of a mixture containing α–chloralose (80 mg/kg) and urethane (800 mg/kg). Adequate depth of anesthesia was determined by absence of corneal or pedal reflexes. A water-circulating pad maintained body temperature. A left femoral artery was catheterized for measurement of arterial blood pressure (ABP), and a left femoral vein was catheterized for administration of drugs. Heart rate (HR) was obtained from the R-wave of the electrocardiogram (lead I). Following tracheal cannulation, rats were ventilated with oxygen rich room air. End-tidal P_{CO2} (Capstar-100, Cwe Inc) was continuously monitored to ensure it was within normal limits (35 to 40 mmHg). Rats were paralyzed with continuous infusion of gallamine trethiodide. Adequate depth of anesthesia following paralysis was determined by lack of pressor responses to noxious foot pinch. Supplemental

doses of anesthesia equal to 10% of initial dose were given as needed. All animals were allowed to stabilize for at least 2 hours following surgery to ensure stability of recorded variables.

2.2.4 Recording of Sympathetic Nerve Activity

A left flank incision was utilized to view and isolate a left renal and a postganglionic splanchnic sympathetic nerve from the surrounding tissue.[177] Nerve bundles were mounted on separate stainless steel wire electrodes (A-M Systems 0.127-mm OD) and covered with silicon-based impression material (Coltene, Light Body). The signal was directed to an AC amplifier (P511, Grass Technologies) equipped with half-amplitude filters (band pass, 100 to 1,000 Hz) and a 60-Hz notch filter. The processed signal was rectified, integrated (10-ms time constant), and digitized at a frequency of 5,000 Hz using a 1401 Micro3 analog-to-digital converter and Spike 2 software (Version 7.04, Cambridge Electronic Design, Cambridge, UK).

2.2.5 PVN Microinjection

Animals were placed in a stereotaxic head frame with the skull level between bregma and lambda. The dura was exposed by removing a small piece of the skull and a single-barreled glass microinjector pipette was lowered vertically into the PVN. Stereotaxic coordinates used were as follows (in mm): 1.2 to 1.6 caudal to bregma, 0.5 lateral to midline, and 7.0 to 7.2 ventral to dura. The SK channel blocker apamin (Sigma) was dissolved in saline and the pH was adjusted to 7.2. The SK channel activator CyPPA (Tocris) was dissolved in DMSO. Apamin (12.5 pmol) or CyPPA (5 nmol) were administered via bilateral PVN microinjection in a volume of 50 nl per side with a pneumatic pump (WPI). The micropipette was withdrawn between bilateral microinjections and the approximate interval between bilateral injections was ~2 minutes. Following each experiment, Chicago blue dye (2% in saline, 50 nl) was injected into the PVN to mark the injection sites and provide an estimate of drug diffusion area. Brains were removed and post-fixed in 4% paraformaldehyde and then transferred to 30% sucrose-PBS. The hypothalamus, including the PVN area,

was sliced in coronal sections and microinjection sites were visualized under brightfield microscopy.

2.2.6 Punched Brain Tissues from Rats

Separate groups of NS control and AngII-salt HTN rats were deeply anesthetized with 5% isoflurane and then decapitated. Brains were quickly removed and were put in the rat brain matrix pre-frozen with dry ice. The hypothalamic PVN were punched out with a 12-gauge needle (inner diameter 1.5 mm). To identify hypothalamic PVN tissue, the optic tract was identified and a 1 mm thick brain section was taken from the rostral end point of the optic tract. Samples were frozen in liquid nitrogen and stored at -80^{o}C for western blot analysis of SK channel protein.

2.2.7 Western Blot Analysis of SK Channel Protein

Frozen brain tissues were homogenized in buffer (50 mM Tris-base, 1.0 mM EDTA, 150 mM NaCl, SDS (0.1%), TritonX-100 (1%), sodium deoxycholate (1%), 1 mM PMSF, pH 7.4, Sigma) complete with protease inhibitors (Leupeptin 0.1 mM and phenylmethylsulfony fluoride 0.3 mM, Sigma) and stirred for 30 min at 4°C. Centrifugation with 12000 *rpm* at 4°C was performed for 5 min. The supernatant was collected and the protein concentration was determined in triplicate by a Bio-Rad DC protein assay Kit at absorbance of 750 nm using Bovine Serum Albumin as a standard. Aliquots were stored at −80°C until analyzed, at which time the 75 μg protein of each sample was separated using sodium dodecyl sulfate-polyacrylamide gel (10%) electrophoresis (SDS-PAGE) followed by electrophoretic transfer of proteins from the gel to a nitrocellulose membrane (Bio-Rad). The membranes were blocked with 5% non-fat milk for 1 hr at room temperature, washed three times, and probed with a primary rabbit KCa2.1, KCa2.2 and KCa2.3 antibodies (Alomone) (1:500) or mouse anti-β-actin (Santa Cruz) overnight at 4°C. The membranes were incubated with goat anti-rabbit IgG-HRP secondary antibodies or goat anti-mouse IgG-HRP secondary antibodies (Santa Cruz) for 1 hr at room temperature, and then detected with enhanced chemiluminescence.

2.2.8 Data Analysis

Summary data are expressed as mean ± SE. SSNA and RSNA were determined as an average of the rectified, integrated signal. Baseline values of all variables were obtained by averaging a 10-min segment of data immediately preceding PVN microinjection in anesthetized rats. SSNA, RSNA, MAP and HR responses to apamin or CyPPA were obtained by averaging a 2-min period centered on the maximal response. Data are presented as percent (%) change from baseline after subtracting background noise determined with bolus injection of the ganglionic blocker hexamethonium (30 mg/kg). Data were analyzed by one-way ANOVA. Post-hoc analysis was performed with Newman-Keuls Multiple Comparison Test. Differences were considered statistically significant at a critical value of $p < 0.05$.

2.3 Results

2.3.1 AngII-salt HTN

Baseline hemodynamic variables from anesthetized animals (n=34) are shown in Table 2.1. ABP was significantly elevated in the AngII-salt HTN group compared to normotensive control rats on a NS diet. Subcutaneous infusion of AngII alone elevated ABP, but the increase did not reach statistical significance, whereas HS alone had no effect on ABP. HR was not significantly different among any of the groups.

Table 2.1 Baseline MAP and HR in anesthetized rats

Group	n	MAP (mmHg)	HR (bpm)
NS control	8	102 ± 6	366 ± 17
AngII-salt HTN	12	123 ± 3 *	399 ± 10
HS	7	106 ± 6	352 ± 7
AngII	7	112 ± 5	370 ± 17

Values are mean ± standard error; n= number of rats; HR-heart rate; MAP-mean arterial pressure; NS-normal salt (0.4%); AngII-angiotensin II; HS-high salt (2%); HTN-hypertension; * P<0.05 vs NS Control.

2.3.2 Effects of PVN-Injected SK Channel Blocker on SSNA, RSNA, MAP and HR

Consistent with data we previously published,[111] bilateral microinjection of the SK channel blocker apamin into the PVN markedly increased SSNA, RSNA, MAP and HR in control rats fed a NS diet. Figure 2.1 demonstrates representative raw tracings from a rat with a NS diet (left) before and after bilateral microinjection of apamin (12.5 pmol, 50 nl) into the PVN. This dose of apamin was previously shown to be the minimum dose to elicit a maximum ABP and SNA response in the PVN.[111] Collectively (n=8) PVN apamin increased SSNA (+263.5 ± 39.7%), RSNA (+179.8 ± 19.3%), MAP (+36.7 ± 4.4 mmHg) and HR (+37.7 ± 12.3 beats/min) as shown in Figure 2.3 summary data.

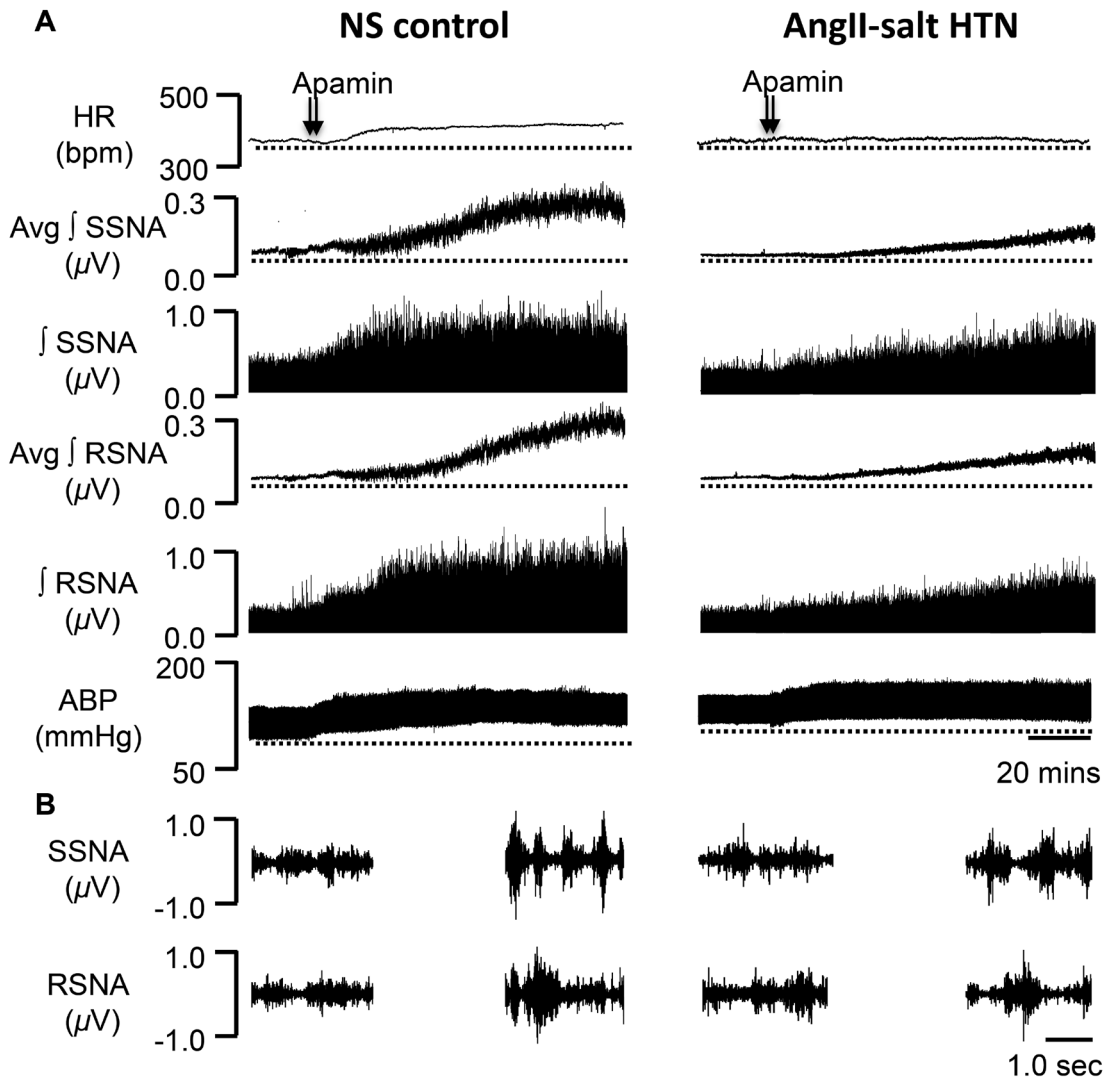

Figure 2.1 Representative traces in response to PVN apamin. Heart rate (HR), splanchnic sympathetic nerve activity (SSNA), renal SNA (RSNA) and arterial blood pressure (ABP) responses to bilateral paraventricular nucleus (PVN) microinjection of apamin (12.5 pmol) in a rat with normal salt (NS) control (left) and a rat with AngII-salt hypertension (HTN, right). **A**: bilateral PVN injection (50 nl each) of apamin (arrowheads) markedly increased HR, SSNA, RSNA and ABP in NS control whereas the responses were obviously attenuated in AngII-salt HTN compared to NS control. **B**: *Left*, 5s trace of SSNA (*top*) and RSNA (*bottom*) prior to injection of apamin into PVN. *Right* 5s trace of SSNA (*top*) and RSNA (*bottom*) after injection of apamin into PVN.

The main goal of this study was to determine *in vivo* whether SK channel function is altered in the PVN in rats with AngII-salt HTN. The right column of Figure 2.1 shows a representative response to bilateral PVN microinjection of

apamin (12.5 pmol, 50 nl) in a rat with AngII-salt HTN. In contrast to normotensive control rats with a NS diet, summary data (n=7) presented in Figure 2.3 demonstrates that maximum increases in SSNA, RSNA and MAP elicited by PVN apamin were significantly attenuated in AngII-salt HTN rats (+36.4 ± 15.7%, $p < 0.05$ versus NS for SSNA; +25.3 ± 16.2%, $p < 0.05$ versus NS for RSNA; +11.3 ± 6.2 mmHg, $p < 0.05$ versus NS for MAP). While the increase in HR evoked by PVN apamin was blunted in rats with AngII-salt HTN compared to NS control group, it did not reach statistical significance (+4.8 ± 8.1 beats/min, $p > 0.05$ versus NS).

A secondary goal of the present study was to examine the relative contributions of a HS diet only or subcutaneous infusion of AngII (150 ng/kg/min) alone to PVN SK channel dysfunction. Figure 2.2 shows a representative response to bilateral PVN microinjection of apamin (12.5 pmol, 50 nl) in a rat on a HS diet (left). Summary data (n=7) presented in Figure 2.3 demonstrates that maximum increases in SSNA, RSNA, and MAP elicited by PVN apamin were significantly attenuated in rats with a HS diet (+125.5 ± 21.5%, $p < 0.05$ versus NS for SSNA; +62.9 ± 17.3%, $p < 0.05$ versus NS for RSNA; +19.9 ± 5.3 mmHg, $p < 0.05$ versus NS for MAP). Similarly, the increase in HR evoked by PVN apamin was blunted in rats with a HS diet, but did not reach statistical significance (+15.1 ± 10.9 beats/min, $p > 0.05$ versus NS). While there is no statistically significant difference, the sympathoexcitatory and pressor responses elicited by PVN apamin in the HS group are less blunted compared to that in AngII-salt HTN animals.

Representative raw tracings of bilateral PVN microinjection of apamin (12.5 pmol, 50 nl) in a rat with subcutaneous infusion of AngII alone are depicted in the right column of Figure 2.2. Interestingly, although the RSNA responses to PVN apamin (+80.4 ± 35.2%, $p < 0$ .05 versus NS) in rats with subcutaneous infusion of AngII alone were significantly attenuated compared to control rats with a NS diet, SSNA (+208.7 ± 66.11%), MAP (+35.3 ± 2.1 mmHg) and HR (+16 ± 5.4 beats/min) responses to PVN apamin in rats with AngII treatment

alone (n=7) shown in Figure 2.3 were not statistically different ($p > 0.05$) from that in rats with a NS diet.

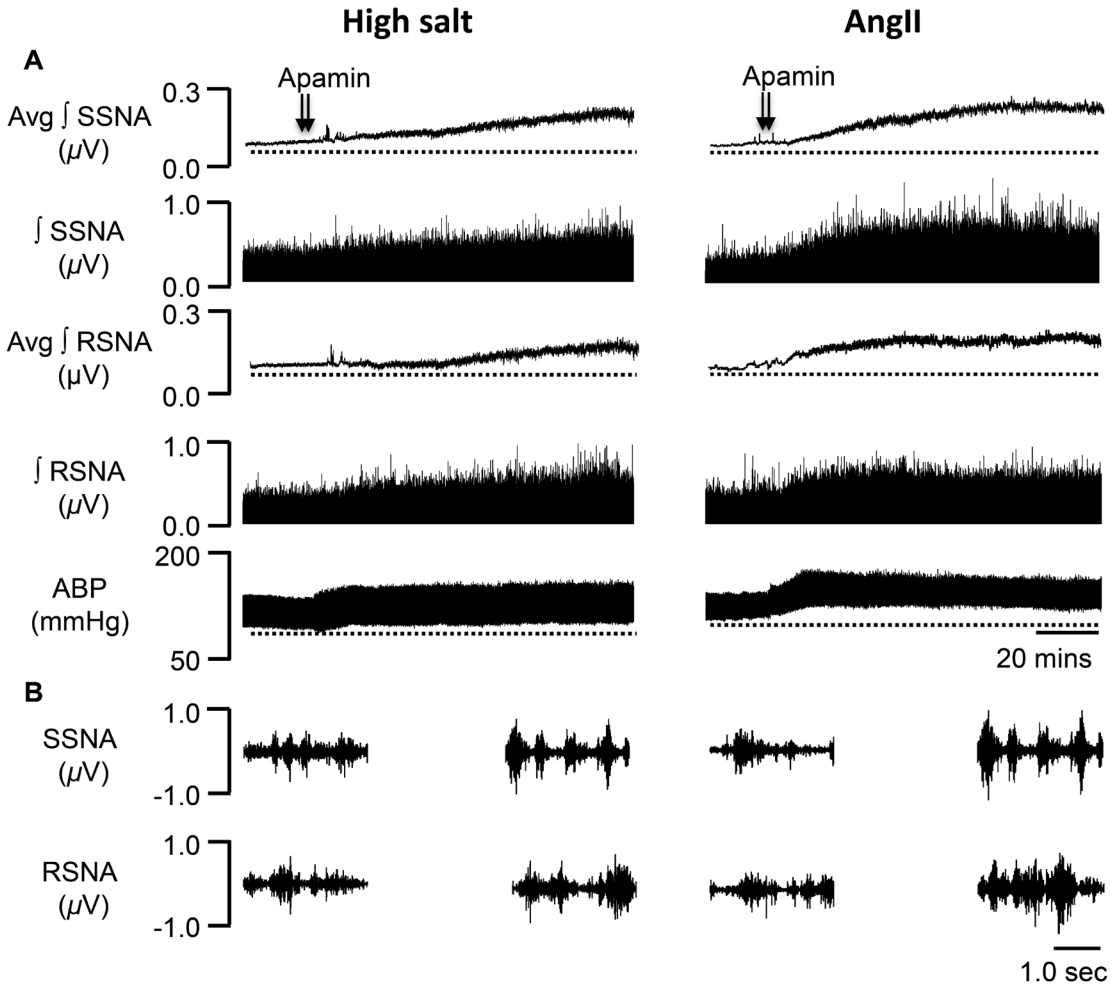

Figure 2.2 Representative traces in response to PVN apamin in NS and AngII only. SSNA, RSNA and ABP responses to bilateral PVN microinjection of apamin (12.5 pmol) in a rat with a high salt (HS) diet alone (left) or systemic Angiotensin II (AngII) infusion alone (right). **A**: bilateral PVN injection (50 nl each) of apamin (arrowheads) in a rat with a HS intake increased SSNA, RSNA and ABP in a similar manner to a rat with AngII-salt HTN (Figure 1, right). Bilateral injection (50 nl each) of apamin (arrowheads) in a rat with systemic AngII infusion increased ABP in a similar manner to a rat with NS control whereas SSNA and RSNA responses were obviously attenuated compared to the NS control (Figure 1, left). **B**: *Left*, 5s trace of SSNA (*top*) and RSNA (*bottom*) prior to injection of apamin into PVN. *Right* 5s trace of SSNA (*top*) and RSNA (*bottom*) after injection of apamin into PVN.

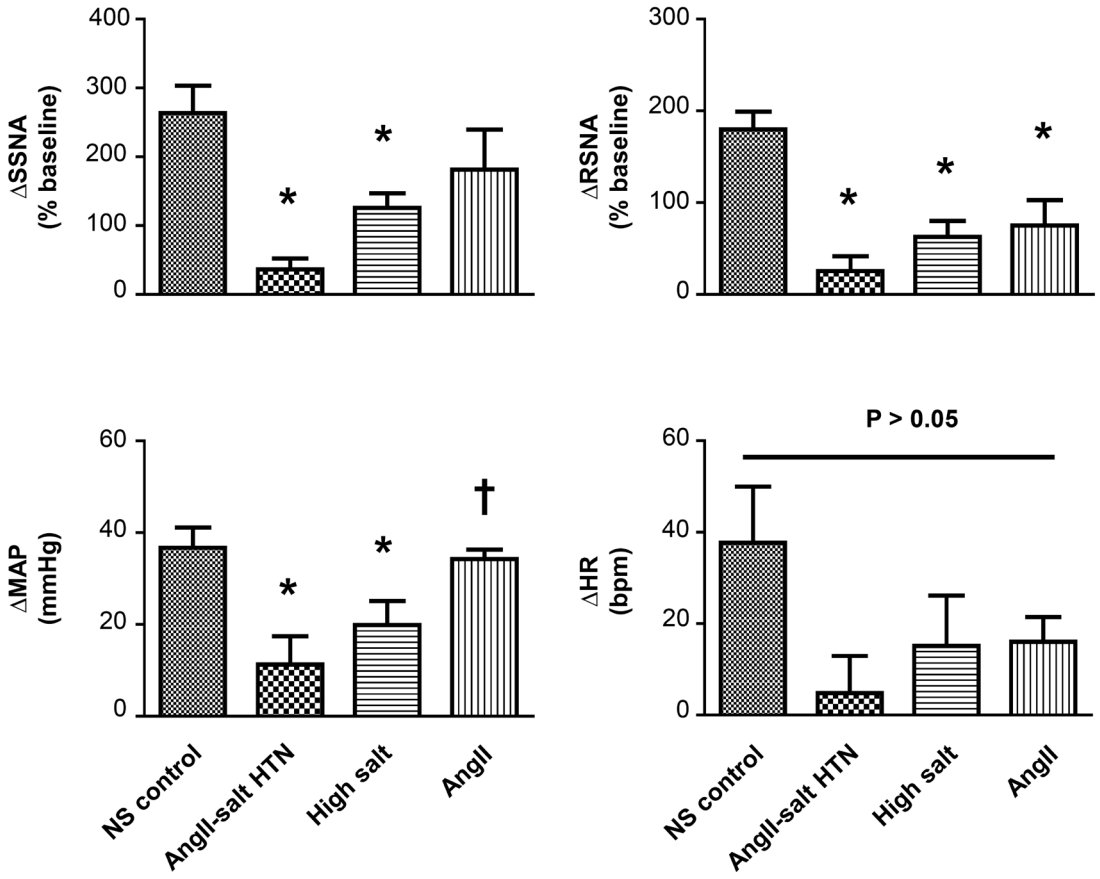

Figure 2.3 Summary data showing the changes in SSNA, RSNA, MAP and HR in response to bilateral microinjection of apamin into the PVN in NS (normal salt) control, AngII-salt HTN (hypertension), HS (high salt) alone, and systemic AngII infusion alone groups. *p<0.05 vs NS controls; † vs AngII-salt HTN (1-way ANOVA; Newman Keuls Multiple Comparison Test).

2.3.3 Effects of PVN-Injected SK Channel Activator on SSNA, RSNA, MAP and HR

Initial experiments demonstrated loss of PVN SK channel function in AngII-salt HTN. In an effort to further determine the role of SK channels in regulating sympathetic outflow in this disease model, we performed bilateral microinjections of the SK channel activator, CyPPA (5.0 nmol, 50nL/each) into the PVN. This dose of CyPPA has been reported to effectively activate the SK channels *in vivo.*[111] CyPPA microinjection (n=5) into the PVN did not significantly alter SSNA (+14.2 ± 4%), RSNA (+7.0 ± 8%), MAP (-5.2 ± 3.1

mmHg), and HR (0.2 ± 7.0 beats/min) compared to baseline (p > 0.05 vs. baseline).

2.3.4 Histological Analysis

Histological examinations of coronal brain slices from similar rostral-caudal positions were performed in order to estimate drug diffusion area within the hypothalamus. Figure 2.4A demonstrates a composite dye diffusion area made by overlying slices from several different brains to show the outermost distribution of dye. Figure 2.4B shows a representative of a single injection tracing within the PVN. Dye distribution was largely contained within the area encompassing the PVN. Note that the composite dye diffusion area demonstrated in Figure 2.4A is larger than any single tracing from an individual brain but represents the widest possible distribution of injected dye for the entire group.

2.3.5 Comparison of SK Channel Protein Expression

We compared the protein expression (western blot analysis) of SK1-3 channels in the hypothalamic PVN between normotensive control rats with a NS diet (n=7) and AngII-salt HTN animals (n=7). No statistically significant difference in PVN SK1-3 expression was detected between NS control and AngII-salt HTN animals (Figure 2.5A&B).

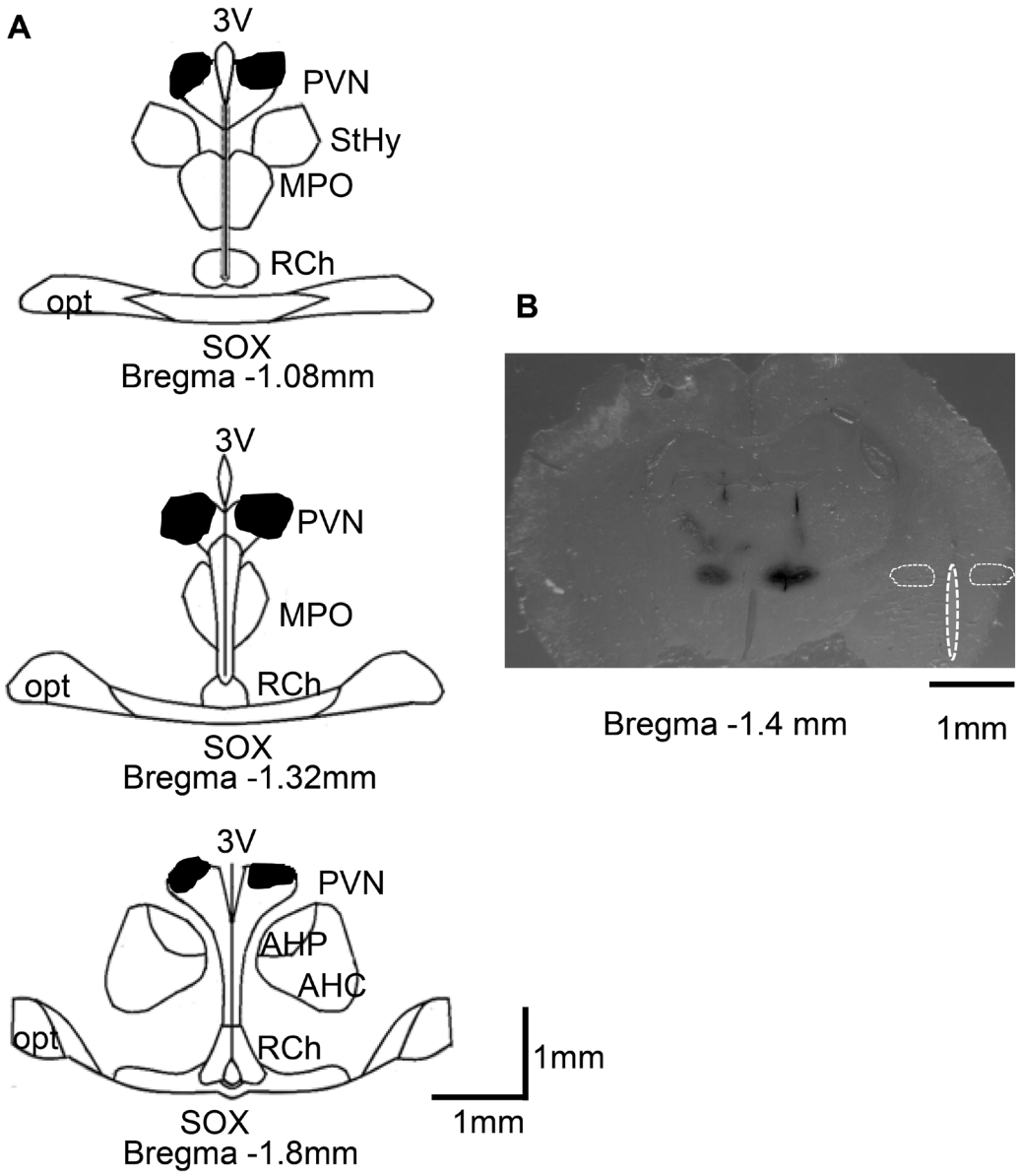

Figure 2.4 Schematic representation of coronal sections throughout the rat hypothalamus. A: shaded areas indicate brain regions exposed to dye utilized to mark the injection sites bilaterally. The shape of each area was determined by overlaying tracings of the outermost diffusion area of injected dye (50 nl) observed on each section through the paraventricular nucleus (PVN). B: representative single bilateral injection of dye within the PVN (50nl of 2% Chicago blue dye, each). AH, anterior hypothalamic area; 3V, third cerebral ventricle; RCh, retrochiasmatic area; MPO, medial preoptic nucleus; opt, optic tract; SOX, supraopticdecussation; StHy, striohypothalamic nucleus.

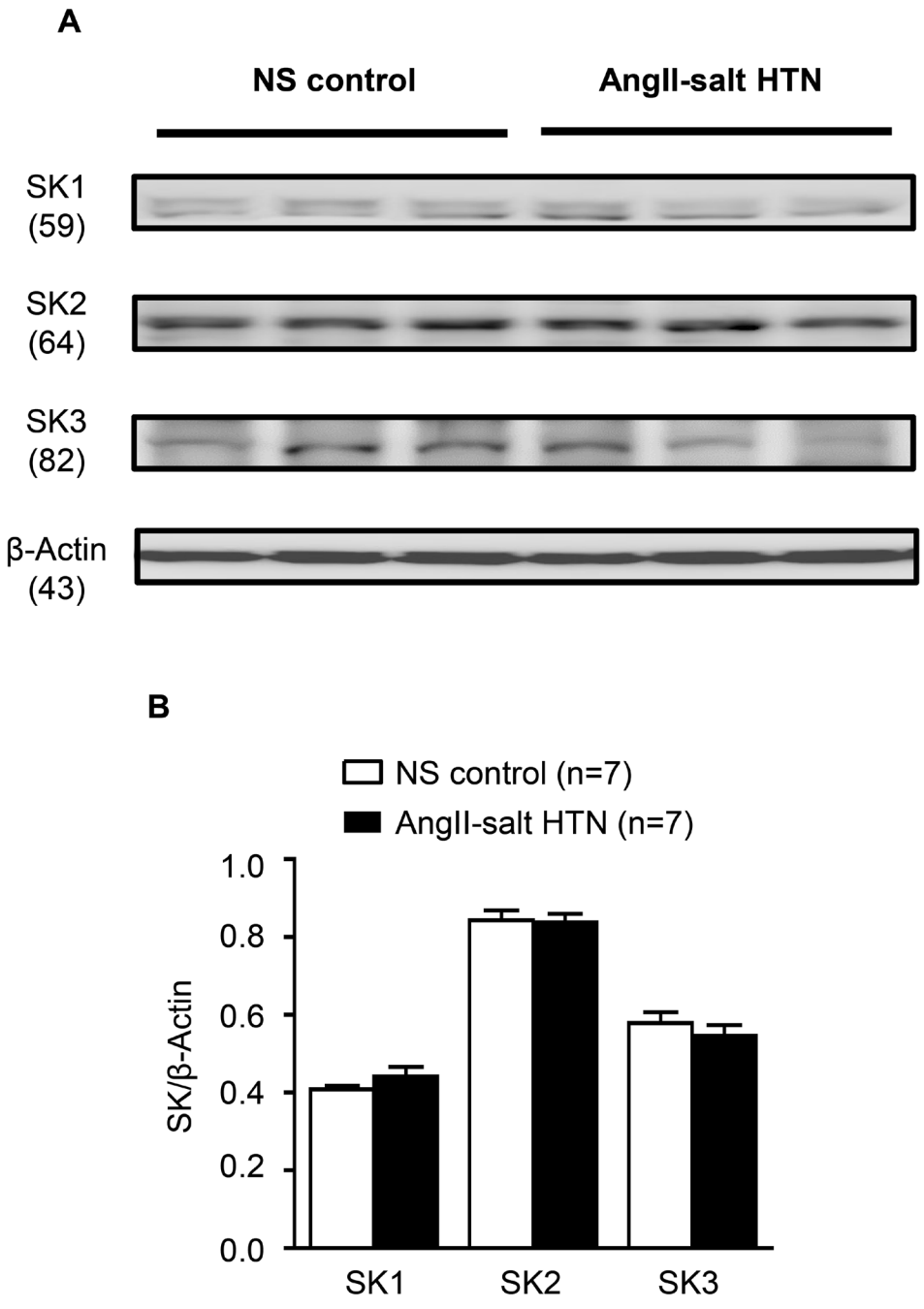

Figure 2.5 Expression of SK1-3 channels in hypothalamic PVN. A: Western blot analysis showing protein expression of SK1-3 channels between rats with NS control group and AngII-salt HTN animals. B: Summary data showing no significant statistical difference in protein expression of SK1-3 channels in the punched PVN between NS control group (n=7) and AngII-salt HTN animals (n=7). All values were normalized to β-actin.

2.4 Discussion

The PVN is a key site for the integration of SNA, and increased PVN neuronal activity is essential to maintain the elevated levels of ABP in AngII-salt HTN.[79, 121] Here, we demonstrate a down-regulation of SK channel function in the PVN, which may underlie the central neuronal mechanisms of increased sympathetic outflow in rats with AngII-salt HTN. We report three novel findings. First, SSNA, RSNA and MAP responses to SK channel blockade in the PVN were attenuated in AngII-salt HTN compared to normotensive rats with a NS diet indicating a loss of PVN SK channel function in animals with treatment of systemic infusion of angiotensin II in combination with a HS (2% NaCl) diet. Second, SSNA, RSNA and MAP responses to PVN SK channel blockade in rats with a HS diet alone were attenuated compared to control animals with a NS intake in a similar manner to the AngII-salt HTN group indicating that perhaps HS intake is a larger contributor to SK channel dysfunction in the PVN in animals with AngII-salt HTN. Lastly, while SNA responses to PVN apamin trended towards an attenuated response, with only RSNA demonstrating a significant difference in rats with systemic AngII infusion only, MAP responses were similar to animals with a NS diet. This evidence indicates that HS intake, rather than the systemic infusion of AngII, may play an important role in down-regulating SK channel function in PVN contributing to the elevated sympathetic outflow in AngII-salt HTN.

Previous studies have demonstrated chronic Ang II-salt treatment induces a neurogenic hypertension,[74, 79, 178] however, little is known yet about the cellular mechanisms that contribute to the elevated sympathetic outflow in this hypertensive model. The current study is the first to demonstrate impairment in SK channel function in the PVN of rats with AngII-salt HTN *in vivo*. In line with our previous work,[111] SK channel blockade in the PVN in normal rats elicited a significant augmentation in SSNA and RSNA displaying the contribution of SK channel inhibition to PVN neuronal excitability and its influence on sympathoexcitation. In the current study, SSNA, RSNA and ABP

responses to SK channel blockade in the PVN were substantially attenuated in rats with AngII-salt HTN compared to control animals with NS intake indicating a large degree of SK channel dysfunction. SK channel function in AngII-salt HTN rats has previously been studied using an *in vitro* whole-cell patch clamp design under brain slice preparation to examine pre-sympathetic PVN neurons[144]. Similar to the present study, it was demonstrated that blocking SK channels of pre-sympathetic PVN neuron significantly increased neuronal discharge in control rats with NS intake, but had less effect on AngII-salt HTN group indicating reduced SK channel activity. Loss of SK channel function diminishes the mAHP and can lead to the loss of spike frequency adaptation in pre-sympathetic PVN neurons that help govern SNA. PVN-RVLM neurons from the AngII-salt group had a greater subthreshold depolarizing input resistance in response to ramp current injection and demonstrated an after-depolarizing potential (ADP) as opposed to the mAHP noted in control neurons. Both the increased depolarizing input resistance and revealed ADP can potentially lead to increased excitability of PVN-RVLM neurons.[144] The mechanism(s) whereby PVN SK channel dysfunction translates into elevated SNA remain to be fully determined. PVN neurons have axon projections to several autonomic control centers including the RVLM, the nucleus tractus solitarii in the dorsal brain stem, and the spinal IML.[105, 142, 179] Augmented excitability of the above pre-sympathetic PVN neurons has the potential to increase SNA through multiple pathways within the SNS.

The current study sought to determine the contribution of SK channels among PVN neurons to the sympathetic outflow in rats with AngII-salt HTN. The AngII-salt model HTN depends on the interaction of circulating AngII and dietary salt.[72] Studies examining depressor responses to ganglionic blockade and whole-body norepinephrine spillover demonstrate that the neurogenic component of AngII-salt HTN depends on the level of dietary salt.[74, 76, 178] A novel aspect of this study was our examination of the separate component of the AngII-salt model on PVN SK channel function. Our data demonstrates that SSNA, RSNA and ABP responses to PVN apamin were not significantly

different between rats with AngII-salt HTN and HS diet only, although the HS intake alone failed to increase ABP. These data suggest that perhaps dietary HS intake is a larger contributor to loss of SK channel function than circulating AngII. The attenuated SNA and MAP responses to PVN SK channel blockade in rats consuming only a HS diet indicate that SK channel dysfunction may be a primary contributor to the elevated sympathetic outflow in rats with AngII-salt HTN.

Despite a large body of epidemiological studies indicating that excess dietary salt is a primary contributor to essential HTN,[180-182] the effects of a HS diet alone on neuronal excitability in the PVN remains largely undetermined. HS intake alone is generally not sufficient to produce HTN in rats, however, it has been demonstrated that excess dietary salt has the ability to sensitize neural circuitry (pathways) within the sympathetic nervous system.[183-186] Microinjection of apamin into the PVN of rats fed a HS diet elicited attenuated ABP and SNA responses compared to control rats fed a NS diet (Fig. 2.3). This loss of SK channel function in the PVN of HS treated rats potentially primes the SNS through loss of spike frequency adaptation within pre-sympathetic PVN neurons. Our data is of considerable interest when taken into account with previous studies demonstrating augmentations in excitability of the SNS after HS treatment, including one very recent study indicating that HS diet alone contributes to exaggerated SNA and ABP responses to various excitatory stimuli.[187] The current study shows that a HS diet alone has the ability sensitize the neural circuitry in the PVN. The loss of SK channel function in the animals with HS intake provides a possible mechanism whereby a HS diet potentially alters membrane properties to influence the excitability of pre-sympathetic PVN neurons. The sensitization of the PVN in the current study, and the RVLM in previous studies, occurs in the absence of HTN and provides a potential mechanism that can cause exaggerated SNS responses that contribute to neurogenic HTN.

The effects of HS diet on neuronal membrane properties and excitability in cardiovascular control areas of the brain is of great interest and will require considerable attention in future studies.

In order to determine the role AngII may have in altering PVN SK channel function, we examined responses to PVN apamin in subcutaneous AngII infused rats on a NS diet. Both SSNA and RSNA responses to PVN SK channel blockade were attenuated compared to control rats with a NS diet, although SSNA did not demonstrate statistical significance compared to NS control group. In contrast, MAP responses to apamin were similar between the NS and AngII groups (Fig 2.3). AngII alone appears to have less of a role in SK channel dysfunction than dietary HS intake and PVN apamin elicited a differential response between SSNA and RSNA. This is of particular interest considering evidence indicating HS diet plays a larger role in the neurogenic component of AngII-salt HTN.[73, 75] Loss of SK channel function due to HS diet likely plays a dominant role in the development of the neurogenic phase of AngII-salt HTN. The mechanisms responsible for the different effect of PVN apamin on the SSNA and RSNA in AngII infused rats are not clear. The augmented sensory outflow from the circumventricular organs to the PVN due to systemic Ang II infusion may potentially target specific subpopulations of neurons leading to a differential SNA response to PVN SK channel blockade. Future studies are needed to investigate the mechanism for the differential between SNA and MAP responses to PVN apamin in rats with systemic administration of AngII.

We have demonstrated a loss of SK channel function in the PVN in AngII-salt HTN utilizing both *in vivo* (Fig. 2.3) and *in vitro* approaches;[144] however, our data also indicates that SK1-3 channel protein is not different between NS control and AngII-salt HTN groups (Fig. 2.5). This potentially suggests that down-regulation of SK channels in AngII-salt HTN are due to loss of function as opposed to a difference in the number of channels expressed within the pre-sympathetic PVN neurons.

In addition, studies examining other regions of central nervous system have demonstrated SK channel expression in astrocytes[188] and microglia,[189, 190] and punched PVN tissue would not differentiate between cell types. One recent study also has demonstrated no difference in SK channel expression level between Wistar-Kyoto and SHR supporting the notion that protein expression of SK channels is not altered in hypertensive rats[143] It also showed that PVN SK channel dysfunction in SHR involves altered casein kinase II (CK2) activity that disrupts the Ca^{2+}-calmodulin complex thereby reducing SK channel activity.[143] Interestingly, the present study demonstrates that PVN microinjection of the SK channel activator, CyPPA has no influence on SNA and ABP in AngII-salt HTN. CyPPA is known to significantly increase the Ca^{2+} sensitivity of SK channels[191] and our data indicate that disruption of intracellular Ca^{2+} dynamics less likely contribute to the down-regulation of SK channel activity in the PVN in this chronic disease model of AngII-salt HTN. The mechanism(s) responsible for the reduced activity of SK channel in the PVN in rats with AngII-salt HTN require further attention in future studies.

This is the first study to demonstrate PVN SK channel dysfunction in rats with AngII-salt HTN utilizing an *in vivo* whole animal design. While *in vivo* experimental designs preserve the substantial number of synaptic and reflex systems, potentially lost using *in vitro* preparations, there still remain limitations that must be recognized. The current study required the use of anesthesia, which has the ability to influence cardiovascular responses.[192] The effects of anesthesia on hemodynamic balance may potentially be reflected by the lack of HR differences in responses to PVN apamin among our treatment groups. Furthermore, there is a possibility that microinjected drugs spread outside the area of the PVN. To exclude this possibility, we examined the diffusion of Chicago blue dye microinjected at the end of the experiment and present a composite demonstrating the largest diffusion area. Our current data and a previously published report from our group indicate that the estimated diffusion area is confined close to the PVN.[111]

In summary, the present study suggests that reduced SK channel activity in the PVN contributes to Ang II-salt HTN. Interestingly, reduced function of SK channels was present in the HS treated group in the absence of hypertension. This indicates that SK channel dysfunction is more than likely not secondary to the development of hypertension. Lastly, in examining the individual contributions of systemic AngII treatment and dietary HS intake to reduce PVN SK channel activity, we demonstrate that dietary HS intake plays a larger role in PVN SK channel dysfunction compared to circulating AngII. This data supports available evidence suggesting that the neurogenic component of Ang II-salt HTN is primarily dependent on the level of dietary salt.

2.5 Perspectives

HTN is one of the main risk factors for the development of cardiovascular disease. As such, determination of the mechanisms responsible for the development, and maintenance of HTN are of great importance in identifying targets for possible intervention in disease progression. SK channels are unique, in that, blockade within the PVN elicits robust increases in SNA (~+250-300%) and ABP (~+30 mmHg); demonstrating their significant involvement in inhibiting the pre-sympathetic PVN neuronal excitability/activity [111]. The present study supports the notion that intrinsic cellular mechanisms may play a significant role in AngII-salt HTN. Restoration of SK channel function potentially provides a significant target for attenuating the activation of sympathetic nervous system in neurogenic HTN.

2.6 Acknowledgments

We gratefully acknowledge Mingjun Gu for excellent technical assistance. This study was funded by the American Heart Association 11SDG7420029 (ZYS) 10SDG2640130 (QHC) and National Institute of Health 1-R15-HL-122952 (QHC).

Chapter 3.

High Salt intake Augments Excitability of Pre-Sympathetic PVN Neurons through Dysfunction of Endoplasmic Reticulum Ca^{2+} Stores.[2]

3.1 Introduction

Elevated dietary salt intake is a major contributor to the pathogenesis of hypertension (HTN),[193, 194] and estimates suggest that 25% of normotensive and 50-60% of hypertensive individuals demonstrate salt-sensitivity.[195, 196] Dietary salt exerts influence through several systems including renal, vascular, and hormonal actions;[194] however, recent evidence indicates that the central nervous system (CNS) plays a prominent role in salt sensitive HTN through augmented sympathetic nerve activity (SNA).[72, 74] Despite a wide body of evidence demonstrating the adverse cardiovascular effects of salt-sensitivity, the mechanism(s) whereby dietary salt augments SNA have yet to be fully elucidated.

The hypothalamic paraventricular nucleus (PVN) is a prominent regulatory center for the sympathetic nervous system. Pre-sympathetic neurons in the PVN receive excitatory synaptic input from the forebrain circumventricular organs[98, 197] and project to the excitatory centers in the brain stem and spinal cord that drive SNA.[105] Studies have demonstrated that enhanced PVN neuronal activity supports the augmented SNA in several models of neurogenic HTN.[79, 121, 166]

Augmented PVN neuronal activity in neurogenic HTN can arise through a variety of synaptic mechanisms including loss of GABA inhibition[174] and augmented excitatory neurotransmitter signaling including glutamate and

[2] The material contained in this chapter has been submitted to *Circulation Research*. Copyright transfer agreement will become effective when accepted for publication.

angiotensin II.[171] Furthermore, alterations of intrinsic membrane properties that influence PVN neuronal excitability also play an important role in neurogenic HTN. Our lab[198] and others[143] have recently demonstrated that dysfunction of small conductance Ca^{2+}-activated K^+ (SK) channels contribute to neurogenic HTN. The endoplasmic reticulum (ER) serves as a Ca^{2+} store and Ca^{2+} release from the ER is a prominent activator of SK channels.

Recent reports indicate the brain ER stress is a mediator of neurogenic HTN, yet the mechanisms remain unclear.[154, 199, 200] We tested the hypothesis that inhibition of the ER Ca^{2+} store with thapsigargin (TG) would augment SNA in vivo and neuronal excitability in vitro. Additionally, we have previously demonstrated SK channel dysfunction and enhanced sympatheoexcitation in rats fed a 2% high salt (HS) diet;[198] therefore, we further examined whether HS diet influences ER Ca^{2+} store function. We hypothesized that HS intake would inhibit ER Ca^{2+} store function in pre-sympathetic PVN neurons, which may be an underlying mechanism to sympathoexcitation in salt-sensitive HTN. Portions of this data have been presented in abstract form.[201, 202]

3.2 Methods

3.2.1 Animals

Male Sprague-Dawley rats (n=61, 250-350g) purchased from Charles River Labs (Wilmington, MA) were housed in a temperature-controlled room (22-23C) with a 12:12 hour light-dark cycle. Tap water was available ad libitum. Animals in the normal salt (NS) treatment group received standard laboratory chow (0.4% NaCl) ad libitum for 4 weeks whereas the HS treatment group was fed a 2% NaCl diet ad libitum for 4 weeks. All experimental and surgical procedures were carried out under the guidelines of the National Institutes of Health *Guide for the Care and Use of Laboratory Animals* with the approval of the Institutional Animal Care and Use Committee of Michigan Technological University.

3.2.2 Microinjection Experiment Preparation

On the day of the experiment, rats were anesthetized with a mixture containing α–chlorolose (80 mg/kg) and urethane (800 mg/kg). Body temperature was maintained at 37°C with a water circulating pad. Catheters were implanted into the left femoral artery and vein in order to record arterial blood pressure (ABP) and administer drugs, respectively. Heart rate (HR) was obtained from the R-wave of the electrocardiogram (lead I). Rats were paralyzed with gallamine triethiodide, ventilated with O_2-rich room air, and end-tidal PCO_2 was monitored and maintained within normal limits (33-40 mmHg). Adequate depth of anesthesia was determined by lack of withdrawal reflex to noxious foot pinch prior to paralysis and absence of pressor response to noxious foot pinch following paralysis with supplemental doses of anesthesia equal to 10% of the initial dose given as needed. All animals were allowed to stabilize at least 2 h following surgery.

3.2.3 Recording of Sympathetic Nerve Activity (SNA)

Rats were prepared for recording of splanchnic (SSNA) and renal (RSNA) SNA according to protocols previously described.[111, 198] Briefly, a left flank incision was made and a left renal nerve and a postganglionic splanchnic nerve were separated from surrounding tissue. Nerve bundles were mounted on separate silver wire electrodes (-mm diameter, A-M Systems) and covered with silicon-based impression material (Coltene, Light Body). The signal was directed to an alternating current amplifier (P511, Grass Technologies) equipped with half-amplitude filters (band pass, 100-1,000 Hz) and a 60-Hz notch filter. The processed signal was rectified, integrated (10-ms time constant), and digitized at a frequency of 5,000 Hz using a 1401 Micro3 analog-to-digital converter and Spike 2 software (version 7.04, Cambridge Electronic Design, Cambridge, UK).

3.2.4 Paraventricular Nucleus (PVN) Microinjection

PVN microinjections were performed as previously described.[111, 198] Animals were placed in a stereotaxic head frame and the skull was leveled

between bregma and lambda. A small section of the skull was removed in order to expose the dura, and a single-barreled glass microinjector pipette was lowered vertically into the PVN. The stereotaxic coordinates used were as follows: 1.2 to 1.6 mm caudal to bregma, 0.5 mm lateral to midline, and 7.0 to 7.2 mm ventral to dura. After a 20-minute baseline period, thapsigargin (TG; 100nl), an inhibitor of the endoplasmic reticulum (ER) Ca^{2+} ATPase (Tocris), or vehicle (DMSO; 100nl) was injected bilaterally into the PVN. The micropipette was withdrawn between injections and bilateral injections were separated by 2 minutes. Variables were recorded for 2 hours following microinjection.

3.2.5 Retrograde Labeling

Five to 7 days prior to neuronal excitability recording, PVN neurons were retrogradely labeled from the ipsilateral rostral ventrolateral medulla (RVLM) as previously described.[142, 144] Briefly, rats were anesthetized with isoflurane (3% in O_2) and placed in a stereotaxic frame. The cerebellum was exposed through a small burr hole and a glass micropipette was lowered into the pressor region of the RVLM (coordinates: −12.7 mm caudal to bregma, 1.8 mm lateral to midline and 8.9 mm below the skull). A pneumatic pump was utilized to inject Flurospheres (150nl, Life Technologies) into the RVLM. Animals received daily subcutaneous injection of penicillin G (30,000 units) and meloxicam (1 mg/kg) for three days post-surgery. Tracer location was verified histologically post-mortem.

3.2.6 Electrophysiology

Five to seven days post-retrograde tracer injection, rats were anesthetized with isoflurane (3% in O_2) and decapitated. The brain was removed and chilled in ice-cold cutting solution containing (in mM): 206 sucrose, 2 KCl, 2 $MgSO_4$, 1.25 NaH_2PO_4, 26 $NaHCO_3$, 1 $CaCl_2$, 1 $MgCl_2$, 10 d-glucose, and 0.4 ascorbic acid, osmolarity 295-302 mosmol L^{-1} measured with an osmometer (Wescor), pH 7.3-7.4, continuously gassed with 95:5 CO_2:O_2 to maintain pH and pO_2. A brain block was cut including the PVN region and affixed to a vibrating microtome (Leica VT 1000S; Leica, Nussloch, Germany).

Coronal sections of 250 μm thickness were cut, and the slices transferred to a holding container of artificial cerebral spinal fluid (ACSF) maintained at 30 °C, continuously gassed with 95:5 CO_2:O_2, containing (in mM): 125 NaCl, 2 KCl, 2 $MgSO_4$, 1.25 NaH_2PO_4, 26 $NaHCO_3$, 2 $CaCl_2$, 10 d-glucose, and 0.4 ascorbic acid (osmolality: 295–302 mosmol L^{-1}; pH 7.3-7.4) and allowed to recover for 1 hr. Following recovery, slices were transferred to a glass-bottomed recording chamber and viewed through an upright microscope (E600FN, Nikon) equipped with DIC optics, epi-fluorescence, an infrared (IR) filter and an IR-sensitive video camera (C2400, Hamamatsu, Bridgewater, NJ). Patch electrodes were pulled from borosilicate glass capillaries and polished to a tip resistance of 4–8 MΩ. Electrodes were filled with a solution containing (in mM) 135 K-gluconate, 10 HEPES, 0.1 EGTA, 1.0 $MgCl_2$, 1.0 NaCl, 2.0 Na_2ATP, and 0.5 Na_2GTP (osmolality: 280–285 mosmol L^{-1}; pH 7.3). Upon achievement of a gigaohm seal and whole cell configuration, cell capacitance, access resistance and resting membrane potential (V_m) were monitored to ensure stability. Cells that met the following criteria were included in data set: Action potential amplitude ≥ 50mV from threshold to the peak, input resistance ($R_{input)}$ larger than 0.5 GΩ when hyperpolarizing current injections of -20pA were delivered from a holding potential of -80mV, resting V_m negative to -50mV, and less than 20% change in series resistance during recording.

3.2.7 Testing Neuronal Excitability

Neuronal excitability from NS and HS rats was studied in current-clamp mode. V_m was adjusted to -80mV by injecting continuous negative current, and a series of square-wave current injections was delivered in increments of +25 pA, for a duration of 800 ms each. To determine action potential voltage threshold (V_t) and depolarizing R_{input} below V_t, ramp current injections (0.2 pA ms^{-1}, 1,000 ms) were made from a potential of -80 mV. Effects of ER Ca^{2+} store inhibition with TG on neuronal excitability were determined by comparing current evoked V_m and spike frequency responses under control conditions, and

following bath application of TG. Responses were recorded from separate groups of NS and HS PVN-RVLM neurons.

3.2.8 Western Blot measurements of SERCA Protein

Western blot measurements for SERCA1, SERCA2 and SERCA3 channel protein were performed as previously described.[111] Briefly, PVN from adult male rats (n=8 for the 0.4% NaCl control group, n = 8 for the 2% NaCl group) were removed and quickly frozen on dry ice. Frozen PVN tissue (100 mg) was homogenized in 400 µl of buffer (50 mM Tris base, 1.0 mM EDTA, 150 mM NaCl, 0.1% SDS, 1% Triton X-100, 1% sodium deoxycholate, and 1 mM PMSF, pH 7.4, Sigma) complete with protease inhibitors (0.1 mM leupeptin and 0.3 mM PMSF, Sigma) and stirred for 30 min at 4°C. A centrifugal spin with 12,000 rpm at 4°C was performed for 5 min. The supernatant was collected, and the protein concentration was determined in triplicate by a Bio-Rad DC protein assay kit at absorbance of 750 nm using BSA as a standard. Aliquots were stored at -80°C until analyzed, at which time the protein was separated using a SDS-polyacrylamide gel (10%) with electrophoresis followed by the electrophoretic transfer of proteins from the gel to a nitrocellulose membrane (Bio-Rad). Membranes were blocked with 5% nonfat milk for 1 h at room temperature, washed three times, and probed with the following primary antibodies: Goat anti-SERCA1 goat anti-SERCA2 antibody, or goat anti-SERCA3 antibody (Santa Cruz Biotechnology) or with mouse anti-β Actin overnight at 4°C. After three 10-min washes in Trisbuffered saline-0.05% Tween 20, membranes were incubated with donkey anti-goat horseradish peroxidase-conjugated IgG or goat anti-mouse horseradish peroxidase-conjugated IgG secondary antibodies (Santa Cruz Biotechnology) for 1 h at room temperature and then detected with enhanced chemiluminescence.

3.2.9 Chemicals

All chemicals were obtained from Sigma-Aldrich (St Louis, MO) except for TTX (Tocris), TEA (Company), and TG (Tocris).

3.2.10 Data Analysis

Summary data are expressed as mean ± SE. SSNA and RSNA were determined as an average of the rectified, integrated signal. Baseline values were obtained by averaging a 10-min window of data immediately prior to PVN microinjection. Responses to PVN microinjection were obtained by averaging a 2-min segment centered on the maximal response quantified after subtraction of background noise obtained following bolus injection of the ganglionic blocker hexamethonium (30 mg/kg, IV). Data were analyzed by one-way ANOVA and unpaired t-test where appropriate. Post hoc analysis was performed with Newman-Keuls multiple-comparison test. Differences were considered statistically significant at a critical value of $P < 0.05$.

3.3 Results

3.3.1 Depletion of PVN ER Ca^{2+} stores Augments SNA and ABP

In order to determine the contribution of the PVN neuronal ER Ca^{2+} stores in regulating SNA and ABP, we performed bilateral microinjection of TG into the PVN. PVN microinjection of TG elicited robust increases in SNA and ABP demonstrated in the raw trace data in Figure 3.1. Maximum increases in SSNA, RSNA and mean arterial pressure (MAP) elicited by PVN TG (0.75 nmol/100nl; n=6) were 92±6% ($P<0.05$ vs. vehicle), 72±6% ($P<0.05$ vs. vehicle), and 10±2mmHg ($P<0.05$ vs. vehicle), respectively as shown in Figure 3.2. Microinjection of TG (0.15nmol, n=4; 0.3nmol, n=5; 0.75nmol, n=6; 1.5nmol n=5) augmented SSNA, RSNA, and ABP in a dose dependent manner whereas bilateral microinjection of vehicle (DMSO, 100nL) into the PVN failed to elicit any significant response ($P>0.05$ vs baseline) in SNA, ABP or HR (Figs. 3.1 and 3.2). There were no significant differences in HR between any TG treatment dose and vehicle control (Fig. 3.2). Bilateral microinjection of TG (0.75nmol, 100nl) outside of the PVN (~2.5mm lateral to midline) failed to produce any significant change in SSNA (10.5±8.1%), RSNA (4.4±7.1%) or ABP (1±1 mmHg) respectively, indicating that the effects of TG appear to be site specific (Table 3.1). In addition, the maximally effective dose of TG was injected into

the femoral vein in order to exclude the possible influence of peripheral actions. IV administration of TG had no significant effect on resting SSNA, RSNA, MAP and HR (Table 3.1).

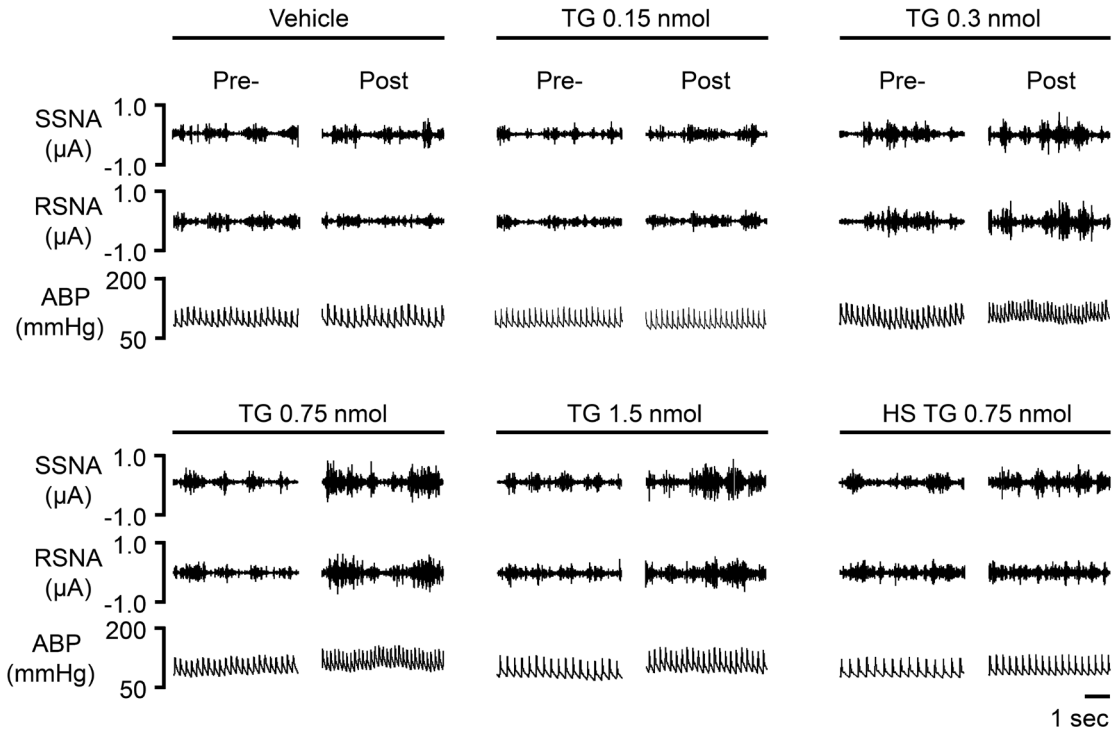

Figure 3.1 Representative raw tracings of splanchnic sympathetic nerve activity (SSNA), renal sympathetic nerve activity (RSNA) and arterial blood pressure (ABP) in response to paraventricular nucleus (PVN) microinjection of graded doses (vehicle, 0.15, 0.30, 0.75, 1.5 nmol) of the ER Ca^{2+} ATPase inhibitor thapsigargin (TG); HS-high salt diet (2%).

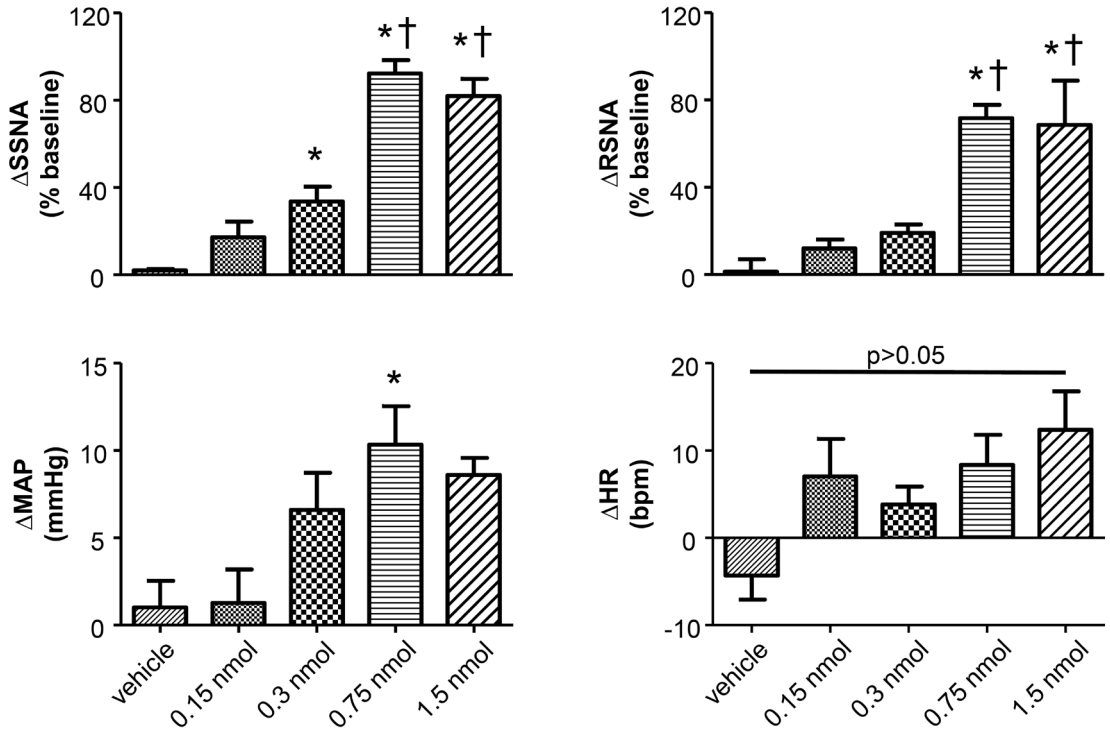

Figure 3.2 Summary data showing changes in SSNA, RSNA, mean arterial pressure (MAP), and heart rate (HR) in response to bilateral microinjections of varying doses of TG (vehicle, 0.15nmol, 0.3nmol, 0.75nmol, and 1.5nmol) into the PVN. Graded concentrations of TG elicited a dose-dependent increase in recorded variables. *P<0.05 vs. vehicle; †P<0.05 vs. 0.3nmol.

Table 3.1 Effects of control injections on MAP, HR, SSNA, and RSNA in NS control rats.

Injected Compound	n	MAP, mmHg		HR, beats/min		SSNA, μV		RSNA, μV	
		Pre	Post	Pre	Post	Pre	Post	Pre	Post
DMSO, PVN	3	111 ± 7	112 ± 6	352 ± 35	348 ± 34	0.03 ± 0.001	0.03 ± 0.005	0.02 ± 0.003	0.02 ± 0.004
Anatomy Control (TG out of PVN)	5	111 ± 6	112 ± 6	337 ± 19	334 ± 22	0.02 ± 0.002	0.02 ± 0.002	0.04 ± 0.008	0.02 ± 0.007
TG, Intravenous	4	111 ± 8	107 ± 10	343 ± 23	344 ± 21	0.03 ± 0.003	0.02 ± 0.003	0.04 ± 0.009	0.02 ± 0.01

Values are mean ± SE; n = number of rats; SSNA, splanchnic sympathetic nerve activity; RSNA, renal sympathetic nerve activity; MAP, mean arterial pressure; HR, heart rate; TG, thapsigargin; PVN, paraventricular nucleus.

3.3.2 HS Diet Disrupts PVN ER Ca^{2+} Store Function Contributing to Sympathoexcitation

A major goal of this study was to determine whether disruption of ER Ca^{2+} store function contributes to sympathoexcitation. Figure 3.3 *left* demonstrates representative raw tracings before, and after bilateral microinjection of TG from the NS treatment group. Figure 3.3, *right*, demonstrates a representative response to bilateral PVN microinjection of TG (0.75nmol, 100nl) from the HS treatment group with a significantly attenuated response compared to NS. Microinjection of 0.75nmol TG was utilized for comparison, as it was the minimum dose to elicit a maximum response in control rats (Fig. 3.1 & 3.2). Maximum increases in SSNA (33±6%) and RSNA (26±5%), were significantly attenuated compared to NS ($P<0.05$ NS vs. HS) as demonstrated by summary data in Figure 3.4. There were no significant differences in MAP (7±2 mmHg) and HR (5±3 bpm) between NS and HS treatment groups (Fig. 3.4).

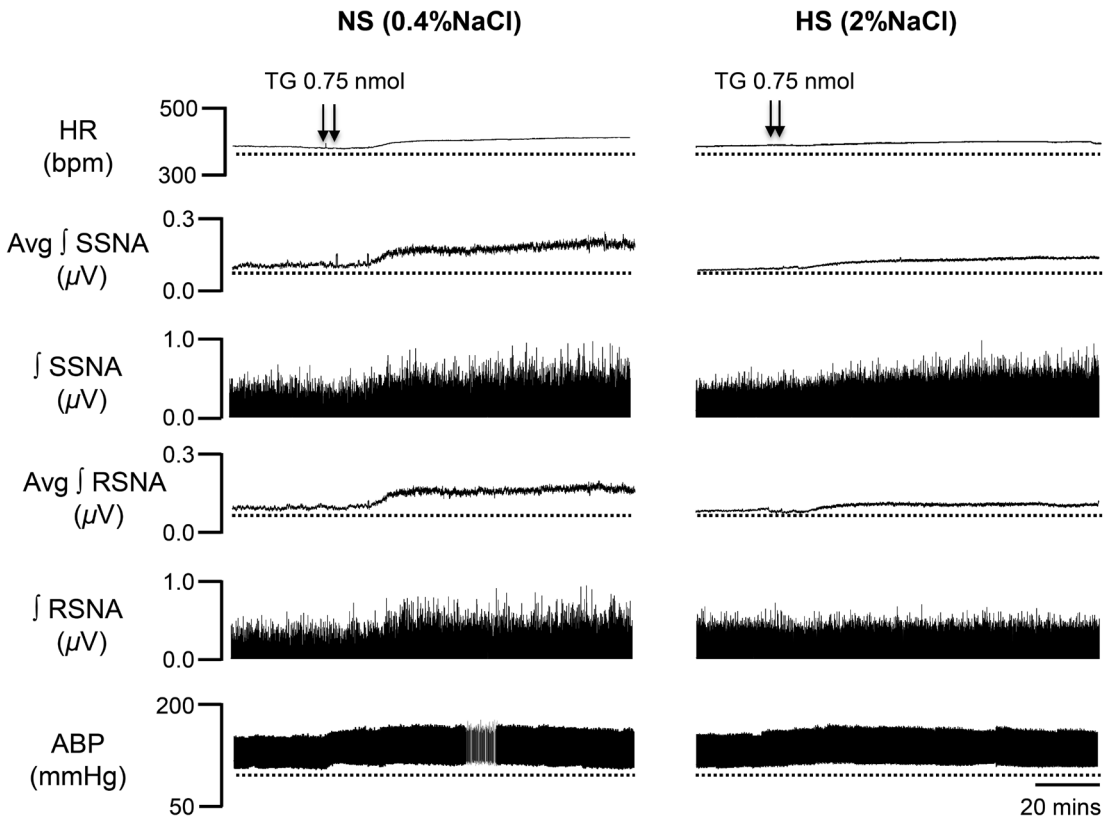

Figure 3.3 Representative traces showing HR, SSNA, RSNA, and ABP responses to bilateral PVN microinjection of TG (0.75nmol) in a rat on a 0.4% normal salt (NS) diet (*left),* and a 2% high salt (HS) (*right*). Bilateral PVN microinjection (100 nl each) of TG (arrowheads) markedly increased HR, SSNA, RSNA and ABP in a NS diet rat, whereas responses were attenuated in a rat fed a HS diet. Avg, average; ∫, integrated.

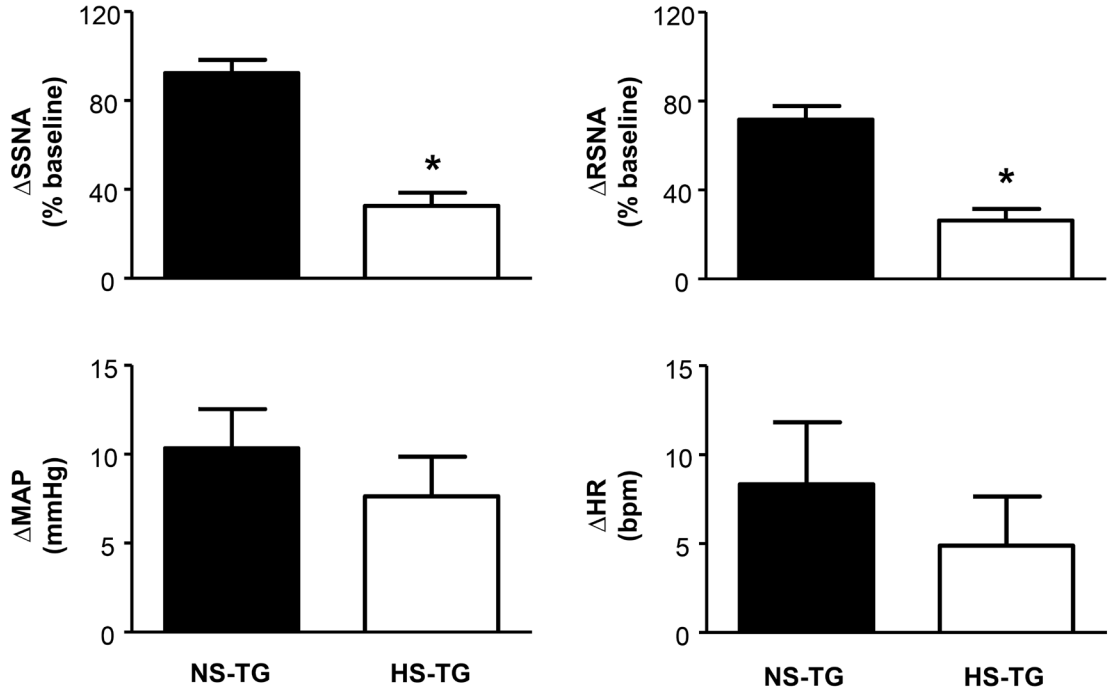

Figure 3.4 Summary data showing peak changes in SSNA, RSNA, MAP and HR after bilateral PVN microinjection of TG (0.75nmol) in normal salt (NS) and high salt (HS) rats. Note that SSNA and RSNA responses to PVN TG were significantly attenuated in HS rats compared to NS. *P<0.05 HS vs. NS.

3.3.3 HS Diet Disrupts ER Ca^{2+} Store Function Contributing to Augmented Excitability of PVN-RVLM Neurons

Similar to previous reports, PVN-RVLM neurons lacked spontaneous discharge at resting Vm;[142, 144] however, depolarizing current injections consistently evoked repetitive action potential firing. The role of the ER Ca^{2+} store in regulating excitability of PVN-RVLM neurons was examined by comparing the relationship between graded current injections and the evoked discharge in the absence and presence of TG (0.5 M). Figure 3.5A shows representative discharge responses to a 200pA depolarizing current pulse in the absence (*top*) and presence of the ER Ca^{2+} ATPase inhibitor, TG (*bottom*). Under control conditions, firing frequency in response to a 200pA current injection in neurons from NS rats (n=8, 22±2 Hz) was significantly lower than HS (n=7, 37±4 Hz, P<0.05 vs. NS control) (Fig. 3.5B & C, *left* vs. *right*).

Interestingly, inhibition of the ER Ca^{2+} store via bath application of TG significantly augmented firing frequency in the NS group (n=6, 30±4 Hz, P<0.05 vs. NS control), but not HS (n= 6, 32±6 Hz, P>0.05 vs HS control) (Fig. 3.5C & D). Furthermore, the slope of firing frequency in response to graded current injection was significantly greater in HS neurons (0.16±0.01, P<0.05 vs. NS control) compared to NS group (0.10±0.01) (Fig 5C & D). Bath application of TG significantly increased the slope of firing frequency in response to graded current injections in NS group (0.14±0.01, P<0.05 vs NS control), yet had no significant effects on HS neurons (0.15±0.01, P>0.05 vs HS control) (Fig 3.5C & D).

3.3.4 HS Disruption of ER Ca^{2+} Store Reduces Spike-Frequency Adaptation in PVN-RVLM Neurons

We have previously demonstrated that loss of SK channel function in AngII-salt HTN augments excitability of PVN-RVLM neurons through loss of spike-frequency adaptation (SFA).[144] Additionally, we recently reported SK channel dysfunction due to 2% HS diet treatment.[198] Therefore, we examined whether the increased excitability of PVN-RVLM neurons due to ER Ca^{2+} store dysfunction was associated with a decrease in SFA. Figure 3.6 Illustrates the slope of the inter-spike interval (ISI)-ISI number curve over trains of action potentials in response to a 200pA current injection in PVN-RVLM neurons from NS (*left*) and HS (*right*) rats. The slope of the linear fit of the ISI-ISI number curve was significantly (P<0.05) greater in NS (2.2±0.2, P<0.05 vs. HS) compared to HS (1.5±0.1) indicating that spike-frequency adaptation is reduced in HS neurons under control conditions (Fig. 3.6B). Additionally, TG significantly decreased the slope of ISI-ISI number curve in NS (1.1±0.1, P<0.05 vs. NS control) group indicating that inhibition of the ER Ca^{2+} store reduces spike-frequency adaptation (Fig. 3.6B, *left*). Interestingly, slope was unchanged in the HS group (1.3±0.1, P>0.05 vs. control) following application of TG (Fig. 3.6B, *right*). Bath application of TG (0.5 M) had no significant effects on any passive membrane properties (Table 3.2).

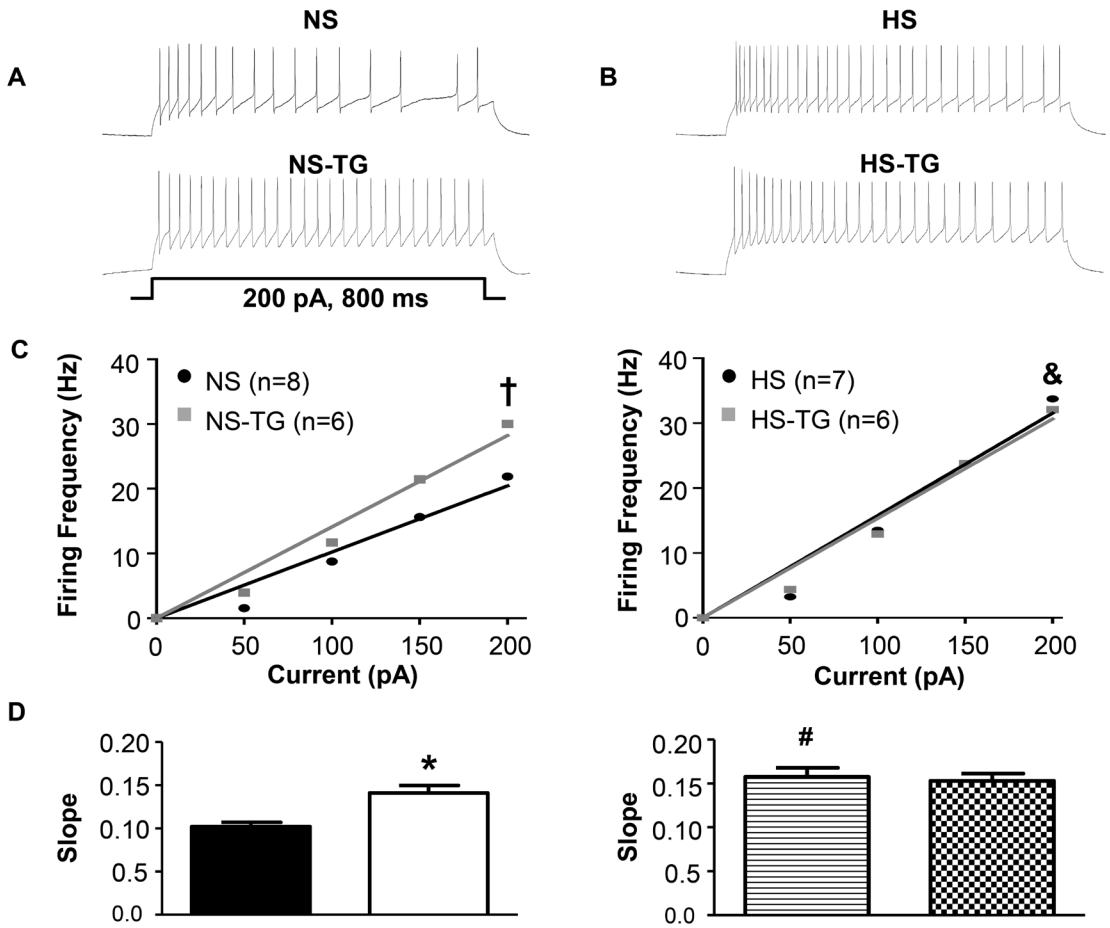

Figure 3.5 Effects of ER Ca^{2+} store inhibition with TG on excitability of PVN-RVLM neurons from NS *left* and HS *right* rats. **A.** Voltage traces illustrating neuronal excitability in response to a 200pA current injection in PVN-RVLM neurons from NS rats in the absence (*top*, control) and presence (*bottom*) of the ER Ca^{2+} ATPase inhibitor TG. **B**. Representative responses of PVN-RVLM neurons from HS rats to 200pA current injection in the absence (*top*) and presence (*bottom*) of TG. **C.** Linear response demonstrating the slope of firing frequency in response to graded current injection (0-200pA) in PVN-RVLM neurons in the absence and presence of TG in NS (*left*) and HS (*right*) neurons. TG increased firing frequency in the NS group, but not HS. Note that firing frequency in response to 200pA depolarizing current injection was increased in HS (*right*) compared to NS (*left*). **D.** Summary data showing slope of firing frequency in response to graded current injection before and after bath application of TG in NS (*left*) and HS (*right*) rats. Inhibition of the ER Ca^{2+} store with TG augmented the slope in NS (*left*), but not HS (*right*) neurons. Note that in control conditions, the slope was significantly greater in HS neurons. NS-normal salt; HS-high salt; TG-thapsigargin. †P<0.05 NS vs. NS –TG; &P<0.05 NS vs. HS; *P<0.05 NS vs. NS-TG; #p<0.05 NS vs. HS.

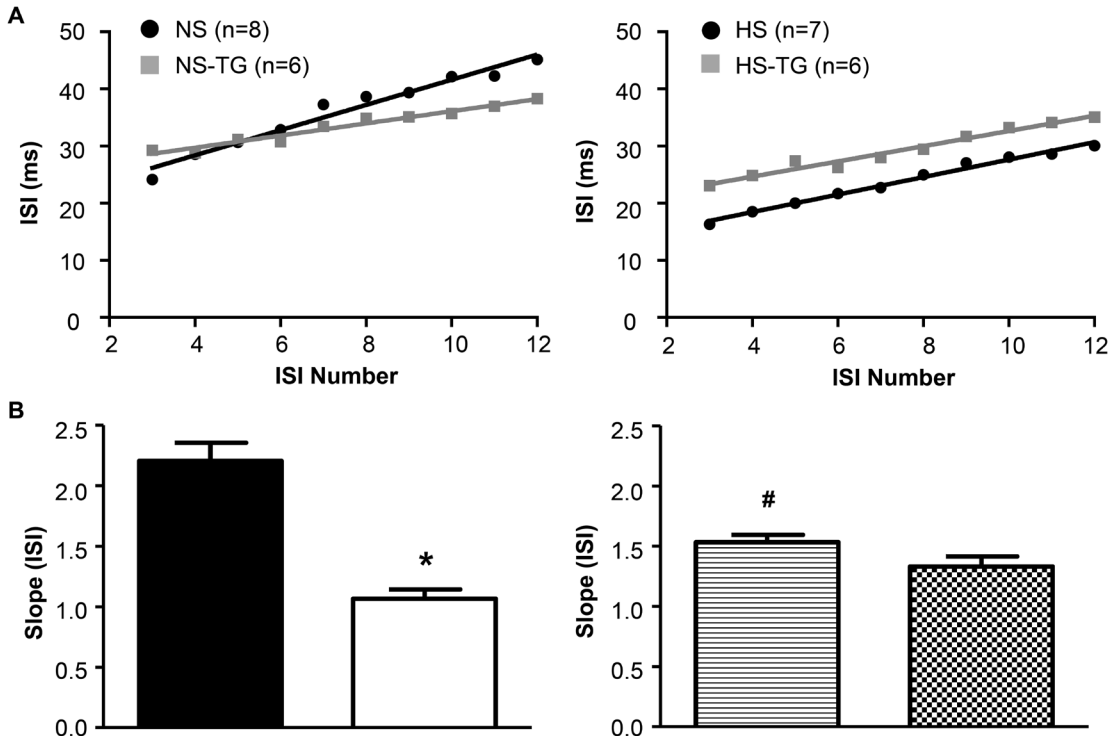

Figure 3.6 Effects of ER Ca^{2+} store inhibition with TG on spike-frequency adaptation in PVN-RVLM neurons. **A.** Linear response of inter-spike interval (ISI)-ISI number over trains of action potentials in response to 200pA current injection in PVN-RVLM neurons from NS l*eft* and HS *right* treatment groups before and after bath application of TG. **B**. Summary data showing slope of the ISI-ISI number response to 200pA current injection was diminished in HS rats compared to NS revealing greater spike frequency adaptation in NS neurons. TG attenuated the slope of ISI in NS (*left*), but not HS (*right*) neurons. NS-normal salt; HS-high salt; TG-thapsigargin. *P<0.05 NS vs. NS-TG; #p<0.05 NS vs. HS.

Table 3.2 Passive membrane properties of PVN-RVLM neurons.

Group	n	V_m (mV)	C_m (pF)	R_{input} (GΩ)	V_t (mV)
NS	8	-58.8 ± 2.2	52.8 ± 3.7	0.62 ± 0.03	-41.7 ± 1.9
NS TG	6	-58.5 ± 2.6	39.7 ± 4.8	0.78 ± 0.14	-43.7 ± 1.3
HS	7	-52.4 ± 2.2	39.7 ± 4.5	0.76 ± 0.08	-39.8 ± 1.1
HS TG	6	-58.0 ± 2.6	47.5 ± 6.6	0.70 ± 0.10	-36.7 ± 2.3

Values are mean ± SE, n = number of neurons, V_m, resting membrane potential; C_m, membrane capacitance; R_{input}, depolarizing input resistance; V_t, sub-threshold of membrane potential to fire action potential.

3.3.5 Comparison of PVN SERCA Protein Expression

In order to further explore potential mechanisms for ER Ca^{2+} store dysfunction due to HS diet, we compared protein expression (Western blot analysis) of SERCA1-3 in the hypothalamic PVN between rats on a NS diet (0.4% NaCl, n=8) for 4 weeks, or a HS salt diet (2% NaCl, n=8) for 4 weeks. Contrary to our hypothesis, expression of SERCA1 was significantly increased by a HS diet (Fig. 3.7). SERCA2 expression tended to be increased by HS diet; however, the difference did not reach statistical significance. SERCA3 was not detected in the PVN (data not showed here).

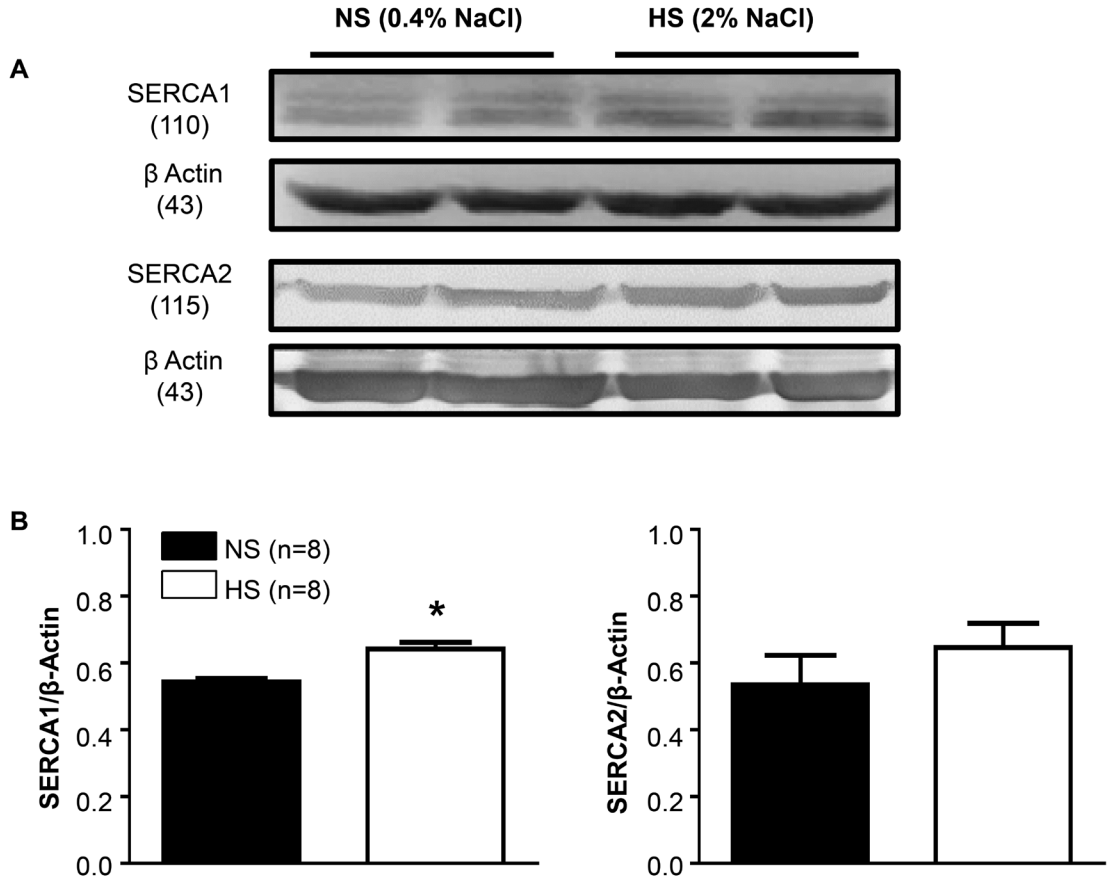

Figure 3.7 Expression of SERCA1 and SERCA2 in the PVN. **A:** Western blot analysis showing protein expression of SERCA1 and SERCA2 in PVN in animals with either NS (0.4% NaCl) control or HS (2% NaCl) group. **B:** Summary data showing HS intake significantly increased protein expression of SERCA1 in the PVN. SERCA2 levels tended to be increased, but the difference did not demonstrate statistical significance. All values were normalized to β actin. *P<0.05 vs. NS control.

3.3.6 Histology

Injection sites were marked with 2% Chicago blue dye (100nl). Coronal slices through the rostral caudal plane encompassing the PVN were examined to ensure microinjections were confined to the PVN as previously described by our laboratory.[198] Figure 3.8 shows the composite diffusion area of injected dye compiled by overlying brain slices from separate rats to demonstrate the outermost diffusion area. Distribution of injected dye was largely confined to the area encompassing the PVN.

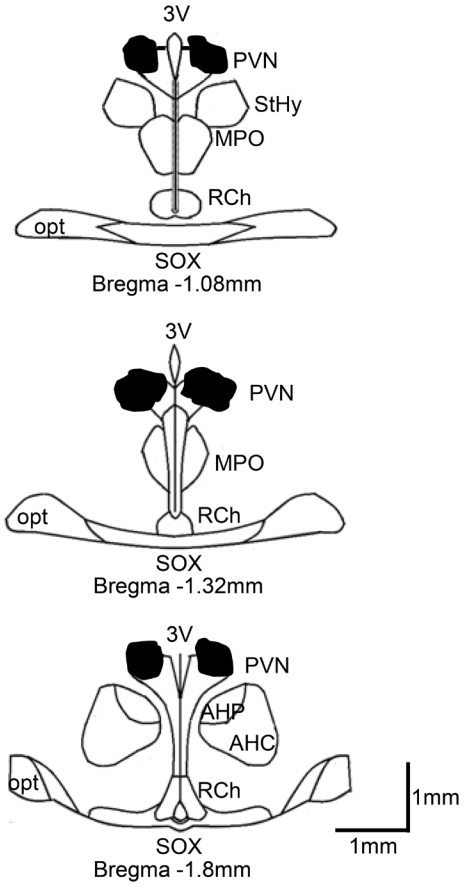

Figure 3.8 Schematic drawings of coronal sections throughout the rat hypothalamus. A: Shaded area indicates spread of injected dye used to mark the injection sites in the bilateral PVN. The shape of each area was determined by overlaying tracings of the outermost diffusion area of injected dye (100 nl) through the rostral-caudal plane of the PVN. AH, anterior hypothalamic area; 3V, third cerebral ventricle; RCh, retrochiasmatic area; MPO, medial preoptic nucleus; opt, optic tract; SOX, supraopticdecussation; StHy, striohypothalamic nucleus.

3.4 Discussion

The PVN is a key regulatory center for SNA, and disinhibition of PVN neurons contributes to the augmented sympathetic outflow in neurogenic HTN. Here, we demonstrate the importance of PVN ER Ca^{2+} store function in regulating SNA and ABP in vivo, and neuronal excitability in vitro. Bilateral PVN microinjection of TG, the ER Ca^{2+}ATPase inhibitor known to deplete the ER Ca^{2+} store,[203] augmented SSNA, RSNA and MAP in a dose-dependent manner demonstrating that the ER Ca^{2+} store plays a significant role in modulating SNA and ABP. Interestingly, sympathoexcitatory responses to PVN TG were significantly blunted in rats fed a 2% HS diet for 4 weeks indicating dysfunction of the ER Ca^{2+} store. Importantly, we also demonstrate augmented neuronal excitability in PVN neurons with axon projections to the RVLM (PVN-RVLM) in rats fed a HS diet. Bath application of TG significantly augmented excitability of PVN-RVLM neurons in rats with a NS diet yet had no significant effect in animals with a HS diet. These results indicate that loss of ER Ca^{2+} store function likely plays a role in the augmented neuronal excitability due to chronic HS intake. Finally, PVN protein expression of SERCA1 and SERCA2 were upregulated in HS rats, which suggests that compensatory mechanisms have been evoked to oppose the dysfunction of ER Ca^{2+} stores in response to chronic HS intake. Therefore, we conclude that dysfunction of the ER Ca^{2+} store in pre-sympathetic PVN neurons represents a novel mechanism contributing to sympathoexcitation evoked by HS intake.

The sympathetic nervous system plays a prominent role in the pathogenesis and maintenance of salt-sensitive HTN.[204] HTN induced by chronic infusion of AngII combined with a 2% HS diet (AngII-salt) is a well-established animal model of salt-sensitive HTN.[72] Previous studies using chronic protocols have established that sympathetic activation is largely responsible for HTN in this model.[73, 76, 77, 205] Furthermore, the neurogenic aspect of the AngII-salt model is primarily mediated by dietary salt.[74, 75] Our lab has recently demonstrated that dysfunction of SK channels in the PVN

contributes to sympathoexcitation in AngII-salt HTN using both in vivo and in vitro approach.[144, 198] Interestingly, we showed that SK channel dysfunction is present in normotensive rats fed a 2% HS diet.[198] Importantly, in the present study, we demonstrate that excitability of PVN-RVLM neurons is augmented by 2% HS diet. Taken together with previous results, our current data indicate that HS-induced augmented excitability of pre-sympathetic PVN neurons in not secondary to the development of HTN and likely represents an important primary mechanism contributing to sympathoexcitation induced by HS intake.

Enhanced neuronal activity among PVN neurons has been noted in a variety of cardiovascular diseases characterized by high sympathetic outflow including heart failure and HTN.[121, 165] Recently, Bardgett et al demonstrated that acute inhibition of the PVN via microinjection muscimol significantly attenuated SNA and MAP in AngII-salt HTN. This provides strong evidence that PVN neuronal activity is required to maintain the augmented sympathetic outflow and blood pressure in this model of neurogenic HTN.[79] Less is known about the cellular mechanisms that are responsible for the augmented PVN neuronal activity in neurogenic HTN. The present study is the first to demonstrate the importance of ER Ca^{2+} stores in regulating PVN neuronal activity/excitability.

Depletion of ER Ca^{2+} store via bilateral microinjection of TG, an inhibitor of the ER Ca^{2+} ATPase, significantly augmented SSNA, RSNA and MAP. Importantly this response demonstrated dose dependence helping to rule out non-specific drug actions that potentially contribute to sympathoexcitation. Additionally we performed control experiments by delivering TG via IV catheter, and microinjection outside the PVN (2.5mm lateral to midline) in separate experiments. Neither of these two control deliveries resulted in a significant change in SNA or ABP, which further demonstrates that action of the drug in our acute experimental model likely depends on actions within the PVN. Furthermore, spread of injected dye (100nl) following experiments was largely confined to the PVN. PVN neurons influence sympathetic activity through axon projections to the prominent autonomic control centers such as the RVLM, the

spinal IML and the nucleus tractus solitarri.[105, 179] Sympathoexcitatory responses to PVN TG are likely mediated through these projections to significantly influence ongoing levels of SNA.

In order to further investigate the underlying cellular mechanisms of ER Ca^{2+} stores in the PVN in regulating SNA and ABP, we utilized whole-cell current clamp to examine excitability of pre-sympathetic PVN-RVLM neurons identified by retrograde labelling under brain slice preparation. Inhibition of the ER Ca^{2+} store via bath application of TG augmented excitability of PVN-RVLM neurons (Fig. 3.5). TG is an inhibitor of the ER Ca^{2+} ATPase which pumps Ca^{2+} into the ER to maintain high Ca^{2+} levels within the ER and preserves intra-neuronal Ca^{2+} homeostasis.[203] Therefore, inhibition of the ER Ca^{2+} ATPase by TG would eventually result in a depletion of the ER Ca^{2+} store which likely contributes to the dysfunction of Ca^{2+} activated K^+ channels including SK channels and augmented neuronal excitability.[158] This possibility is supported by our previous report showing that Ca^{2+} free bath application significantly diminished SK currents and blockade of SK channels increased excitability among PVN-RVLM neurons.[142] Our recent findings showing that Ca^{2+} chelators BAPTA and EGTA, significantly increased both in vivo SNA and in vitro neuronal excitability of PVN-RVLM neurons also support this possibility.[206] Moreover, the present study demonstrates that TG inhibits spike frequency adaptation (SFA) among PVN-RVLM neurons contributing to increased excitability (Fig. 3.6), which lends further support to the possibility since we previously reported that reductions in SFA contribute to the increased excitability of PVN-RVLM neurons following SK channel blockade. [142] Whether reduced SK current underlie the mechanisms of TG elicited increases in excitability of PVN-RVLM neurons remains further study in the future.

The ER is an important regulator of intracellular Ca^{2+} hemostasis. Here, we also present a novel mechanism whereby HS diet disrupts ER Ca^{2+} stores in the pre-sympathetic PVN neurons. SSNA, RSNA and MAP responses to PVN microinjection of TG were significantly attenuated in HS rats indicating that Ca^{2+} store function is altered by HS treatment. In order to further explore

mechanisms whereby HS diet contributes to augmented activity/excitability of PVN neurons, we examined PVN-RVLM neurons with whole-cell patch clamp techniques. Interesting, we found that firing frequency in response to a 200pA current injection is significantly augmented in HS neurons. Additionally, the slope of the linear response to graded current injections is significantly augmented in HS neurons. We have previously reported that excitability of PVN-RVLM neurons is augmented in AngII-salt HTN[144] and results from the present study further indicate that excitability of PVN-RVLM neurons is augmented by HS diet alone in the absence of HTN. Interestingly, bath application of TG had no significant effect on either firing frequency in response to 200pA current injection, or the slope of firing frequency in response to graded current injection in HS rats indicating that dysfunction of the ER Ca^{2+} store likely contributes to the augmented PVN neuronal excitability in HS rats. In order to explore possible mechanisms for the augmented excitability of PVN-RVLM neurons due to HS intake, we compared SFA in NS and HS neurons. SFA was significantly attenuated in HS neurons indicated by a reduction in the slope of ISI-ISI number curve and bath application of TG did not significantly alter SFA in HS neurons. SK channel is Ca^{2+} dependent and a primary mediator of SFA.[141, 207] Therefore, we expect that the reduced SFA in HS neurons could be due to reduced SK channel activation through diminished ER Ca^{2+} signaling.

SERCA2 is ubiquitously expressed throughout the CNS, whereas SERCA3 has only demonstrated expression in Purkinje fibers of cerebellum; however, little is known regarding SERCA1 expression in the CNS.[208, 209] The present study has demonstrated a disruption of ER Ca^{2+} stores in the PVN in animals with a HS diet using both in vivo and in vitro approaches. Initially, we have hypothesized that a down-regulation of SERCA1-2 might contribute to the dysfunction of ER Ca^{2+} stores. Surprisingly, our data indicates that protein expression of SERCA1 is significantly augmented and SERCA2 levels tended to be increased in punched PVN tissue from HS rats (Fig. 3.7). Our data demonstrating altered ER Ca^{2+} regulation in response to HS Diet indicates dysfunction of the ER Ca^{2+} ATPase and we speculate that the augmented

SERCA1-2 expression may be a compensatory mechanism to maintain ER Ca^{2+} homeostasis. SERCA function and expression remains largely to be explored in the CNS and we are the first to report the expression of SERCA1-2 protein in the PVN.

SERCA pumps are widely expressed throughout the body, but little is known regarding altered expression levels in the CNS due to pathological conditions. Studies in cardiomyocytes indicate that catecholamines increase SERCA2 expression.[210, 211] further studies in cardiomyocytes demonstrate that SERCA2 expression can be augmented through the anti-apoptotic protein, Bcl-2.[212] SERCA pumps are highly conserved throughout a variety of cell types and future studies are needed to examine if a similar protective mechanism exists in PVN neurons due to HS intake. It's also important to note that punched PVN tissue contains both magnocellular and parvocellular neurons, as well as astrocytes and glial cells. Therefore, we are cautious in our interpretation of the data since the diverse population of neural cells in the PVN that may have functions and projections that have no influence on sympathetic outflow.

In the current study, we have examined ER Ca^{2+} store function through inhibition of ER Ca^{2+} uptake with TG, an inhibitor of the ER Ca^{2+} ATPase. Future investigation is required to determine if alterations in release of ER Ca^{2+} contributes to augmented neuronal excitability due to HS diet. Release of ER Ca^{2+} is primarily mediated through two distinct types of ligand gated Ca^{2+} channels including the inositol 1,4,5-triphosphate receptor (InsP3R) and the ryanodine receptor (RyR). Release of ER Ca^{2+} through the InsP3R is activated primarily through synaptic activity whereas RyR activation occurs primarily through Ca^{2+} induced Ca^{2+} release (CICR).[156] During trains of action potentials, Ca^{2+} entry through voltage dependent Ca^{2+} channels (VDCCs) stimulates CICR from RYR, resulting in a significant elevation of cytoplasmic Ca^{2+}.[158] CICR during action potentials is a key activator of SK channels, and therefore, can significantly influence neuronal excitability.[207] Whether HS diet induces alterations in ER Ca^{2+} release in the pre-sympathetic PVN remains to be determined.

3.5 Perspectives

HTN is a major risk factor for cardiovascular disease and the majority of cases demonstrate sensitivity to dietary salt. While salt-sensitive HTN depends on complex interactions involving multiple body systems including renal and vascular, recent studies have demonstrated the importance of the SNS. Due to the prevalence of essential HTN, identification of new treatment targets is imperative to the overall health of society. The present study identifies a novel mechanism whereby disruption of Ca^{2+} homeostasis in the ER contributes to enhanced sympathoexcitation and augmented neuronal excitability due to HS diet. In the present study, PVN microinjection of TG augmented SNA and ABP in vivo, and neuronal excitability in vitro demonstrating the contribution of the ER in regulating sympathetic outflow. In contrast, sympathoexcitatory responses to PVN TG were significantly attenuated in HS rats and bath application of TG had no significant influence on excitability of PVN-RVLM neurons indicting dysfunction of the ER Ca^{2+} store. The ER is a new and novel treatment target due to its involvement in a multitude of cellular process and we are only beginning to understand the role it plays in mediating neuronal excitability and sympathetic activation. Future studies are needed to elucidate the molecular mechanisms that underlie HS diet induced ER dysfunction.

3.6 Acknowledgments

We gratefully acknowledge Mingjun Gu for excellent technical assistance. This study was funded by the American Heart Association grant 11SDG7420029 (ZYS) 10SDG2640130 (QHC) and National Institute of Health HL122952 (QHC).

Chapter 4.
Summary, Limitations, and Future Directions

4.1 Summary

Cardiovascular disease is the leading cause of death in the United States.[1] Reducing the incidence of CVD would have a significant impact on the overall health of the population, and in many cases, improve quality of life. HTN is also very prevalent in the United States and is a major risk factor for the development of CVD.[1] Evidence suggests that approximately 25% of individuals with normal blood pressure, and 50-60% of individuals diagnosed with HTN demonstrate sensitivity to salt.[195, 196] The CNS plays a major role in the pathogenesis and maintenance of salt-sensitive hypertension through augmented activity of the SNS.[67, 72] The overall goal of our research is to identify central neural mechanisms that contribute to sympathoexcitation due to HS intake, in order to develop new targets for the treatment of salt-sensitive HTN.

Salt-sensitive hypertension involves excess activation of the SNS. Neuronal activity in the hypothalamic PVN is augmented in AngII-salt HTN and PVN neuronal activity is required to maintain the high SNA and ABP in this model of salt-sensitive HTN.[79] Previous work from our lab demonstrates that SK channel dysfunction is a key contributor to augmented excitability among PVN-RVLM neurons.[144] In **study 1**, we demonstrate that sympathoexcitatory responses to PVN SK channel blockade are attenuated in AngII-salt hypertension. Furthermore, we report that SK1-3 protein levels in punched PVN tissue were not different between normotensive control and AngII-salt HTN. These results indicate that dysfunction of SK channels contributes to sympathoexcitation in AngII-salt HTN. SK channels are powerful negative feedback regulators of excitability, and normally function to suppress PVN neuronal excitability.[142] Interestingly, we also demonstrate SK channel dysfunction in HS only rats that are normotensive. These results indicate that

dietary salt likely plays a dominant role in down-regulating SK channel function in the PVN.

In **study 1** we demonstrate SK channel dysfunction in the PVN of AngII-salt hypertensive rats. Additionally, SK channel dysfunction has been reported in IML projecting PVN neurons in spontaneously hypertensive rats as well.[143] Therefore, we sought to examine mechanisms that contribute to PVN SK channel dysfunction. Ca^{2+} release from the ER Ca^{2+} store during action potentials is a prominent activator of SK channels.[207] Recent reports indicate that brain ER stress plays a role in the pathogenesis of hypertension characterized by high sympathetic outflow.[154, 199, 200] In **study 2** we examined the functional role of the endoplasmic reticulum in regulating neuronal excitability in vitro and sympathetic nerve activity and blood pressure in vivo. We demonstrate that inhibition of ER Ca^{2+} store function with PVN microinjection of TG augments sympathetic nerve activity and blood pressure. In addition, bath application of TG significantly augments excitability of PVN-RVLM neurons. Interestingly, excitability of PVN-RVLM neurons was significantly augmented in HS treated rats compared to control, and we further demonstrate that dysfunction of the ER Ca^{2+} store contributes to the augmented neuronal excitability. Finally, SFA is primarily mediated by Ca^{2+} activated K^+ channels including SK, and we report that SFA is diminished in HS rats. Furthermore, bath application of TG significantly diminished SFA in control rats yet had no effect in the HS treatment group. These results indicate that loss of ER Ca^{2+} store function due to HS intake contributes to augmented neuronal excitability likely through diminished function of Ca^{2+} activated K^+ channels.

4.2 Limitations

Several limitations must be recognized for the preceding studies. All of our whole animal studies utilized anesthetized animal preparations. Anesthesia could potentially impact the cardiovascular responses to PVN microinjection of apamin or TG.[192] Future studies will employ telemetry recordings of SNA and

ABP in order to elucidate the impact of SK channel function in conscious, free-moving animals. We utilize pharmacological agents including ion channel and transporter blockers in these studies, and it's important to recognize that these agents may have non-specific effects. In a previous study we performed control experiments with apamin including determination of a dose dependent response, microinjection outside of the PVN to determine site specificity, as well as IV injection to rule out peripheral actions of the apamin.[111] Furthermore, in study 1, we marked injection sites with Chicago Blue dye and examined distribution of the dye to confirm that distribution was primarily within the PVN. In study 2 we also examined the dose dependent response of TG in order to find the minimum dose that elicits a maximum response in SNA and ABP and rule out potential non-specific effects. Additionally, we performed control injections outside of the PVN (2.5mm lateral to midline), as well as IV injection of the minimum effective dose to rule out peripheral actions. Additionally, we confirmed that spread of injected dye following experiments was largely confined to the PVN.

It's important to note that both of the primary drugs we utilized in study 1 and study 2 cannot be used in human studies. The methodology utilized in the current research involves targeted delivery to specific brain areas that are not accessible in humans. Apamin is a component of bee venom and acts as a neurotoxin. Apamin administered peripherally in sub-lethal doses results in seizures in mice, and marked changes in neuronal structure in neuronal cultures during chronic bath application.[213, 214] Chronic application of TG induces brain ER stress in live animals and cellular apoptosis through diminished ER Ca^{2+} handling both *in vivo* and *in vitro*.[149, 154, 203] The goal of our research is to ultimately develop new treatment strategies in humans and alternative approaches will have to be developed for studies involving human intervention.

It's also important to recognize that other brain regions besides the PVN contribute to the high sympathetic outflow in salt-sensitive HTN. The CVO's including the OVLT and SFO contribute to salt-sensitive HTN.[215, 216] Additionally, the RVLM is a key driver of tonic SNA.[7] Evidence demonstrates

that HS intake augments angiotensinergic activity within the RVLM contributing to augmented sympathetic outflow.[183, 217] Further information suggests that excess salt intake sensitizes neurons in the RVLM contributing to exaggerated SNA and ABP responses to excitatory and inhibitory stimuli.[184, 218] Recent evidence indicates that increases in cerebrospinal (CSF) fluid Na^+ concentration activates RVLM neurons to produce exaggerated elevations in SNA.[219] Our lab examines alterations in the PVN that contribute to salt-sensitive HTN; however, we recognize that other CNS sites likely provide significant contributions to salt-sensitive hypertension.

4.3 Future Studies

Our goal is to elucidate central neural mechanisms responsible for the high sympathetic outflow due to HS intake. We have demonstrated that PVN SK channel dysfunction contributes to augmented excitability of PVN-RVLM neurons *in vitro*, and sympathoexcitation *in vivo*. We seek to test the overall hypothesis that HS intake augments excitability of PVN neurons making them susceptible to further stimuli such as AngII or stress to induce HTN. We demonstrate in study 1 that HS intake induces SK channel dysfunction even in the absence of HTN. In addition, in study 2 we demonstrate augmented excitability of PVN-RVLM in HS rats that have not developed HTN.

Ongoing studies in our lab demonstrate SK channel dysfunction in Dahl salt-sensitive rats. Dahl rats are an ideal model to perform a treatment study in that they only require high salt food to become hypertensive. We plan to perform continuous infusion of an SK channel positive modulator in the PVN of Dahl salt-sensitive rats. We hypothesize that maintaining SK channel function in the PVN will attenuate hypertension. We will further explore SK channel function utilizing viral vectors to knock out, or overexpress SK channels in Dahl salt-sensitive rats in order to determine their contribution in a chronic model.

We further seek to identify the mechanism(s) responsible for SK channel dysfunction due to HS intake. In study 2 we demonstrate the contribution of the

ER in regulating neuronal excitability *in vitro*, and SNA and ABP *in vivo*. We demonstrate that dysfunction of the ER Ca^{2+} store augments PVN neuronal excitability likely through less activation of Ca^{2+} activated K^+ channels including SK. The ER is only one source of Ca^{2+} that activates SK channels (Fig 1.8) and we have only used a blocker of ER Ca^{2+} uptake. Further studies are required to examine release of ER Ca^{2+} from IP3 and RYR sources. Additionally, ongoing studies in the lab are examining the interaction of NMDA glutamate receptors, AT1R's, and VDCC's with SK channels. Future studies will also examine whether alterations in the Ca^{2+}-calmodulin complex contribute to SK channel dysfunction in AngII-salt HTN.

4.4 Conclusions

This dissertation reports novel findings that potentially provide new treatment targets for salt-sensitive HTN. First, we report that SK channel dysfunction in the PVN is a key contributor to the augmented sympathetic outflow in AngII-salt HTN. Additionally, we report that HS intake likely plays a dominant role in reducing SK channel function in the PVN. Secondly, demonstrate the importance of the ER Ca^{2+} store in regulating PVN neuronal excitability *in vitro*, and SNA and ABP *in vivo*. Finally we report that the dysfunction of the ER Ca^{2+} store contributes to augmented PVN neuronal excitability due to HS diet, likely through reduced activity of Ca^{2+} activated K^+ channels including SK. These finding provide new and valuable information into the central neural mechanisms contributing to salt-sensitive HTN.

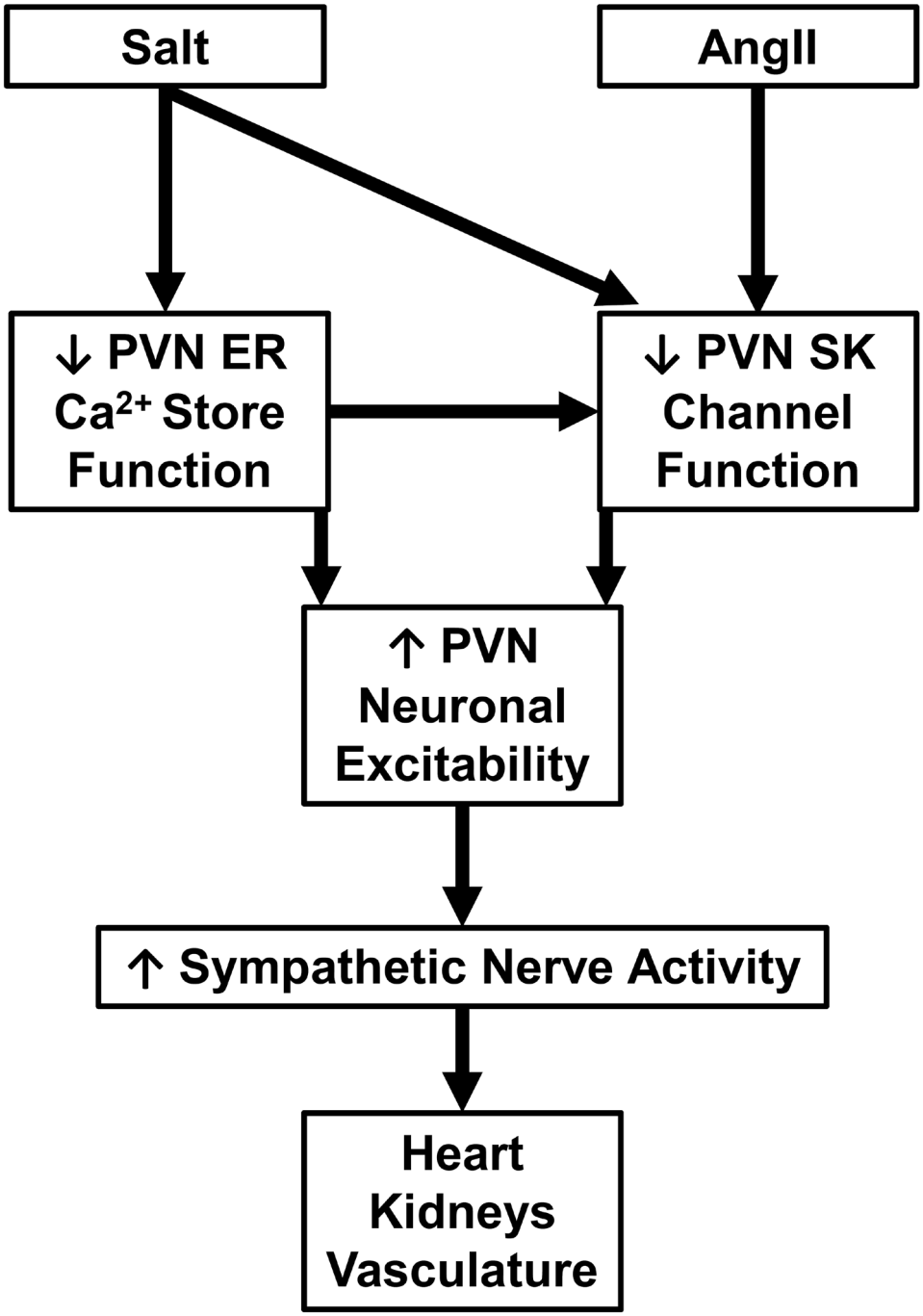

Figure 4.1 Summary of mechanisms contributing to sympathoexcitation in Study 1 and Study 2. AngII-salt HTN involves reduced SK channel function in the PVN (Study 1). Diminished ER Ca^{2+} store function contributes to augmented PVN neuronal excitability (Study 2). Augmented excitability of PVN neurons increases sympathetic nerve activity targeting the heart, kidneys and vasculature to increase arterial blood pressure.

References

1. Mozaffarian D, Benjamin EJ, Go AS, Arnett DK, Blaha MJ, Cushman M, Das SR, de Ferranti S, Despres JP, Fullerton HJ, Howard VJ, Huffman MD, Isasi CR, Jimenez MC, Judd SE, Kissela BM, Lichtman JH, Lisabeth LD, Liu S, Mackey RH, Magid DJ, McGuire DK, Mohler ER, 3rd, Moy CS, Muntner P, Mussolino ME, Nasir K, Neumar RW, Nichol G, Palaniappan L, Pandey DK, Reeves MJ, Rodriguez CJ, Rosamond W, Sorlie PD, Stein J, Towfighi A, Turan TN, Virani SS, Woo D, Yeh RW, Turner MB, American Heart Association Statistics C and Stroke Statistics S. Heart Disease and Stroke Statistics-2016 Update: A Report From the American Heart Association. *Circulation*. 2016;133:e38-e360.

2. Rowell LB. *Human cardiovascular control*: Oxford University Press, USA; 1993.

3. Chobanian AV, Bakris GL, Black HR, Cushman WC, Green LA, Izzo JL, Jr., Jones DW, Materson BJ, Oparil S, Wright JT, Jr., Roccella EJ, Joint National Committee on Prevention DE, Treatment of High Blood Pressure. National Heart L, Blood I and National High Blood Pressure Education Program Coordinating C. Seventh report of the Joint National Committee on Prevention, Detection, Evaluation, and Treatment of High Blood Pressure. *Hypertension*. 2003;42:1206-52.

4. Pickering TG, Gribbin B, Petersen ES, Cunningham DJ and Sleight P. Effects of autonomic blockade on the baroreflex in man at rest and during exercise. *Circ Res*. 1972;30:177-85.

5. Ciriello J. Brainstem projections of aortic baroreceptor afferent fibers in the rat. *Neurosci Lett*. 1983;36:37-42.

6. Polson JW, Potts PD, Li YW and Dampney RA. Fos expression in neurons projecting to the pressor region in the rostral ventrolateral medulla after sustained hypertension in conscious rabbits. *Neuroscience*. 1995;67:107-23.

7. Schreihofer AM, Stornetta RL and Guyenet PG. Regulation of sympathetic tone and arterial pressure by rostral ventrolateral medulla after depletion of C1 cells in rat. *J Physiol*. 2000;529 Pt 1:221-36.

8. Ross CA, Ruggiero DA, Park DH, Joh TH, Sved AF, Fernandez-Pardal J, Saavedra JM and Reis DJ. Tonic vasomotor control by the rostral ventrolateral medulla: effect of electrical or chemical stimulation of the area containing C1 adrenaline neurons on arterial pressure, heart rate, and plasma catecholamines and vasopressin. *J Neurosci*. 1984;4:474-94.

9. Ross CA, Ruggiero DA, Joh TH, Park DH and Reis DJ. Rostral ventrolateral medulla: selective projections to the thoracic autonomic cell column from the region containing C1 adrenaline neurons. *J Comp Neurol*. 1984;228:168-85.

10. Kandel ER, Schwartz JH and Jessell TM. *Principles of neural science*: McGraw-hill New York; 2000.

11. Cowley AW, Jr. Long-term control of arterial blood pressure. *Physiological reviews*. 1992;72:231-300.

12. Guyton AC, Coleman TG, Cowley AV, Jr., Scheel KW, Manning RD, Jr. and Norman RA, Jr. Arterial pressure regulation. Overriding dominance of the kidneys in long-term regulation and in hypertension. *Am J Med*. 1972;52:584-94.

13. Guyton AC. Blood pressure control--special role of the kidneys and body fluids. *Science*. 1991;252:1813-6.

14. Andersson B. Thirst--and brain control of water balance. *Am Sci*. 1971;59:408-15.

15. Marks L and Maxwell M. Tigerstedt and the discovery of renin. An historical note. *Hypertension*. 1979;1:384-388.

16. Tigerstedt R and Bergman P. Niere und kreislauf1. *Skandinavisches Archiv für Physiologie*. 1898;8:223-271.

17. Epstein AN, Fitzsimons JT and Rolls BJ. Drinking induced by injection of angiotensin into the rain of the rat. *J Physiol*. 1970;210:457-74.

18. Epstein AN, Fitzsimons JT and Simons BJ. Drinking caused by the intracranial injection of angiotensin into the rat. *J Physiol*. 1969;200:98P-100P.

19. Sakai RR, Nicolaidis S and Epstein AN. Salt appetite is suppressed by interference with angiotensin II and aldosterone. *Am J Physiol*. 1986;251:R762-8.

20. Zhang DM, Stellar E and Epstein AN. Together intracranial angiotensin and systemic mineralocorticoid produce avidity for salt in the rat. *Physiol Behav*. 1984;32:677-81.

21. Hall JE, Guyton AC, Smith MJ, Jr. and Coleman TG. Blood pressure and renal function during chronic changes in sodium intake: role of angiotensin. *Am J Physiol*. 1980;239:F271-80.

22. Hall JE, Mizelle HL, Hildebrandt DA and Brands MW. Abnormal pressure natriuresis. A cause or a consequence of hypertension? *Hypertension*. 1990;15:547-59.

23. Mizelle HL, Montani JP, Hester RL, Didlake RH and Hall JE. Role of pressure natriuresis in long-term control of renal electrolyte excretion. *Hypertension*. 1993;22:102-10.

24. Cowley AW and McCaa RE. Acute and chronic dose-response relationships for angiotensin, aldosterone, and arterial pressure at varying levels of sodium intake. *Circ Res*. 1976;39:788-97.

25. Hall JE. Control of sodium excretion by angiotensin II: intrarenal mechanisms and blood pressure regulation. *Am J Physiol*. 1986;250:R960-72.

26. DeClue JW, Guyton AC, Cowley AW, Jr., Coleman TG, Norman RA, Jr. and McCaa RE. Subpressor angiotensin infusion, renal sodium handling, and salt-induced hypertension in the dog. *Circ Res*. 1978;43:503-12.

27. Lohmeier TE and Cowley AW, Jr. Hypertensive and renal effects of chronic low level intrarenal angiotensin infusion in the dog. *Circ Res*. 1979;44:154-60.

28. Bianchi G, Fox U, Di Francesco GF, Giovanetti AM and Pagetti D. Blood pressure changes produced by kidney cross-transplantation between

spontaneously hypertensive rats and normotensive rats. *Clin Sci Mol Med*. 1974;47:435-48.

29. Dahl LK and Heine M. Primary role of renal homografts in setting chronic blood pressure levels in rats. *Circ Res*. 1975;36:692-6.

30. Dahl LK, Heine M and Thompson K. Genetic influence of the kidneys on blood pressure. Evidence from chronic renal homografts in rats with opposite predispositions to hypertension. *Circ Res*. 1974;34:94-101.

31. Hamlyn JM, Blaustein MP, Bova S, DuCharme DW, Harris DW, Mandel F, Mathews WR and Ludens JH. Identification and characterization of a ouabain-like compound from human plasma. *Proc Natl Acad Sci U S A*. 1991;88:6259-63.

32. Hamlyn JM, Ringel R, Schaeffer J, Levinson PD, Hamilton BP, Kowarski AA and Blaustein MP. A circulating inhibitor of (Na+ + K+)ATPase associated with essential hypertension. *Nature*. 1982;300:650-2.

33. Manunta P, Hamilton BP and Hamlyn JM. Salt intake and depletion increase circulating levels of endogenous ouabain in normal men. *Am J Physiol Regul Integr Comp Physiol*. 2006;290:R553-9.

34. Pierdomenico SD, Bucci A, Manunta P, Rivera R, Ferrandi M, Hamlyn JM, Lapenna D, Cuccurullo F and Mezzetti A. Endogenous ouabain and hemodynamic and left ventricular geometric patterns in essential hypertension. *Am J Hypertens*. 2001;14:44-50.

35. Rossi G, Manunta P, Hamlyn JM, Pavan E, De Toni R, Semplicini A and Pessina AC. Immunoreactive endogenous ouabain in primary aldosteronism and essential hypertension: relationship with plasma renin, aldosterone and blood pressure levels. *J Hypertens*. 1995;13:1181-91.

36. Ferrandi M, Manunta P, Rivera R, Bianchi G and Ferrari P. Role of the ouabain-like factor and Na-K pump in rat and human genetic hypertension. *Clin Exp Hypertens*. 1998;20:629-39.

37. Leenen FH, Harmsen E and Yu H. Dietary sodium and central vs. peripheral ouabain-like activity in Dahl salt-sensitive vs. salt-resistant rats. *Am J Physiol*. 1994;267:H1916-20.

38. Takada T, Nakagawa M, Ura N, Kaide J, Yoshida H and Shimamoto K. Endogenous immunoreactive ouabain-like and digoxin-like factors in reduced renal mass hypertensive rats. *Hypertens Res*. 1998;21:193-9.

39. Bragulat E and de la Sierra A. Salt intake, endothelial dysfunction, and salt-sensitive hypertension. *J Clin Hypertens (Greenwich)*. 2002;4:41-6.

40. Bragulat E, de la Sierra A, Antonio MT and Coca A. Endothelial dysfunction in salt-sensitive essential hypertension. *Hypertension*. 2001;37:444-8.

41. Panza JA, Casino PR, Kilcoyne CM and Quyyumi AA. Role of endothelium-derived nitric oxide in the abnormal endothelium-dependent vascular relaxation of patients with essential hypertension. *Circulation*. 1993;87:1468-74.

42. Panza JA, Quyyumi AA, Brush JE, Jr. and Epstein SE. Abnormal endothelium-dependent vascular relaxation in patients with essential hypertension. *The New England journal of medicine*. 1990;323:22-7.

43. Lockette W, Otsuka Y and Carretero O. The loss of endothelium-dependent vascular relaxation in hypertension. *Hypertension*. 1986;8:II61-6.

44. Tesfamariam B and Halpern W. Endothelium-dependent and endothelium-independent vasodilation in resistance arteries from hypertensive rats. *Hypertension*. 1988;11:440-4.

45. Zicha J, Dobesova Z and Kunes J. Relative deficiency of nitric oxide-dependent vasodilation in salt-hypertensive Dahl rats: the possible role of superoxide anions. *J Hypertens*. 2001;19:247-54.

46. Palmer RM, Ashton DS and Moncada S. Vascular endothelial cells synthesize nitric oxide from L-arginine. *Nature*. 1988;333:664-6.

47. Beckman JS, Beckman TW, Chen J, Marshall PA and Freeman BA. Apparent hydroxyl radical production by peroxynitrite: implications for endothelial injury from nitric oxide and superoxide. *Proc Natl Acad Sci U S A*. 1990;87:1620-4.

48. Cai H and Harrison DG. Endothelial dysfunction in cardiovascular diseases: the role of oxidant stress. *Circ Res*. 2000;87:840-4.

49. Duffy SJ, Keaney JF, Jr., Holbrook M, Gokce N, Swerdloff PL, Frei B and Vita JA. Short- and long-term black tea consumption reverses endothelial dysfunction in patients with coronary artery disease. *Circulation*. 2001;104:151-6.

50. Heitzer T, Just H and Munzel T. Antioxidant vitamin C improves endothelial dysfunction in chronic smokers. *Circulation*. 1996;94:6-9.

51. Levine GN, Frei B, Koulouris SN, Gerhard MD, Keaney JF, Jr. and Vita JA. Ascorbic acid reverses endothelial vasomotor dysfunction in patients with coronary artery disease. *Circulation*. 1996;93:1107-13.

52. Solzbach U, Hornig B, Jeserich M and Just H. Vitamin C improves endothelial dysfunction of epicardial coronary arteries in hypertensive patients. *Circulation*. 1997;96:1513-9.

53. Goldstein DS. Plasma catecholamines and essential hypertension. An analytical review. *Hypertension*. 1983;5:86-99.

54. Anderson EA, Sinkey CA, Lawton WJ and Mark AL. Elevated sympathetic nerve activity in borderline hypertensive humans. Evidence from direct intraneural recordings. *Hypertension*. 1989;14:177-83.

55. Grassi G, Cattaneo BM, Seravalle G, Lanfranchi A and Mancia G. Baroreflex control of sympathetic nerve activity in essential and secondary hypertension. *Hypertension*. 1998;31:68-72.

56. Meyrelles SS, Tinucci T, Hollanda HE and Mion D, Jr. Baroreflex control of muscle sympathetic nerve activity in mild hypertension. *Am J Hypertens*. 1997;10:162-7.

57. Grassi G, Colombo M, Seravalle G, Spaziani D and Mancia G. Dissociation between muscle and skin sympathetic nerve activity in essential hypertension, obesity, and congestive heart failure. *Hypertension*. 1998;31:64-7.

58. Hering D, Kara T, Kucharska W, Somers VK and Narkiewicz K. High-normal blood pressure is associated with increased resting sympathetic activity but normal responses to stress tests. *Blood Press*. 2013;22:183-7.

59. Matsukawa T, Mano T, Gotoh E and Ishii M. Elevated sympathetic nerve activity in patients with accelerated essential hypertension. *J Clin Invest*. 1993;92:25-8.

60. Yamada Y, Miyajima E, Tochikubo O, Matsukawa T and Ishii M. Age-related changes in muscle sympathetic nerve activity in essential hypertension. *Hypertension*. 1989;13:870-7.

61. Schlaich MP, Lambert E, Kaye DM, Krozowski Z, Campbell DJ, Lambert G, Hastings J, Aggarwal A and Esler MD. Sympathetic augmentation in hypertension: role of nerve firing, norepinephrine reuptake, and Angiotensin neuromodulation. *Hypertension*. 2004;43:169-75.

62. Esler M, Jackman G, Bobik A, Leonard P, Kelleher D, Skews H, Jennings G and Korner P. Norepinephrine kinetics in essential hypertension. Defective neuronal uptake of norepinephrine in some patients. *Hypertension*. 1981;3:149-56.

63. Esler M, Jackman G, Leonard P, Bobik A, Skews H, Jennings G, Kelleher D and Korner P. Determination of noradrenaline uptake, spillover to plasma and plasma concentration in patients with essential hypertension. *Clin Sci (Lond)*. 1980;59 Suppl 6:311s-313s.

64. Esler M, Jennings G, Biviano B, Lambert G and Hasking G. Mechanism of elevated plasma noradrenaline in the course of essential hypertension. *J Cardiovasc Pharmacol*. 1986;8:S39-S43.

65. Esler M, Lambert G and Jennings G. Regional norepinephrine turnover in human hypertension. *Clin Exp Hypertens A*. 1989;11 Suppl 1:75-89.

66. Gordon FJ, Matsuguchi H and Mark AL. Abnormal baroreflex control of heart rate in prehypertensive and hypertensive Dahl genetically salt-sensitive rats. *Hypertension*. 1981;3:I135-41.

67. Takeshita A, Mark AL and Brody MJ. Prevention of salt-induced hypertension in the Dahl strain by 6-hydroxydopamine. *Am J Physiol*. 1979;236:H48-52.

68. Genain CP, Reddy SR, Ott CE, Van Loon GR and Kotchen TA. Failure of salt loading to inhibit tissue norepinephrine turnover in prehypertensive Dahl salt-sensitive rats. *Hypertension*. 1988;12:568-573.

69. Fujita T, Henry WL, Bartter FC, Lake CR and Delea CS. Factors influencing blood pressure in salt-sensitive patients with hypertension. *The American journal of medicine*. 1980;69:334-344.

70. Koolen MI and van Brummelen P. Adrenergic activity and peripheral hemodynamics in relation to sodium sensitivity in patients with essential hypertension. *Hypertension*. 1984;6:820-825.

71. Krieger JE, Liard JF and Cowley AW, Jr. Hemodynamics, fluid volume, and hormonal responses to chronic high-salt intake in dogs. *Am J Physiol*. 1990;259:H1629-36.

72. Osborn JW, Fink GD, Sved AF, Toney GM and Raizada MK. Circulating angiotensin II and dietary salt: converging signals for neurogenic hypertension. *Curr Hypertens Rep*. 2007;9:228-35.

73. King AJ and Fink GD. Chronic low-dose angiotensin II infusion increases venomotor tone by neurogenic mechanisms. *Hypertension*. 2006;48:927-33.

74. King AJ, Novotny M, Swain GM and Fink GD. Whole body norepinephrine kinetics in ANG II-salt hypertension in the rat. *Am J Physiol Regul Integr Comp Physiol*. 2008;294:R1262-7.

75. Osborn JW, Olson DM, Guzman P, Toney GM and Fink GD. The neurogenic phase of angiotensin II-salt hypertension is prevented by chronic intracerebroventricular administration of benzamil. *Physiol Rep*. 2014;2:e00245.

76. King AJ, Osborn JW and Fink GD. Splanchnic circulation is a critical neural target in angiotensin II salt hypertension in rats. *Hypertension*. 2007;50:547-56.

77. Yoshimoto M, Miki K, Fink GD, King A and Osborn JW. Chronic angiotensin II infusion causes differential responses in regional sympathetic nerve activity in rats. *Hypertension*. 2010;55:644-51.

78. Luft FC, Wilcox CS, Unger T, Kuhn R, Demmert G, Rohmeiss P, Ganten D and Sterzel RB. Angiotensin-induced hypertension in the rat. Sympathetic nerve activity and prostaglandins. *Hypertension*. 1989;14:396-403.

79. Bardgett ME, Holbein WW, Herrera-Rosales M and Toney GM. Ang II-salt hypertension depends on neuronal activity in the hypothalamic paraventricular nucleus but not on local actions of tumor necrosis factor-alpha. *Hypertension*. 2014;63:527-34.

80. Holmes JH and Gregersen MI. Observations on drinking induced by hypertonic solutions. *Am J Physiol*. 1950;162:326-37.

81. Olsson K. Dipsogenic effects of intracarotid infusions of various hyperosmolal solutions. *Acta Physiol Scand*. 1971;85:517-522.

82. Eriksson L, Fernandez O and Olsson K. Differences in the antidiuretic response to intracarotid infusions of various hypertonic solutions in the conscious goat. *Acta Physiol Scand*. 1971;83:554-62.

83. Jewell PA and Verney E. An experimental attempt to determine the site of the neurohypophysial osmoreceptors in the dog. *Philosophical Transactions of the Royal Society of London Series B, Biological Sciences*. 1957:197-324.

84. Thrasher TN, Brown CJ, Keil LC and Ramsay DJ. Thirst and vasopressin release in the dog: an osmoreceptor or sodium receptor mechanism? *Am J Physiol*. 1980;238:R333-9.

85. Buggy J and Fisher AE. Anteroventral third ventricle site of action for angiotensin induced thirst. *Pharmacol Biochem Behav*. 1976;4:651-60.

86. Buggy J and Johnson AK. Angiotensin-induced thirst: effects of third ventricle obstruction and periventricular ablation. *Brain Res*. 1978;149:117-28.

87. Buggy J and Jonhson AK. Preoptic-hypothalamic periventricular lesions: thirst deficits and hypernatremia. *Am J Physiol*. 1977;233:R44-52.

88. Johnson AK, Hoffman WE and Buggy J. Attenuated pressor responses to intracranially injected stimuli and altered antidiuretic activity following preoptic-hypothalamic periventricular ablation. *Brain Res*. 1978;157:161-6.

89. Mendelsohn FA, Quirion R, Saavedra JM, Aguilera G and Catt KJ. Autoradiographic localization of angiotensin II receptors in rat brain. *Proc Natl Acad Sci U S A*. 1984;81:1575-9.

90. Mangiapane ML and Simpson JB. Subfornical organ lesions reduce the pressor effect of systemic angiotensin II. *Neuroendocrinology*. 1980;31:380-4.

91. Lind RW, Van Hoesen GW and Johnson AK. An HRP study of the connections of the subfornical organ of the rat. *J Comp Neurol*. 1982;210:265-77.

92. Miselis RR, Shapiro RE and Hand PJ. Subfornical organ efferents to neural systems for control of body water. *Science*. 1979;205:1022-5.

93. Prager-Khoutorsky M and Bourque CW. Anatomical organization of the rat organum vasculosum laminae terminalis. *Am J Physiol Regul Integr Comp Physiol*. 2015;309:R324-37.

94. Ciura S and Bourque CW. Transient receptor potential vanilloid 1 is required for intrinsic osmoreception in organum vasculosum lamina terminalis neurons and for normal thirst responses to systemic hyperosmolality. *J Neurosci*. 2006;26:9069-75.

95. Ciura S, Liedtke W and Bourque CW. Hypertonicity sensing in organum vasculosum lamina terminalis neurons: a mechanical process involving TRPV1 but not TRPV4. *J Neurosci*. 2011;31:14669-76.

96. Miller RL, Wang MH, Gray PA, Salkoff LB and Loewy AD. ENaC-expressing neurons in the sensory circumventricular organs become c-Fos activated following systemic sodium changes. *Am J Physiol Regul Integr Comp Physiol*. 2013;305:R1141-52.

97. McKinley MJ, Bicknell RJ, Hards D, McAllen RM, Vivas L, Weisinger RS and Oldfield BJ. Efferent neural pathways of the lamina terminalis subserving osmoregulation. *Prog Brain Res*. 1992;91:395-402.

98. Shi P, Martinez MA, Calderon AS, Chen Q, Cunningham JT and Toney GM. Intra-carotid hyperosmotic stimulation increases Fos staining in forebrain organum vasculosum laminae terminalis neurones that project to the hypothalamic paraventricular nucleus. *J Physiol*. 2008;586:5231-45.

99. Shi P, Stocker SD and Toney GM. Organum vasculosum laminae terminalis contributes to increased sympathetic nerve activity induced by central hyperosmolality. *Am J Physiol Regul Integr Comp Physiol*. 2007;293:R2279-89.
100. Ono T, Nishino H, Sasaka K, Muramoto K, Yano I and Simpson A. Paraventricular nucleus connections to spinal cord and pituitary. *Neurosci Lett*. 1978;10:141-6.
101. Swanson LW and Sawchenko PE. Paraventricular nucleus: a site for the integration of neuroendocrine and autonomic mechanisms. *Neuroendocrinology*. 1980;31:410-7.
102. Swanson LW and Kuypers HG. The paraventricular nucleus of the hypothalamus: cytoarchitectonic subdivisions and organization of projections to the pituitary, dorsal vagal complex, and spinal cord as demonstrated by retrograde fluorescence double-labeling methods. *J Comp Neurol*. 1980;194:555-70.
103. Sawchenko PE and Swanson LW. Immunohistochemical identification of neurons in the paraventricular nucleus of the hypothalamus that project to the medulla or to the spinal cord in the rat. *J Comp Neurol*. 1982;205:260-72.
104. Pyner S and Coote JH. Identification of branching paraventricular neurons of the hypothalamus that project to the rostroventrolateral medulla and spinal cord. *Neuroscience*. 2000;100:549-56.
105. Chen QH and Toney GM. Identification and characterization of two functionally distinct groups of spinal cord-projecting paraventricular nucleus neurons with sympathetic-related activity. *Neuroscience*. 2003;118:797-807.
106. Martin DS, Segura T and Haywood JR. Cardiovascular responses to bicuculline in the paraventricular nucleus of the rat. *Hypertension*. 1991;18:48-55.
107. Martins-Pinge MC, Mueller PJ, Foley CM, Heesch CM and Hasser EM. Regulation of arterial pressure by the paraventricular nucleus in conscious rats: interactions among glutamate, GABA, and nitric oxide. *Front Physiol*. 2012;3:490.

108. Chen QH, Haywood JR and Toney GM. Sympathoexcitation by PVN-injected bicuculline requires activation of excitatory amino acid receptors. *Hypertension*. 2003;42:725-31.

109. Chen QH and Toney GM. Responses to GABA-A receptor blockade in the hypothalamic PVN are attenuated by local AT1 receptor antagonism. *Am J Physiol Regul Integr Comp Physiol*. 2003;285:R1231-9.

110. Zhang K and Patel KP. Effect of nitric oxide within the paraventricular nucleus on renal sympathetic nerve discharge: role of GABA. *Am J Physiol*. 1998;275:R728-34.

111. Gui L, LaGrange LP, Larson RA, Gu M, Zhu J and Chen QH. Role of small conductance calcium-activated potassium channels expressed in PVN in regulating sympathetic nerve activity and arterial blood pressure in rats. *Am J Physiol Regul Integr Comp Physiol*. 2012;303:R301-10.

112. Xu B, Zheng H and Patel KP. Enhanced activation of RVLM-projecting PVN neurons in rats with chronic heart failure. *Am J Physiol Heart Circ Physiol*. 2012;302:H1700-11.

113. Zhang K, Li YF and Patel KP. Blunted nitric oxide-mediated inhibition of renal nerve discharge within PVN of rats with heart failure. *Am J Physiol Heart Circ Physiol*. 2001;281:H995-1004.

114. Zheng H, Li YF, Wang W and Patel KP. Enhanced angiotensin-mediated excitation of renal sympathetic nerve activity within the paraventricular nucleus of anesthetized rats with heart failure. *Am J Physiol Regul Integr Comp Physiol*. 2009;297:R1364-74.

115. Zheng H, Sharma NM, Liu X and Patel KP. Exercise training normalizes enhanced sympathetic activation from the paraventricular nucleus in chronic heart failure: role of angiotensin II. *Am J Physiol Regul Integr Comp Physiol*. 2012;303:R387-94.

116. Freeman KL and Brooks VL. AT(1) and glutamatergic receptors in paraventricular nucleus support blood pressure during water deprivation. *Am J Physiol Regul Integr Comp Physiol*. 2007;292:R1675-82.

117. Holbein WW, Bardgett ME and Toney GM. Blood pressure is maintained during dehydration by hypothalamic paraventricular nucleus-driven tonic sympathetic nerve activity. *J Physiol*. 2014;592:3783-99.
118. Stocker SD, Hunwick KJ and Toney GM. Hypothalamic paraventricular nucleus differentially supports lumbar and renal sympathetic outflow in water-deprived rats. *J Physiol*. 2005;563:249-63.
119. Stocker SD, Simmons JR, Stornetta RL, Toney GM and Guyenet PG. Water deprivation activates a glutamatergic projection from the hypothalamic paraventricular nucleus to the rostral ventrolateral medulla. *J Comp Neurol*. 2006;494:673-85.
120. Goto A, Ikeda T, Tobian L, Iwai J and Johnson MA. Brain lesions in the paraventricular nuclei and catecholaminergic neurons minimize salt hypertension in Dahl salt-sensitive rats. *Clin Sci (Lond)*. 1981;61 Suppl 7:53s-55s.
121. Allen AM. Inhibition of the hypothalamic paraventricular nucleus in spontaneously hypertensive rats dramatically reduces sympathetic vasomotor tone. *Hypertension*. 2002;39:275-80.
122. Takeda K, Nakata T, Takesako T, Itoh H, Hirata M, Kawasaki S, Hayashi J, Oguro M, Sasaki S and Nakagawa M. Sympathetic inhibition and attenuation of spontaneous hypertension by PVN lesions in rats. *Brain Res*. 1991;543:296-300.
123. Herzig TC, Buchholz RA and Haywood JR. Effects of paraventricular nucleus lesions on chronic renal hypertension. *Am J Physiol*. 1991;261:H860-7.
124. Li YF, Jackson KL, Stern JE, Rabeler B and Patel KP. Interaction between glutamate and GABA systems in the integration of sympathetic outflow by the paraventricular nucleus of the hypothalamus. *Am J Physiol Heart Circ Physiol*. 2006;291:H2847-56.
125. Gabor A and Leenen FH. Cardiovascular effects of angiotensin II and glutamate in the PVN of Dahl salt-sensitive rats. *Brain Res*. 2012;1447:28-37.

126. Huang BS and Leenen FH. Both brain angiotensin II and "ouabain" contribute to sympathoexcitation and hypertension in Dahl S rats on high salt intake. *Hypertension*. 1998;32:1028-33.

127. Wang JM, Veerasingham SJ, Tan J and Leenen FH. Effects of high salt intake on brain AT1 receptor densities in Dahl rats. *Am J Physiol Heart Circ Physiol*. 2003;285:H1949-55.

128. Ito S, Komatsu K, Tsukamoto K, Kanmatsuse K and Sved AF. Ventrolateral medulla AT1 receptors support blood pressure in hypertensive rats. *Hypertension*. 2002;40:552-9.

129. Li DP and Pan HL. Plasticity of GABAergic control of hypothalamic presympathetic neurons in hypertension. *Am J Physiol Heart Circ Physiol*. 2006;290:H1110-9.

130. Li DP and Pan HL. Increased group I metabotropic glutamate receptor activity in paraventricular nucleus supports elevated sympathetic vasomotor tone in hypertension. *Am J Physiol Regul Integr Comp Physiol*. 2010;299:R552-61.

131. Li DP, Yang Q, Pan HM and Pan HL. Pre- and postsynaptic plasticity underlying augmented glutamatergic inputs to hypothalamic presympathetic neurons in spontaneously hypertensive rats. *J Physiol*. 2008;586:1637-47.

132. Li DP, Yang Q, Pan HM and Pan HL. Plasticity of pre- and postsynaptic GABAB receptor function in the paraventricular nucleus in spontaneously hypertensive rats. *Am J Physiol Heart Circ Physiol*. 2008;295:H807-15.

133. Ye ZY, Li DP, Li L and Pan HL. Protein kinase CK2 increases glutamatergic input in the hypothalamus and sympathetic vasomotor tone in hypertension. *J Neurosci*. 2011;31:8271-9.

134. Sonner PM and Stern JE. Functional role of A-type potassium currents in rat presympathetic PVN neurones. *J Physiol*. 2007;582:1219-38.

135. Sonner PM, Filosa JA and Stern JE. Diminished A-type potassium current and altered firing properties in presympathetic PVN neurones in renovascular hypertensive rats. *J Physiol*. 2008;586:1605-22.

136. Adelman JP, Maylie J and Sah P. Small-conductance Ca2+-activated K+ channels: form and function. *Annu Rev Physiol*. 2012;74:245-69.

137. Faber ES, Delaney AJ and Sah P. SK channels regulate excitatory synaptic transmission and plasticity in the lateral amygdala. *Nat Neurosci*. 2005;8:635-41.

138. Kohler M, Hirschberg B, Bond CT, Kinzie JM, Marrion NV, Maylie J and Adelman JP. Small-conductance, calcium-activated potassium channels from mammalian brain. *Science*. 1996;273:1709-14.

139. Pedarzani P, McCutcheon JE, Rogge G, Jensen BS, Christophersen P, Hougaard C, Strobaek D and Stocker M. Specific enhancement of SK channel activity selectively potentiates the afterhyperpolarizing current I(AHP) and modulates the firing properties of hippocampal pyramidal neurons. *J Biol Chem*. 2005;280:41404-11.

140. Stocker M. Ca(2+)-activated K+ channels: molecular determinants and function of the SK family. *Nat Rev Neurosci*. 2004;5:758-70.

141. Stocker M, Krause M and Pedarzani P. An apamin-sensitive Ca2+-activated K+ current in hippocampal pyramidal neurons. *Proc Natl Acad Sci U S A*. 1999;96:4662-7.

142. Chen QH and Toney GM. Excitability of paraventricular nucleus neurones that project to the rostral ventrolateral medulla is regulated by small-conductance Ca2+-activated K+ channels. *J Physiol*. 2009;587:4235-47.

143. Pachuau J, Li DP, Chen SR, Lee HA and Pan HL. Protein kinase CK2 contributes to diminished small conductance Ca(2+) -activated K(+) channel activity of hypothalamic pre-sympathetic neurons in hypertension. *J Neurochem*. 2014;130:657-67.

144. Chen QH, Andrade MA, Calderon AS and Toney GM. Hypertension induced by angiotensin II and a high salt diet involves reduced SK current and increased excitability of RVLM projecting PVN neurons. *J Neurophysiol*. 2010;104:2329-37.

145. Ron D and Walter P. Signal integration in the endoplasmic reticulum unfolded protein response. *Nat Rev Mol Cell Biol*. 2007;8:519-29.

146. Harding HP, Zhang Y and Ron D. Protein translation and folding are coupled by an endoplasmic-reticulum-resident kinase. *Nature*. 1999;397:271-4.
147. Kleizen B and Braakman I. Protein folding and quality control in the endoplasmic reticulum. *Curr Opin Cell Biol*. 2004;16:343-9.
148. Sitia R and Braakman I. Quality control in the endoplasmic reticulum protein factory. *Nature*. 2003;426:891-4.
149. Paschen W. Dependence of vital cell function on endoplasmic reticulum calcium levels: implications for the mechanisms underlying neuronal cell injury in different pathological states. *Cell Calcium*. 2001;29:1-11.
150. Rutkowski DT and Kaufman RJ. A trip to the ER: coping with stress. *Trends Cell Biol*. 2004;14:20-8.
151. Schubert U, Anton LC, Gibbs J, Norbury CC, Yewdell JW and Bennink JR. Rapid degradation of a large fraction of newly synthesized proteins by proteasomes. *Nature*. 2000;404:770-4.
152. Banhegyi G, Baumeister P, Benedetti A, Dong D, Fu Y, Lee AS, Li J, Mao C, Margittai E, Ni M, Paschen W, Piccirella S, Senesi S, Sitia R, Wang M and Yang W. Endoplasmic reticulum stress. *Ann N Y Acad Sci*. 2007;1113:58-71.
153. Purkayastha S, Zhang H, Zhang G, Ahmed Z, Wang Y and Cai D. Neural dysregulation of peripheral insulin action and blood pressure by brain endoplasmic reticulum stress. *Proc Natl Acad Sci U S A*. 2011;108:2939-44.
154. Young CN, Cao X, Guruju MR, Pierce JP, Morgan DA, Wang G, Iadecola C, Mark AL and Davisson RL. ER stress in the brain subfornical organ mediates angiotensin-dependent hypertension. *J Clin Invest*. 2012;122:3960-4.
155. Brini M, Cali T, Ottolini D and Carafoli E. Neuronal calcium signaling: function and dysfunction. *Cell Mol Life Sci*. 2014;71:2787-814.
156. Solovyova N and Verkhratsky A. Neuronal endoplasmic reticulum acts as a single functional Ca2+ store shared by ryanodine and inositol-1,4,5-trisphosphate receptors as revealed by intra-ER [Ca2+] recordings in single rat sensory neurones. *Pflugers Arch*. 2003;446:447-54.

157. Suarez C, Tornadu IG, Cristina C, Vela J, Iglesias AG, Libertun C, Diaz-Torga G and Becu-Villalobos D. Angiotensin and calcium signaling in the pituitary and hypothalamus. *Cell Mol Neurobiol*. 2002;22:315-33.

158. Akita T and Kuba K. Functional triads consisting of ryanodine receptors, Ca(2+) channels, and Ca(2+)-activated K(+) channels in bullfrog sympathetic neurons. Plastic modulation of action potential. *The Journal of general physiology*. 2000;116:697-720.

159. Cordoba-Rodriguez R, Moore KA, Kao JP and Weinreich D. Calcium regulation of a slow post-spike hyperpolarization in vagal afferent neurons. *Proc Natl Acad Sci U S A*. 1999;96:7650-7.

160. Honda K, Negoro H, Dyball RE, Higuchi T and Takano S. The osmoreceptor complex in the rat: evidence for interactions between the supraoptic and other diencephalic nuclei. *J Physiol*. 1990;431:225-41.

161. Ferguson AV and Bains JS. Actions of angiotensin in the subfornical organ and area postrema: implications for long term control of autonomic output. *Clin Exp Pharmacol Physiol*. 1997;24:96-101.

162. Simpson JB. The circumventricular organs and the central actions of angiotensin. *Neuroendocrinology*. 1981;32:248-56.

163. Gutman MB, Ciriello J and Mogenson GJ. Effects of plasma angiotensin II and hypernatremia on subfornical organ neurons. *Am J Physiol*. 1988;254:R746-54.

164. Miselis RR. The efferent projections of the subfornical organ of the rat: a circumventricular organ within a neural network subserving water balance. *Brain Res*. 1981;230:1-23.

165. Patel KP. Role of paraventricular nucleus in mediating sympathetic outflow in heart failure. *Heart Fail Rev*. 2000;5:73-86.

166. Herzig TC, Buchholz RA and Haywood JR. Effects of paraventricular nucleus lesions on chronic renal hypertension. *Am J Physiol*. 1991;261:H860-7.

167. Takeda K, Nakata T, Takesako T, Itoh H, Hirata M, Kawasaki S, Hayashi J, Oguro M, Sasaki S and Nakagawa M. Sympathetic inhibition and attenuation

of spontaneous hypertension by PVN lesions in rats. *Brain Res*. 1991;543:296-300.

168. Li DP, Yang Q, Pan HM and Pan HL. Pre- and postsynaptic plasticity underlying augmented glutamatergic inputs to hypothalamic presympathetic neurons in spontaneously hypertensive rats. *J Physiol*. 2008;586:1637-47.

169. Li DP, Byan HS and Pan HL. Switch to glutamate receptor 2-lacking AMPA receptors increases neuronal excitability in hypothalamus and sympathetic drive in hypertension. *J Neurosci*. 2012;32:372-80.

170. Gabor A and Leenen FH. Central mineralocorticoid receptors and the role of angiotensin II and glutamate in the paraventricular nucleus of rats with angiotensin II-induced hypertension. *Hypertension*. 2013;61:1083-90.

171. Gabor A and Leenen FH. Cardiovascular effects of angiotensin II and glutamate in the PVN of Dahl salt-sensitive rats. *Brain Res*. 2012;1447:28-37.

172. Park JB, Jo JY, Zheng H, Patel KP and Stern JE. Regulation of tonic GABA inhibitory function, presympathetic neuronal activity and sympathetic outflow from the paraventricular nucleus by astroglial GABA transporters. *J Physiol*. 2009;587:4645-60.

173. Chen QH and Toney GM. Responses to GABA-A receptor blockade in the hypothalamic PVN are attenuated by local AT1 receptor antagonism. *Am J Physiol Regul Integr Comp Physiol*. 2003;285:R1231-9.

174. Martin DS and Haywood JR. Reduced GABA inhibition of sympathetic function in renal-wrapped hypertensive rats. *Am J Physiol*. 1998;275:R1523-9.

175. Li DP and Pan HL. Plasticity of GABAergic control of hypothalamic presympathetic neurons in hypertension. *Am J Physiol Heart Circ Physiol*. 2006;290:H1110-9.

176. Sonner PM, Filosa JA and Stern JE. Diminished A-type potassium current and altered firing properties in presympathetic PVN neurones in renovascular hypertensive rats. *J Physiol*. 2008;586:1605-22.

177. Stocker SD and Muntzel MS. Recording sympathetic nerve activity chronically in rats: surgery techniques, assessment of nerve activity, and quantification. *Am J Physiol Heart Circ Physiol*. 2013;305:H1407-16.

178. Kuroki MT, Guzman PA, Fink GD and Osborn JW. Time-dependent changes in autonomic control of splanchnic vascular resistance and heart rate in ANG II-salt hypertension. *Am J Physiol Heart Circ Physiol*. 2012;302:H763-9.

179. Michelini LC and Stern JE. Exercise-induced neuronal plasticity in central autonomic networks: role in cardiovascular control. *Exp Physiol*. 2009;94:947-60.

180. MacGregor GA, Markandu ND, Sagnella GA, Singer DR and Cappuccio FP. Double-blind study of three sodium intakes and long-term effects of sodium restriction in essential hypertension. *Lancet*. 1989;2:1244-7.

181. Campese VM. Salt sensitivity in hypertension. Renal and cardiovascular implications. *Hypertension*. 1994;23:531-50.

182. Sacks FM, Svetkey LP, Vollmer WM, Appel LJ, Bray GA, Harsha D, Obarzanek E, Conlin PR, Miller ER, Simons-Morton DG, Karanja N, Lin PH and Grp D-SCR. Effects on blood pressure of reduced dietary sodium and the dietary approaches to stop hypertension (DASH) diet. *New Engl J Med*. 2001;344:3-10.

183. Adams JM, McCarthy JJ and Stocker SD. Excess dietary salt alters angiotensinergic regulation of neurons in the rostral ventrolateral medulla. *Hypertension*. 2008;52:932-7.

184. Adams JM, Madden CJ, Sved AF and Stocker SD. Increased dietary salt enhances sympathoexcitatory and sympathoinhibitory responses from the rostral ventrolateral medulla. *Hypertension*. 2007;50:354-9.

185. Pawloski-Dahm CM and Gordon FJ. Increased dietary salt sensitizes vasomotor neurons of the rostral ventrolateral medulla. *Hypertension*. 1993;22:929-33.

186. Ito S, Gordon FJ and Sved AF. Dietary salt intake alters cardiovascular responses evoked from the rostral ventrolateral medulla. *Am J Physiol*. 1999;276:R1600-7.

187. Simmonds SS, Lay J and Stocker SD. Dietary salt intake exaggerates sympathetic reflexes and increases blood pressure variability in normotensive rats. *Hypertension*. 2014;64:583-9.

188. Armstrong WE, Rubrum A, Teruyama R, Bond CT and Adelman JP. Immunocytochemical localization of small-conductance, calcium-dependent potassium channels in astrocytes of the rat supraoptic nucleus. *J Comp Neurol*. 2005;491:175-85.

189. Hayashi Y, Kawaji K, Sun L, Zhang X, Koyano K, Yokoyama T, Kohsaka S, Inoue K and Nakanishi H. Microglial Ca(2+)-activated K(+) channels are possible molecular targets for the analgesic effects of S-ketamine on neuropathic pain. *J Neurosci*. 2011;31:17370-82.

190. Kaushal V, Koeberle PD, Wang Y and Schlichter LC. The Ca2+-activated K+ channel KCNN4/KCa3.1 contributes to microglia activation and nitric oxide-dependent neurodegeneration. *J Neurosci*. 2007;27:234-44.

191. Hougaard C, Eriksen BL, Jorgensen S, Johansen TH, Dyhring T, Madsen LS, Strobaek D and Christophersen P. Selective positive modulation of the SK3 and SK2 subtypes of small conductance Ca2+-activated K+ channels. *British journal of pharmacology*. 2007;151:655-65.

192. Fluckiger JP, Sonnay M, Boillat N and Atkinson J. Attenuation of the baroreceptor reflex by general anesthetic agents in the normotensive rat. *European journal of pharmacology*. 1985;109:105-9.

193. Appel LJ, Frohlich ED, Hall JE, Pearson TA, Sacco RL, Seals DR, Sacks FM, Smith SC, Jr., Vafiadis DK and Van Horn LV. The importance of population-wide sodium reduction as a means to prevent cardiovascular disease and stroke: a call to action from the American Heart Association. *Circulation*. 2011;123:1138-43.

194. Kotchen TA, Cowley AW, Jr. and Frohlich ED. Salt in health and disease--a delicate balance. *The New England journal of medicine*. 2013;368:2531-2.

195. Weinberger MH. Salt sensitivity of blood pressure in humans. *Hypertension*. 1996;27:481-90.

196. Morimoto A, Uzu T, Fujii T, Nishimura M, Kuroda S, Nakamura S, Inenaga T and Kimura G. Sodium sensitivity and cardiovascular events in patients with essential hypertension. *Lancet*. 1997;350:1734-7.
197. Miselis RR. The efferent projections of the subfornical organ of the rat: a circumventricular organ within a neural network subserving water balance. *Brain Res*. 1981;230:1-23.
198. Larson RA, Gui L, Huber MJ, Chapp AD, Zhu J, LaGrange LP, Shan Z and Chen QH. Sympathoexcitation in ANG II-salt hypertension involves reduced SK channel function in the hypothalamic paraventricular nucleus. *Am J Physiol Heart Circ Physiol*. 2015;308:H1547-55.
199. Chao YM, Lai MD and Chan JY. Redox-sensitive endoplasmic reticulum stress and autophagy at rostral ventrolateral medulla contribute to hypertension in spontaneously hypertensive rats. *Hypertension*. 2013;61:1270-80.
200. Young CN, Li A, Dong FN, Horwath JA, Clark CG and Davisson RL. Endoplasmic reticulum and oxidant stress mediate nuclear factor-kappaB activation in the subfornical organ during angiotensin II hypertension. *Am J Physiol Cell Physiol*. 2015;308:C803-12.
201. Larson R, Gui L, Chapp A, Huber M, Zhu J, Cheng Z, Shan Z and Chen Q-H. Inhibition of endoplasmic reticulum function in PVN by thapsigargin increases neuronal excitability and sympathetic nerve activity (1125.4). *The FASEB Journal*. 2014;28.
202. Larson RA, Chapp AD, Huber MJ, Cheng Z, Shan Z and Chen Q-H. High Salt Intake Augments Excitability of Pre-sympathetic PVN Neurons Through Dysfunction of the Endoplasmic Reticulum Ca2+ ATPase. *Hypertension*. 2015;66:A138-A138.
203. Thastrup O, Cullen PJ, Drobak BK, Hanley MR and Dawson AP. Thapsigargin, a tumor promoter, discharges intracellular Ca2+ stores by specific inhibition of the endoplasmic reticulum Ca2(+)-ATPase. *Proc Natl Acad Sci U S A*. 1990;87:2466-70.
204. Grassi G, Arenare F, Pieruzzi F, Brambilla G and Mancia G. Sympathetic activation in cardiovascular and renal disease. *J Nephrol*. 2009;22:190-5.

205. Osborn JW and Fink GD. Region-specific changes in sympathetic nerve activity in angiotensin II-salt hypertension in the rat. *Exp Physiol*. 2010;95:61-8.
206. Larson RA, Chapp AD, Cheng Z, Shan Z and Chen Q-H. Diminished Intracellular Calcium in the Hypothalamic Paraventricular Nucleus Augments Neuronal Excitability and Sympathetic Nerve Activity. *The FASEB Journal*. 2016;30:757.13.
207. Sah P. Ca(2+)-activated K+ currents in neurones: types, physiological roles and modulation. *Trends Neurosci*. 1996;19:150-4.
208. Baba-Aissa F, Raeymaekers L, Wuytack F, Callewaert G, Dode L, Missiaen L and Casteels R. Purkinje neurons express the SERCA3 isoform of the organellar type Ca(2+)-transport ATPase. *Brain Res Mol Brain Res*. 1996;41:169-74.
209. Baba-Aissa F, Raeymaekers L, Wuytack F, De Greef C, Missiaen L and Casteels R. Distribution of the organellar Ca2+ transport ATPase SERCA2 isoforms in the cat brain. *Brain Res*. 1996;743:141-53.
210. Anwar A, Taimor G, Korkusuz H, Schreckenberg R, Berndt T, Abdallah Y, Piper HM and Schluter KD. PKC-independent signal transduction pathways increase SERCA2 expression in adult rat cardiomyocytes. *Journal of molecular and cellular cardiology*. 2005;39:911-9.
211. Anwar A, Schluter KD, Heger J, Piper HM and Euler G. Enhanced SERCA2A expression improves contractile performance of ventricular cardiomyocytes of rat under adrenergic stimulation. *Pflugers Arch*. 2008;457:485-91.
212. Kuo TH, Kim HR, Zhu L, Yu Y, Lin HM and Tsang W. Modulation of endoplasmic reticulum calcium pump by Bcl-2. *Oncogene*. 1998;17:1903-10.
213. Spoerri PE, Jentsch J and Glees P. Apamin from bee venom: effects of the neurotoxin on cultures of the embryonic mouse cortex. *Neurobiology*. 1973;3:207-14.
214. Spoerri PE, Jentsch J and Glees P. Apamin from bee venom. Effects of the neurotoxin on subcellular particles of neural cultures. *FEBS letters*. 1975;53:143-7.

215. Collister JP, Olson MK, Nahey DB, Vieira AA and Osborn JW. OVLT lesion decreases basal arterial pressure and the chronic hypertensive response to AngII in rats on a high-salt diet. *Physiol Rep*. 2013;1:e00128.

216. Osborn JW, Hendel MD, Collister JP, Ariza-Guzman PA and Fink GD. The role of the subfornical organ in angiotensin II-salt hypertension in the rat. *Exp Physiol*. 2012;97:80-8.

217. Ito S, Hiratsuka M, Komatsu K, Tsukamoto K, Kanmatsuse K and Sved AF. Ventrolateral medulla AT1 receptors support arterial pressure in Dahl salt-sensitive rats. *Hypertension*. 2003;41:744-50.

218. Adams JM, Bardgett ME and Stocker SD. Ventral lamina terminalis mediates enhanced cardiovascular responses of rostral ventrolateral medulla neurons during increased dietary salt. *Hypertension*. 2009;54:308-14.

219. Stocker SD, Lang SM, Simmonds SS, Wenner MM and Farquhar WB. Cerebrospinal Fluid Hypernatremia Elevates Sympathetic Nerve Activity and Blood Pressure via the Rostral Ventrolateral Medulla. *Hypertension*. 2015;66:1184-90.

Appendix A. Raw Data for Study 1.

Table A.1 Raw data for Splanchnic and Renal Sympathetic Nerve Activity for Angiotensin II-Salt treatment group.

	SSNA				RSNA			
Rat	Base (µV)	Max (µV)	%Change	Noise (µV)	Base (µV)	Max (µV)	%Change	Noise (µV)
1	0.086	0.107	32.881	0.023	-	-	-	-
2	0.019	0.021	20.119	0.007	-	-	-	-
3	0.064	0.068	8.990	0.023	0.013	0.013	-5.318	0.006
4	-	-	-	-	0.025	0.035	50.139	0.005
5	0.054	0.060	22.809	0.024	-	-	-	-
6	0.080	0.117	97.409	0.041	-	-	-	-
7	-	-	-	-	0.062	0.102	105.789	0.024
8	-	-	-	-	0.049	0.040	-18.367	-
9	-	-	-	-	0.061	0.062	1.631	-
10	-	-	-	-	0.062	0.086	37.180	-
11	-	-	-	-	0.050	0.053	6.219	-

Table A.2 Raw data for Mean Arterial Blood Pressure and Heart Rate for Angiotensin II-Salt treatment group.

	MAP			HR		
Rat	Base (mmHg)	Max (mmHg)	Delta (mmHg)	Base (mmHg)	Max (mmHg)	Delta (mmHg)
1	-	-	-	309	293	-13
2	145	143	-2	396	369	-27
3	139	131	2	-	-	-
4	-	-	-	424	479	55
5	129	146	17	401	354	-47
6	125	170	45	394	354	-47
7	124	136	12	332	330	-2
8	143	143	0	391	388	-3
9	117	122	5	414	442	28
10	-	-	-	482	487	5
11	-	-	-	413	423	10

SSNA-Splanchnic Sympathetic Nerve Activity; RSNA-Renal Sympathetic Nerve Activity; MAP-Mean Arterial Pressure; HR-Heart Rate.

Table A.3 Raw data for Splanchnic and Renal Sympathetic Nerve Activity for Angiotensin II treatment group.

	SSNA				RSNA			
Rat	**Base (μV)**	**Max (μV)**	**%Change**	**Noise (μV)**	**Base (μV)**	**Max (μV)**	**%Change**	**Noise (μV)**
1	0.058	0.135	245.687	0.027	-	-	-	-
2	0.121	0.170	68.837	0.049	0.008	0.011	64.662	0.004
3	0.091	0.214	374.618	0.059	0.015	0.029	138.198	0.005
4	0.048	0.101	145.504	0.011	0.030	0.052	131.481	0.014
5	-	-	-	-	-	-	-	-
6	-	-	-	-	0.044	0.040	-12.773	0.018
7	0.037	0.051	73.196	0.018	0.040	0.051	53.702	0.019

Table A.4 Raw data for Mean Arterial Blood Pressure and Heart Rate for Angiotensin II treatment group.

	MAP			HR		
Rat	**Base (mmHg)**	**Max (mmHg)**	**Delta (mmHg)**	**Base (mmHg)**	**Max (mmHg)**	**Delta (mmHg)**
1	121	150	29	418	428	10
2	115	154	39	401	413	12
3	118	159	41	375	413	38
4	125	155	30	-	-	-
5	101	140	39	367	372	5
6	87	121	34	303	329	26
7	90	118	28	321	326	5

SSNA-Splanchnic Sympathetic Nerve Activity; RSNA-Renal Sympathetic Nerve Activity; MAP-Mean Arterial Pressure; HR-Heart Rate.

Table A.5 Raw data for Splanchnic and Renal Sympathetic Nerve Activity for High Salt treatment group.

	SSNA				RSNA			
Rat	**Base (μV)**	**Max (μV)**	**%Change**	**Noise (μV)**	**Base (μV)**	**Max (μV)**	**%Change**	**Noise (μV)**
1	0.087	0.184	192.09	0.037	0.019	0.026	47.45	0.005
2	0.065	0.098	125.40	0.039	-	-	-	-
3	0.026	0.044	95.94	0.008	0.099	0.115	38.29	0.056
4	-	-	-	-	0.010	0.013	63.88	0.006
5	0.021	0.023	44.28	0.017	-	-	-	-
6	0.013	0.031	198.94	0.004	0.034	0.064	160.20	0.016
7	0.074	0.084	51.91	0.055	0.045	0.048	15.82	0.030
8	0.043	0.071	180.64	0.028	0.017	0.021	58.68	0.011
9	0.055	0.094	114.62	0.021	0.051	0.073	55.87	0.011

Table A.6 Raw data for Mean Arterial Blood Pressure and Heart Rate for Angiotensin II treatment group.

	MAP			HR		
Rat	**Base (mmHg)**	**Max (mmHg)**	**Delta (mmHg)**	**Base (mmHg)**	**Max (mmHg)**	**Delta (mmHg)**
1	-	-	-	385	342	-43
2	81	118	37	354	392	38
3	127	130	3	365	388	23
4	114	131	17	359	349	-10
5	99	107	8	343	352	9
6	102	134	32	355	374	19
7	-	-	-	-	-	-
8	120	153	33	335	395	60
9	123	132	9	318	343	25

SSNA-Splanchnic Sympathetic Nerve Activity; RSNA-Renal Sympathetic Nerve Activity; MAP-Mean Arterial Pressure; HR-Heart Rate.

Table A.7 Raw data for Splanchnic and Renal Sympathetic Nerve Activity for Normal Salt treatment group.

	SSNA				RSNA			
Rat	Base (μV)	Max (μV)	%Change	Noise (μV)	Base (μV)	Max (μV)	%Change	Noise (μV)
1	0.021	0.058	384.52	0.011	-	-	-	-
2	0.021	0.046	344.28	0.014	-	-	-	-
3	0.022	0.057	337.56	0.012	0.025	0.052	214.76	0.012
4	0.042	0.068	266.96	0.032	-	-	-	-
5	-	-	-	-	0.038	0.056	211.55	0.033
6	-	-	-	-	0.039	0.046	162.70	0.036
7	-	-	-	-	0.041	0.055	200.42	0.033
8	-	-	-	-	0.042	0.056	209.79	0.034
9	0.030	0.046	105.06	0.014	0.058	0.093	136.33	0.032
10	0.034	0.051	79.34	0.013	0.187	0.395	130.91	0.027
11	0.035	0.059	282.09	0.026	0.051	0.076	79.31	0.020
12	0.020	0.051	308.27	0.009	0.042	0.110	272.34	0.017

Table A.8 Raw data for Mean Arterial Blood Pressure and Heart Rate for Angiotensin II treatment group.

	MAP			HR		
Rat	Base (mmHg)	Max (mmHg)	Delta (mmHg)	Base (mmHg)	Max (mmHg)	Delta (mmHg)
1	110	145	35	-	-	-
2	67	113	46	-	-	-
3	107	129	22	460	480	20
4	109	143	34	441	450	9
5	82	125	43	388	478	90
6	116	172	56	325	329	4
7	116	148	32	335	374	39
8	113	123	10	288	348	60
9	-	-	-	-	-	-
10	116	169	53	376	454	78
11	-	-	-	-	-	-
12	110	146	36	353	355	2

SSNA-Splanchnic Sympathetic Nerve Activity; RSNA-Renal Sympathetic Nerve Activity; MAP-Mean Arterial Pressure; HR-Heart Rate.

Table A.9 Raw data for Small Conductance Ca^{2+} Activated K^{+} Channel (1-3) Western Blot Protein Expression.

Flourescent Intensity Normalized to β-actin					
SK1-NS	**SK1-AngII-Salt**	**SK2-NS**	**SK2-AngII-salt**	**SK3-NS**	**SK3-AngII-salt**
0.42	0.48	0.93	0.90	0.66	0.67
0.39	0.37	0.84	0.88	0.67	0.46
0.40	0.33	0.89	0.72	0.62	0.47
0.43	0.48	0.90	0.85	0.59	0.54
0.38	0.46	0.77	0.81	0.50	0.52
0.40	0.47	0.76	0.83	0.51	0.56
0.44	0.50	0.81	0.87	0.50	0.60

SK- Small Conductance Ca2+ Activated K+ Channel; NS-Normal Salt; AngII-salt-AngiotensinII-Salt Hypertension.

Appendix B. Summary Statistics for Study 1.

Table B.1 Mean splanchnic sympathetic nerve activity % change from baseline following PVN microinjection of apamin.

	NS	AngII-salt	HS	AngII
Number of values	8	5	8	5
Mean	263.50	36.44	125.50	181.60
Std. Deviation	112.10	35.13	60.80	129.60
Std. Error	39.65	15.71	21.49	57.94
Lower 95% CI of mean	169.80	-7.17	74.65	20.71
Upper 95% CI of mean	357.30	80.06	176.30	342.40

Table B.2 Mean renal sympathetic nerve activity % change from baseline following PVN microinjection of apamin.

	NS	AngII-salt	HS	AngII
Number of values	8	5	8	5
Mean	179.80	25.32	62.88	75.05
Std. Deviation	57.87	42.83	45.82	62.15
Std. Error	19.29	16.19	17.32	27.79
Lower 95% CI of mean	135.30	-14.29	20.51	-2.11
Upper 95% CI of mean	224.30	64.93	105.30	152.20

Std.-standard; NS-normal salt; AngII -Angiotensin II; HS-high salt; CI-confidence interval.

Table B.3 Mean change from baseline for mean arterial pressure (mmHg) following PVN microinjection of apamin.

	NS	AngII-salt	HS	AngII
Number of values	10	7	7	7
Mean	36.74	11.29	19.86	34.29
Std. Deviation	13.90	16.33	13.93	5.41
Std. Error	4.40	6.17	5.27	2.04
Lower 95% CI of mean	26.79	-3.81	6.97	29.28
Upper 95% CI of mean	46.68	26.39	32.74	39.29

Table B.4 Mean change from baseline for heart rate (beats/minute) following PVN microinjection of apamin.

	NS	AngII-salt	HS	AngII
Number of values	8	9	8	6
Mean	37.70	4.78	15.13	16.00
Std. Deviation	34.69	24.43	31.07	13.25
Std. Error	12.26	8.14	10.99	5.41
Lower 95% CI of mean	8.70	-14.00	-10.85	2.09
Upper 95% CI of mean	66.70	23.56	41.10	29.91

Std.-standard; NS-normal salt; AngII -Angiotensin II; HS-high salt; CI-confidence interval.

Table B.5 One-way ANOVA for splanchnic sympathetic nerve activity % change from baseline following PVN microinjection of apamin.

One-way analysis of variance			
P value	0.002		
Number of groups	4		
F	6.855		
R square	0.4831		
Bartlett's test for equal variances			
Bartlett's statistic (corrected)	7.359		
P value	0.0613		
ANOVA Table	**SS**	**df**	**MS**
Treatment (between columns)	173841	3	57947
Residual (within columns)	185977	22	8454
Total	359818	25	
Newman-Keuls	**Mean Diff.**	**q**	**P < 0.05?**
AngII-salt vs NS	-227.1	6.126	Yes
AngII-salt vs AngII only	-145.1	3.53	No
AngII-salt vs HS	-89.04	---	No
HS vs NS	-138	4.246	Yes
HS vs AngII	-56.09	---	No
AngII vs NS	-81.94	2.211	No

NS-normal salt; AngII -Angiotensin II; HS-high salt

Table B.6 One-way ANOVA for renal sympathetic nerve activity % change from baseline following PVN microinjection of apamin.

One-way analysis of variance			
P value	< 0.0001		
Number of groups	4		
F	13.1		
R square	0.6208		
Bartlett's test for equal variances			
Bartlett's statistic (corrected)	0.984		
P value	0.8051		
ANOVA Table	**SS**	**df**	**MS**
Treatment (between columns)	107810	3	35937
Residual (within columns)	65840	24	2743
Total	173649	27	
Newman-Keuls	**Mean Diff.**	**q**	**P < 0.05?**
AngII-salt vs NS	-154.5	8.276	Yes
AngII-salt vs AngII only	-49.73	2.293	No
AngII-salt vs HS	-37.56	---	No
HS vs NS	-116.9	6.264	Yes
HS vs AngII	-12.17	---	No
AngII vs NS	-104.7	5.07	Yes

NS-normal salt; AngII -Angiotensin II; HS-high salt

Table B.7 One-way ANOVA for change from baseline for mean arterial pressure (mmHg) following PVN microinjection of apamin.

One-way analysis of variance			
P value	0.0018		
Number of groups	4		
F	6.543		
R square	0.4209		
Bartlett's test for equal variances			
Bartlett's statistic (corrected)	6.045		
P value	0.1095		
ANOVA Table	**SS**	**df**	**MS**
Treatment (between columns)	3401	3	1134
Residual (within columns)	4678	27	173.3
Total	8078	30	
Newman-Keuls	**Mean Diff.**	**q**	**P < 0.05?**
AngII-salt vs NS	-25.45	5.548	Yes
AngII-salt vs AngII only	-23	4.623	Yes
AngII-salt vs HS	-8.571	1.723	No
HS vs NS	-16.88	3.68	Yes
HS vs AngII	-14.43	2.9	No
AngII vs NS	-2.449	0.534	No

NS-normal salt; AngII -Angiotensin II; HS-high salt

Table B.8 One-way ANOVA for change from baseline for heart rate (beats/minute) following PVN microinjection of apamin.

One-way analysis of variance			
P value	0.1292		
Number of groups	4		
F	2.059		
R square	0.1862		
Bartlett's test for equal variances			
Bartlett's statistic (corrected)	4.491		
P value	0.2131		
ANOVA Table	**SS**	**df**	**MS**
Treatment (between columns)	4767	3	1589
Residual (within columns)	20835	27	771.7
Total	25602	30	
Newman-Keuls	**Mean Diff.**	**q**	**P < 0.05?**
AngII-salt vs NS	32.92	3.449	No
AngII-salt vs AngII only	-11.22	-	No
AngII-salt vs HS	-10.35	-	No
HS vs NS	22.57	-	No
HS vs AngII	-0.875	-	No
AngII vs NS	21.7	-	No

NS-normal salt; AngII -Angiotensin II; HS-high salt

Appendix C. Raw Data for Study 2.

Table C.1 Raw data for Splanchnic and Renal Sympathetic Nerve Activity for Thapsigargin 0.15nmol treatment group.

	SSNA				RSNA			
Rat	Base (μV)	Max (μV)	%Change	Noise (μV)	Base (μV)	Max (μV)	%Change	Noise (μV)
1	0.063	0.068	18.939	0.037	0.046	0.049	10.000	0.016
2	0.027	0.032	36.913	0.012	0.022	0.024	24.138	0.013
3	0.050	0.052	5.277	0.012	0.050	0.052	5.743	0.020
4	0.047	0.049	7.358	0.017	0.068	0.072	7.984	0.018

Table C.2 Raw data for Mean Arterial Blood Pressure and Heart Rate for Thapsigargin 0.15nmol treatment group.

	MAP			HR		
Rat	Base (mmHg)	Max (mmHg)	Delta (mmHg)	Base (mmHg)	Max (mmHg)	Delta (mmHg)
1	100	99	-1	348	344	-4
2	97	101	4	369	386	17
3	131	128	-3	323	331	8
4	98	103	5	349	356	7

SSNA-Splanchnic Sympathetic Nerve Activity; RSNA-Renal Sympathetic Nerve Activity; MAP-Mean Arterial Pressure; HR-Heart Rate.

Table C.3 Raw data for Splanchnic and Renal Sympathetic Nerve Activity for Thapsigargin 0.30nmol treatment group.

	SSNA				RSNA			
Rat	Base (μV)	Max (μV)	%Change	Noise (μV)	Base (μV)	Max (μV)	%Change	Noise (μV)
1	0.038	0.041	18.497	0.021	0.025	0.029	27.211	0.011
2	0.046	0.061	53.546	0.018	0.016	0.018	26.804	0.006
3	0.023	0.029	45.070	0.009	0.019	0.020	6.604	0.009
4	0.032	0.036	20.833	0.013	0.011	0.012	20.000	0.007
5	0.046	0.052	29.891	0.028	0.037	0.041	14.634	0.008

Table C.4 Raw data for Mean Arterial Blood Pressure and Heart Rate for Thapsigargin 0.30nmol treatment group.

	MAP			HR		
Rat	Base (mmHg)	Max (mmHg)	Delta (mmHg)	Base (mmHg)	Max (mmHg)	Delta (mmHg)
1	124	130	6	311	317	6
2	110	118	8	352	350	-2
3	109	112	3	353	357	4
4	95	109	14	333	334	1
5	136	138	2	340	350	10

SSNA-Splanchnic Sympathetic Nerve Activity; RSNA-Renal Sympathetic Nerve Activity; MAP-Mean Arterial Pressure; HR-Heart Rate.

Table C.5 Raw data for Splanchnic and Renal Sympathetic Nerve Activity for Thapsigargin 0.75nmol treatment group.

	SSNA				RSNA			
Rat	Base (μV)	Max (μV)	%Change	Noise (μV)	Base (μV)	Max (μV)	%Change	Noise (μV)
1	0.025	0.036	83.745	0.012	-	-	-	-
2	0.036	0.054	90.863	0.017	0.021	0.029	86.364	0.012
3	0.028	0.040	79.021	0.014	0.029	0.038	85.714	0.018
4	0.044	0.064	91.781	0.022	0.023	0.030	60.345	0.011
5	0.019	0.030	121.053	0.009	0.016	0.021	57.471	0.007
6	0.052	0.081	86.747	0.019	0.074	0.109	68.279	0.022

Table C.6 Raw data for Mean Arterial Blood Pressure and Heart Rate for Thapsigargin 0.75nmol treatment group.

	MAP			HR		
Rat	Base (mmHg)	Max (mmHg)	Delta (mmHg)	Base (mmHg)	Max (mmHg)	Delta (mmHg)
1	108	125	17	346	370	24
2	123	137	14	337	341	4
3	113	126	13	330	342	12
4	82	92	10	362	368	6
5	110	114	4	373	375	2
6	105	109	4	354	356	2

SSNA-Splanchnic Sympathetic Nerve Activity; RSNA-Renal Sympathetic Nerve Activity; MAP-Mean Arterial Pressure; HR-Heart Rate.

Table C.7 Raw data for Splanchnic and Renal Sympathetic Nerve Activity for Thapsigargin 1.5nmol treatment group.

	SSNA				RSNA			
Rat	Base (μV)	Max (μV)	%Change	Noise (μV)	Base (μV)	Max (μV)	%Change	Noise (μV)
1	0.031	0.044	82.166	0.015	0.020	0.023	28.125	0.007
2	0.022	0.030	71.171	0.011	-	-	-	-
3	0.023	0.031	62.097	0.011	0.032	0.052	112.360	0.014
4	0.020	0.032	109.009	0.009	0.038	0.050	41.554	0.008
5	0.019	0.029	84.821	0.008	0.015	0.024	92.553	0.006

Table C.8 Raw data for Mean Arterial Blood Pressure and Heart Rate for Thapsigargin 1.5nmol treatment group.

	MAP			HR		
Rat	Base (mmHg)	Max (mmHg)	Delta (mmHg)	Base (mmHg)	Max (mmHg)	Delta (mmHg)
1	106	118	12	348	349	1
2	115	123	8	352	375	23
3	114	120	6	322	335	13
4	114	122	8	366	387	21
5	107	116	9	294	298	4

SSNA-Splanchnic Sympathetic Nerve Activity; RSNA-Renal Sympathetic Nerve Activity; MAP-Mean Arterial Pressure; HR-Heart Rate.

Table C.9 Raw data for Splanchnic and Renal Sympathetic Nerve Activity for Thapsigargin 0.75nmol in High Salt diet treatment group.

	SSNA				RSNA			
Rat	Base (µV)	Max (µV)	%Change	Noise (µV)	Base (µV)	Max (µV)	%Change	Noise (µV)
1	0.032	0.038	32.940	0.011	-	-	-	-
2	-	-	-	-	0.013	0.016	34.276	0.005
3	-	-	-	-	0.027	0.031	33.813	0.013
4	0.068	0.085	52.199	0.034	-	-	-	-
5	0.073	0.079	23.556	0.051	0.050	0.054	14.098	0.020
6	0.037	0.043	28.571	0.016	0.009	0.010	44.444	0.006
7	0.019	0.022	54.717	0.014	0.034	0.037	15.217	0.011
8	0.047	0.050	10.248	0.015	0.036	0.039	16.372	0.013

Table C.10 Raw data for Mean Arterial Blood Pressure and Heart Rate for Thapsigargin 0.75nmol in High Salt diet treatment group.

	MAP			HR		
Rat	Base (mmHg)	Max (mmHg)	Delta (mmHg)	Base (mmHg)	Max (mmHg)	Delta (mmHg)
1	104	120	16	318	315	-3
2	99	109	10	328	346	18
3	114	122	8	368	370	2
4	113	124	11	312	320	8
5	80	82	1	248	244	-4
6	114	127	13	304	306	2
7	112	117	5	366	380	14
8	113	110	-3	355	357	2

SSNA-Splanchnic Sympathetic Nerve Activity; RSNA-Renal Sympathetic Nerve Activity; MAP-Mean Arterial Pressure; HR-Heart Rate.

Table C.11 Raw data for Splanchnic and Renal Sympathetic Nerve Activity for Thapsigargin 0.75nmol intravenous infusion.

	SSNA				RSNA			
Rat	Base (μV)	Max (μV)	%Change	Noise (μV)	Base (μV)	Max (μV)	%Change	Noise (μV)
1	-	-	-	-	0.040	0.044	14.232	0.013
2	0.016	0.017	8.974	0.008	0.025	0.026	4.023	0.008
3	0.026	0.027	2.837	0.012	0.071	0.072	1.167	0.020
4	0.026	0.027	6.098	0.010	0.040	0.038	-9.524	0.019

Table C.12 Raw data for Mean Arterial Blood Pressure and Heart Rate for Thapsigargin 0.75nmol in High Salt diet treatment group.

	MAP			HR		
Rat	Base (mmHg)	Max (mmHg)	Delta (mmHg)	Base (mmHg)	Max (mmHg)	Delta (mmHg)
1	120	123	-3	301	306	5
2	114	94	-20	406	403	-3
3	123	125	2	346	343	-3
4	86	87	1	317	322	5

SSNA-Splanchnic Sympathetic Nerve Activity; RSNA-Renal Sympathetic Nerve Activity; MAP-Mean Arterial Pressure; HR-Heart Rate.

Table C.13 Raw data for Splanchnic and Renal Sympathetic Nerve Activity for Thapsigargin 0.75nmol microinjection in the lateral hypothalamus.

	SSNA				RSNA			
Rat	Base (μV)	Max (μV)	%Change	Noise (μV)	Base (μV)	Max (μV)	%Change	Noise (μV)
1	-	-	-	-	0.038	0.036	-7.968	0.013
2	0.023	0.025	15.000	0.013	-	-	-	-
3	0.018	0.021	31.633	0.008	0.028	0.033	24.631	0.008
4	0.024	0.024	-1.563	0.012	0.066	0.065	-1.316	0.020
5	0.029	0.031	-2.985	0.096	0.037	0.037	1.667	0.019

Table C.14 Raw data for Mean Arterial Blood Pressure and Heart Rate for Thapsigargin 0.75nmol in microinjection in the lateral hypothalamus.

	MAP			HR		
Rat	Base (mmHg)	Max (mmHg)	Delta (mmHg)	Base (mmHg)	Max (mmHg)	Delta (mmHg)
1	116	114	-2	318	305	-13
2	121	120	-1	291	294	3
3	114	116	2	405	417	12
4	117	120	3	339	329	-10
5	88	89	1	332	323	-9

SSNA-Splanchnic Sympathetic Nerve Activity; RSNA-Renal Sympathetic Nerve Activity; MAP-Mean Arterial Pressure; HR-Heart Rate.

Table C.15 Raw data for Splanchnic and Renal Sympathetic Nerve Activity for DMSO (vehicle) microinjection in paraventricular nucleus.

	SSNA				RSNA			
Rat	Base (μV)	Max (μV)	%Change	Noise (μV)	Base (μV)	Max (μV)	%Change	Noise (μV)
1	0.038	0.039	3.211	0.016	0.023	0.025	9.756	0.011
2	0.020	0.020	1.695	0.008	0.016	0.015	-10.000	0.006
3	0.026	0.026	1.325	0.011	0.026	0.027	3.468	0.009

Table C.16 Raw data for Mean Arterial Blood Pressure and Heart Rate for DMSO (vehicle) microinjection in paraventricular nucleus.

	MAP			HR		
Rat	Base (mmHg)	Max (mmHg)	Delta (mmHg)	Base (mmHg)	Max (mmHg)	Delta (mmHg)
1	126	125	-1	357	358	1
2	105	105	0	290	284	-6
3	103	107	4	410	402	-8

SSNA-Splanchnic Sympathetic Nerve Activity; RSNA-Renal Sympathetic Nerve Activity; MAP-Mean Arterial Pressure; HR-Heart Rate.

Table C.17 Firing frequency in response to step current injection in PVN-RVLM neurons from normal salt rats.

	NS Control Firing Frequency (Hz)							
Current Injection	**Cell 1**	**Cell 2**	**Cell 3**	**Cell 4**	**Cell 5**	**Cell 6**	**Cell 7**	**Cell 8**
50	1.25	0.00	0.00	3.75	6.25	0.00	1.25	0.00
100	6.25	7.50	11.25	13.75	12.50	7.50	5.00	6.25
150	11.25	12.50	20.00	22.50	16.25	15.00	13.75	13.75
200	15.00	17.50	28.75	30.00	20.00	21.25	21.25	21.25

Table C.18 Firing frequency in response to step current injection in PVN-RVLM neurons from normal salt rats following bath application of Thapsigargin.

	NS Thapsigargin Firing Frequency (Hz)					
Current Injection	**Cell 1**	**Cell 2**	**Cell 3**	**Cell 4**	**Cell 5**	**Cell 6**
50	0.00	6.25	6.25	7.50	1.25	10.00
100	8.75	17.50	16.25	12.50	7.50	33.75
150	22.50	27.50	31.25	18.75	13.75	27.50
200	32.50	37.50	41.25	32.50	17.50	7.50

PVN-paraventricular nucleus; RVLM-rostralventrolateral medulla; NS-normal salt; Hz-Hertz

Table C.19 Firing frequency in response to step current injection in PVN-RVLM neurons from high salt rats.

	HS Control Firing Frequency (Hz)				
Current Injection	**Cell 1**	**Cell 2**	**Cell 3**	**Cell 4**	**Cell 5**
50	5.00	2.50	8.75	0.00	0.00
100	25.00	6.25	18.75	7.50	10.00
150	40.00	16.25	30.00	13.75	18.75
200	47.50	26.25	37.50	21.25	36.25

Table C.20 Firing frequency in response to step current injection in PVN-RVLM neurons from high salt rats following bath application of Thapsigargin.

	HS Thapsigargin Firing Frequency (Hz)					
Current Injection	**Cell 1**	**Cell 2**	**Cell 3**	**Cell 4**	**Cell 5**	**Cell 6**
50	1.25	1.25	5.00	6.25	5.00	7.50
100	6.25	6.25	11.25	15.00	10.00	28.75
150	16.25	15.00	17.50	33.75	17.50	42.50
200	25.00	18.75	23.75	46.25	26.25	52.5

PVN-paraventricular nucleus; RVLM-rostralventrolateral medulla; NS-normal salt; Hz-Hertz

Table C.21 Resting membrane potential (mV) in PVN-RVLM neurons from normal salt and high salt rats.

Cell	NS	NS TG	HS	HS TG
1	-69.00	-50.00	-49.00	-51.00
2	-60.00	-59.00	-55.00	-65.00
3	-61.00	-52.00	-48.00	-65.00
4	-64.00	-59.00	-58.00	-51.00
5	-51.00	-67.00	-60.00	-57.00
6	-55.00	-64.00	-44.00	-59.00
7	-59.00	-	-53.00	-
8	-51.00	-	-	-

Table C.22 Membrane capacitance (pF) in PVN-RVLM neurons from normal salt and high salt rats.

Cell	NS	NS TG	HS	HS TG
1	70.00	39.00	45.00	44.00
2	68.00	33.00	27.00	73.00
3	44.00	31.00	28.00	61.00
4	47.00	44.00	59.00	32.00
5	44.00	61.00	49.00	37.00
6	48.00	30.00	34.00	38.00
7	47.00	-	36.00	-
8	54.00	-	-	-

pF-picofarads; PVN-paraventricular nucleus; RVLM rostral ventrolateral medulla; NS normal salt; HS-high salt; TG-thapsigargin

Table C.23 Depolarizing input resistance (GigaOhm) in PVN-RVLM neurons from normal salt and high salt rats.

Cell	NS	NS TG	HS	HS TG
1	0.67	0.52	0.75	0.66
2	0.53	0.30	0.78	0.55
3	0.64	1.10	0.78	0.62
4	0.59	1.19	0.52	0.90
5	0.78	0.68	0.50	0.82
6	0.60	0.86	0.85	0.66
7	0.64	-	1.12	-
8	0.49	-	-	-

Table C.24 Sub-threshold of membrane potential to fire action potential (mV) in PVN-RVLM neurons from normal salt and high salt rats.

Cell	NS	NS TG	HS	HS TG
1	0.67	0.52	0.75	0.66
2	0.53	0.30	0.78	0.55
3	0.64	1.10	0.78	0.62
4	0.59	1.19	0.52	0.90
5	0.78	0.68	0.50	0.82
6	0.60	0.86	0.85	0.66
7	0.64	-	1.12	-
8	0.49	-	-	-

mV-millivolts; PVN-paraventricular nucleus; RVLM rostral ventrolateral medulla; NS normal salt; HS-high salt; TG-thapsigargin

Table C.25 Inter-spike interval (milliseconds) in PVN-RVLM neurons from normal salt rats.

	Inter-Spike Interval (milliseconds) NS							
AP #	**Cell 1**	**Cell 2**	**Cell 3**	**Cell 4**	**Cell 5**	**Cell 6**	**Cell 7**	**Cell 8**
1	10.95	35.20	15.80	25.00	21.40	31.60	28.40	24.70
2	12.74	39.70	20.60	26.50	25.80	46.40	29.40	27.20
3	13.57	40.80	23.60	26.50	28.30	48.50	35.10	28.90
4	13.83	48.00	27.20	30.20	34.50	45.70	34.60	28.70
5	13.19	54.70	32.50	29.60	39.40	51.30	47.00	30.40
6	13.04	55.50	34.60	28.30	50.60	49.10	44.20	33.90
7	12.92	61.50	37.90	30.60	44.50	46.00	43.50	38.00
8	14.43	58.40	34.00	32.70	50.90	49.60	56.30	40.80
9	12.56	63.40	38.30	31.30	50.40	51.70	49.10	41.50
10	13.89	67.60	36.30	33.30	53.60	50.70	55.20	50.50

Table C.26 Inter-spike interval (milliseconds) in PVN-RVLM neurons from normal salt rats following bath application of thapsigargin.

	Inter-Spike Interval (milliseconds) NS TG					
AP #	**Cell 1**	**Cell 2**	**Cell 3**	**Cell 4**	**Cell 5**	**Cell 6**
1	23.60	29.70	15.30	69.80	13.70	23.50
2	25.00	26.10	19.40	62.00	14.50	26.00
3	26.00	30.80	20.70	64.90	15.90	28.50
4	27.90	25.70	22.70	58.40	16.90	33.00
5	29.20	23.20	23.00	65.00	18.80	41.50
6	30.00	23.70	24.50	64.70	20.60	45.50
7	31.00	23.90	23.70	57.90	22.70	51.50
8	30.10	24.70	24.80	53.60	24.00	57.00
9	29.80	21.10	24.50	61.30	25.10	60.00
10	31.60	25.10	22.10	61.50	25.60	64.00

PVN-paraventricular nucleus; RVLM rostral ventrolateral medulla; NS normal salt; HS-high salt; TG-thapsigargin; AP Action potential

Table C.27 Inter-spike interval (milliseconds) in PVN-RVLM neurons from high salt rats following bath application of thapsigargin.

	Inter-Spike Interval (milliseconds) HS					
AP#	**Cell 1**	**Cell 2**	**Cell 3**	**Cell 4**	**Cell 5**	**Cell 6**
1	16.10	16.50	15.20	26.90	10.00	13.20
2	17.90	19.40	16.60	30.30	13.00	14.00
3	19.00	21.70	17.40	31.00	15.30	15.80
4	20.30	21.20	18.60	36.20	17.50	16.30
5	20.00	23.70	20.20	40.40	15.80	16.20
6	20.00	30.80	23.60	41.40	16.80	17.40
7	21.00	31.00	24.80	45.90	22.90	16.90
8	21.50	30.80	25.20	49.20	23.60	18.10
9	20.80	35.80	23.40	52.30	20.70	18.50
10	21.20	38.10	25.50	51.00	26.10	18.40

Table C.28 Inter-spike interval (milliseconds) in PVN-RVLM neurons from high salt rats following bath application of thapsigargin.

	Inter-Spike Interval (milliseconds) HS TG					
AP #	**Cell 1**	**Cell 2**	**Cell 3**	**Cell 4**	**Cell 5**	**Cell 6**
1	27.00	28.50	36.50	12.70	15.20	18.60
2	29.60	33.50	37.30	14.40	15.50	18.90
3	33.10	37.10	37.30	16.00	16.20	24.60
4	34.30	39.60	33.60	16.10	16.00	17.90
5	34.50	45.60	34.40	16.70	16.70	20.00
6	37.20	48.60	36.90	17.70	18.00	18.20
7	37.60	58.50	37.30	20.50	18.50	17.80
8	42.20	63.00	35.70	20.60	20.10	17.80
9	42.90	66.70	36.90	19.40	21.10	17.80
10	49.80	64.00	37.50	21.50	21.10	16.50

PVN-paraventricular nucleus; RVLM rostral ventrolateral medulla; NS normal salt; HS-high salt; TG-thapsigargin; AP Action potential

Appendix D. Summary Statistics for Study 2.

Table D.1 Mean splanchnic sympathetic nerve activity % change from baseline following PVN microinjection of Thapsigargin in normal rats.

	DMSO	TG 0.15nmol	TG 0.30nmol	TG 0.75nmol	TG 1.5nmol
Number of values	3	4	5	6	5.00
Mean	2.07	17.13	33.56	92.22	81.84
Std. Deviation	1.00	14.48	15.29	14.92	17.67
Std. Error	0.58	7.24	6.84	6.09	7.90
Lower 95% CI of mean	-0.42	-5.91	14.57	76.56	59.90
Upper 95% CI of mean	4.56	40.16	52.55	107.90	103.80

Table D.2 Mean renal sympathetic nerve activity % change from baseline following PVN microinjection of Thapsigargin in normal rats.

	DMSO	TG 0.15nmol	TG 0.30nmol	TG 0.75nmol	TG 1.5nmol
Number of values	3	4	5	5	4.00
Mean	1.10	11.95	19.06	71.62	68.67
Std. Deviation	10.12	8.29	8.68	13.75	40.27
Std. Error	5.84	4.14	3.88	6.15	20.13
Lower 95% CI of mean	-24.03	-1.24	8.28	54.55	4.60
Upper 95% CI of mean	26.23	25.14	29.84	88.69	132.70

DMSO-dimethyl sulfoxide; TG-thapsigargin; Std-standard; CI-confidence interval

Table D.3 Average mean arterial blood pressure change from baseline following PVN microinjection of Thapsigargin in normal rats.

	DMSO	TG 0.15nmol	TG 0.30nmol	TG 0.75nmol	TG 1.5nmol
Number of values	3	4	5	6	5.00
Mean	1.00	1.25	6.60	10.33	8.60
Std. Deviation	2.65	3.86	4.78	5.39	2.19
Std. Error	1.53	1.93	2.14	2.20	0.98
Lower 95% CI of mean	-5.57	-4.90	0.67	4.68	5.88
Upper 95% CI of mean	7.57	7.40	12.53	15.99	11.32

Table D.4 Average heart rate (beats/minute) change from baseline following PVN microinjection of Thapsigargin in normal rats.

	DMSO	TG 0.15nmol	TG 0.30nmol	TG 0.75nmol	TG 1.5nmol
Number of values	3	4	5	6	5.00
Mean	-4.33	7.00	3.80	8.33	12.40
Std. Deviation	4.73	8.60	4.60	8.52	9.84
Std. Error	2.73	4.30	2.06	3.48	4.40
Lower 95% CI of mean	-16.07	-6.69	-1.92	-0.61	0.18
Upper 95% CI of mean	7.41	20.69	9.52	17.28	24.62

DMSO-dimethyl sulfoxide; TG-thapsigargin; Std-standard; CI-confidence interval

Table D.5 Mean splanchnic sympathetic nerve activity % change from baseline following PVN microinjection of Thapsigargin in normal control and high salt rats.

	HS TG	TG IV	TG Lat Hypo
Number of values	6	3	4
Mean	33.71	5.97	10.52
Std. Deviation	17.11	3.07	16.27
Std. Error of Mean	6.99	1.77	8.14
Lower 95% CI of mean	15.75	-1.66	-15.37
Upper 95% CI of mean	51.66	13.60	36.41

Table D.6 Mean renal sympathetic nerve activity % change from baseline following PVN microinjection of Thapsigargin in normal control and high salt rats.

	HS TG	TG IV	TG Lat Hypo
Number of values	6	4	4
Mean	26.37	2.48	4.25
Std. Deviation	12.80	9.77	14.17
Std. Error of Mean	5.23	4.89	7.09
Lower 95% CI of mean	12.93	-13.07	-18.29
Upper 95% CI of mean	39.81	18.02	26.80

TG-thapsigargin; Std-standard; CI-confidence interval; HS-high salt; IV-intravenous; Lat Hypo-Lateral Hypothalamus

Table D.7 Average mean arterial blood pressure change from baseline following PVN microinjection of Thapsigargin in normal control and high salt rats.

	HS TG	TG IV	TG Lat Hypo
Number of values	8	4	5
Mean	7.63	-5.00	0.60
Std. Deviation	6.32	10.23	2.07
Std. Error of Mean	2.24	5.12	0.93
Lower 95% CI of mean	2.34	-21.28	-1.98
Upper 95% CI of mean	12.91	11.28	3.18

Table D.8 Average heart rate (beats/minute) change from baseline following PVN microinjection of Thapsigargin in normal rats.

	HS TG	TG IV	TG Lat Hypo
Number of values	8	4	5
Mean	4.88	1.00	-3.40
Std. Deviation	7.85	4.62	10.55
Std. Error of Mean	2.77	2.31	4.72
Lower 95% CI of mean	-1.68	-6.35	-16.50
Upper 95% CI of mean	11.43	8.35	9.70

TG-thapsigargin; Std-standard; CI-confidence interval; HS-high salt; IV-intravenous; Lat Hypo-Lateral Hypothalamus

Table D.9 One-way ANOVA for splanchnic sympathetic nerve activity % change from baseline following microinjection of thapsigargin in the PVN.

ANOVA summary	
F	32.3
P value	<0.0001
R square	0.8777

Brown-Forsythe test	
F (DFn, DFd)	0.7917 (4, 18)
P value	0.5457

ANOVA table	**SS**	**DF**	**MS**	**F (DFn, DFd)**	**P value**
Treatment (between columns)	28198	4	7050	F (4, 18) = 32.3	P<0.0001
Residual (within columns)	3928	18	218.2		
Total	32126	22			

Newman-Keuls	**Mean Diff.**	**Significant ?**	**Summary**
DMSO vs. TG 0.15nmol	-15.06	No	ns
DMSO vs. TG 0.30nmol	-31.49	Yes	*
DMSO vs. TG 0.75nmol	-90.15	Yes	****
DMSO vs. TG 1.5nmol	-79.77	Yes	****
TG 0.15nmol vs. TG 0.30nmol	-16.44	No	ns
TG 0.15nmol vs. TG 0.75nmol	-75.09	Yes	****
TG 0.15nmol vs. TG 1.5nmol	-64.72	Yes	****
TG 0.30nmol vs. TG 0.75nmol	-58.66	Yes	****
TG 0.30nmol vs. TG 1.5nmol	-48.28	Yes	****
TG 0.75nmol vs. TG 1.5nmol	10.38	No	ns

DMSO-dimethylsulfoxide; TG-thapsigargin

Table D.10 One-way ANOVA for renal sympathetic nerve activity % change from baseline following microinjection of thapsigargin in the PVN.

ANOVA summary	
F	11.36
P value	0.0001
R square	0.7397

Brown-Forsythe test	
F (DFn, DFd)	11.1 (4, 16)
P value	0.0002

ANOVA table	**SS**	**DF**	**MS**	**F (DFn, DFd)**	**P value**
Treatment (between columns)	17990	4	4498	F (4, 16) = 11.36	P<0.001
Residual (within columns)	6332	16	395.7		
Total	24322	20			

Newman-Keuls	**Mean Diff.**	**Significant ?**	**Summary**
DMSO vs. TG 0.15nmol	-10.85	No	ns
DMSO vs. TG 0.30nmol	-17.96	No	ns
DMSO vs. TG 0.75nmol	-70.52	Yes	**
DMSO vs. TG 1.5nmol	-67.57	Yes	**
TG 0.15nmol vs. TG 0.30nmol	-7.11	No	ns
TG 0.15nmol vs. TG 0.75nmol	-59.67	Yes	**
TG 0.15nmol vs. TG 1.5nmol	-56.72	Yes	**
TG 0.30nmol vs. TG 0.75nmol	-52.56	Yes	**
TG 0.30nmol vs. TG 1.5nmol	-49.61	Yes	**
TG 0.75nmol vs. TG 1.5nmol	2.95	No	ns

DMSO-dimethylsulfoxide; TG-thapsigargin

Table D.11 One-way ANOVA for mean arterial blood pressure (mmHg) change from baseline following microinjection of thapsigargin in the PVN.

ANOVA summary	
F	4.446
P value	0.0113
R square	0.497

Brown-Forsythe test	
F (DFn, DFd)	1.36 (4, 18)
P value	0.2869

ANOVA table	**SS**	**DF**	**MS**	**F (DFn, DFd)**	**P value**
Treatment (between columns)	310.7	4	77.68	F (4, 18) = 4.446	P=0.01
Residual (within columns)	314.5	18	17.47		
Total	625.2	22			

Newman-Keuls	**Mean Diff.**	**Significant ?**	**Summary**
DMSO vs. TG 0.15nmol	-0.25	No	ns
DMSO vs. TG 0.3nmol	-5.6	No	ns
DMSO vs. TG 0.75nmol	-9.333	Yes	*
DMSO vs. TG 1.5nmol	-7.6	No	ns
TG 0.15nmol vs. TG 0.3nmol	-5.35	No	ns
TG 0.15nmol vs. TG 0.75nmol	-9.083	Yes	*
TG 0.15nmol vs. TG 1.5nmol	-7.35	No	ns
TG 0.3nmol vs. TG 0.75nmol	-3.733	No	ns
TG 0.3nmol vs. TG 1.5nmol	-2	No	ns
TG 0.75nmol vs. TG 1.5nmol	1.733	No	ns

DMSO-dimethylsulfoxide; TG-thapsigargin

Table D.12 One-way ANOVA for heart rate (beats/minute) change from baseline following microinjection of thapsigargin in the PVN.

ANOVA summary	
F	2.382
P value	0.09
R square	0.3461

Brown-Forsythe test	
F (DFn, DFd)	0.6232 (4, 18)
P value	0.6519

ANOVA table	**SS**	**DF**	**MS**	**F (DFn, DFd)**	**P value**
Treatment (between columns)	583.2	4	145.8	F (4, 18) = 2.382	P=0.09
Residual (within columns)	1102	18	61.22		
Total	1685	22			

Newman-Keuls	**Mean Diff.**	**Significant ?**	**Summary**
DMSO vs. TG 0.15nmol	-11.33	No	ns
DMSO vs. TG 0.3nmol	-8.133	No	ns
DMSO vs. TG 0.75nmol	-12.67	No	ns
DMSO vs. TG 1.5nmol	-16.73	No	ns
TG 0.15nmol vs. TG 0.3nmol	3.2	No	ns
TG 0.15nmol vs. TG 0.75nmol	-1.333	No	ns
TG 0.15nmol vs. TG 1.5nmol	-5.4	No	ns
TG 0.3nmol vs. TG 0.75nmol	-4.533	No	ns
TG 0.3nmol vs. TG 1.5nmol	-8.6	No	ns
TG 0.75nmol vs. TG 1.5nmol	-4.067	No	ns

DMSO-dimethylsulfoxide; TG-thapsigargin

Table D.13 Unpaired t-test for slope of the current injection response in normal and high salt rats before and after bath application of thapsigargin.

	Slope	Slope	Slope
Column A	NS	HS	NS
vs.	vs	vs	vs
Column B	NS TG	HS TG	HS
Unpaired t test			
P value	0.0013	0.8079	0.0017
P value summary	**	ns	**
One- or two-tailed P value?	Two-tailed	Two-tailed	Two-tailed
t, df	t=4.28 df=11	t=0.2504 df=9	t=4.399 df=9

Table D.14 Unpaired t-test for excitability in response to 200pA current injection in normal and high salt rats before and after bath application of thapsigargin.

	Excitability	Excitability	Excitability
Column A	NS	HS	NS
vs.	vs	vs	vs
Column B	NS TG	HS TG	HS
Unpaired t test			
P value	0.0329	0.4399	0.0026
P value summary	**	ns	**
One- or two-tailed P value?	One-tailed	Two-tailed	Two-tailed
t, df	t=2.025 df=12	t=0.8013 df=11	t=3.713 df=13

NS-normal salt; TG-thapsigargin; HS-high salt

Table D.15 Unpaired t-test for slope of inter-spike interval in normal and high salt rats before and after bath application of thapsigargin.

	Slope	**Slope**	**Slope**
Column A	NS	HS	NS
vs.	vs.	vs	vs
Column B	NS TG	HS TG	HS
Unpaired t test			
P value	<0.0001	0.0842	0.0473
P value summary	**	ns	*
One- or two-tailed P value?	Two-tailed	Two-tailed	Two-tailed
t, df	t=6.111 df=12	t=1.917 df=10	t=2.261 df=10

NS-normal salt; TG-thapsigargin; HS-high salt

Appendix E. Chemical Structures

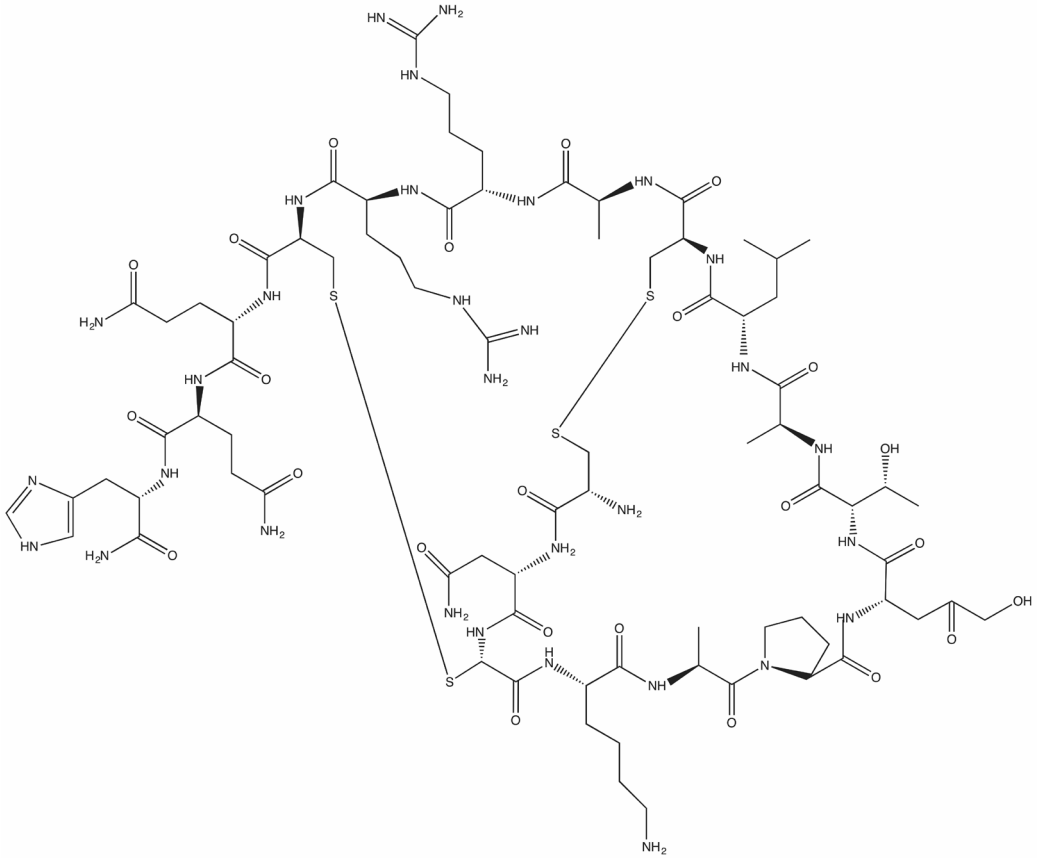

Figure E.1 Representative Chemical Structure of the SK Channel Blocker Apamin

Formula: $C_{79}H_{131}N_{31}O_{24}S_4$
Molecular Weight: 2027.339 g/mol

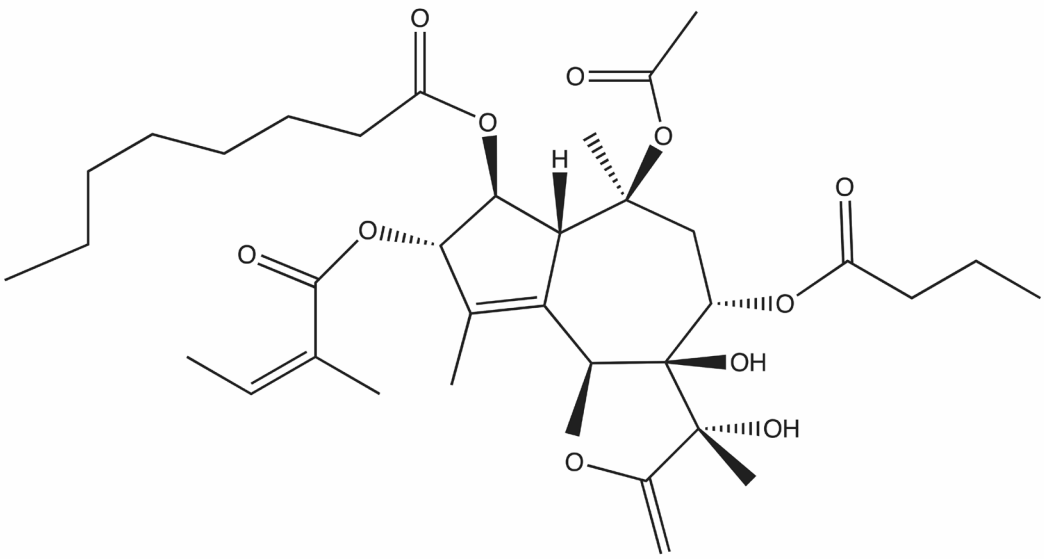

Figure E.2 Representative Chemical Structure of the ER Ca^{2+} ATPase Thapsigargin.

Formula: $C_{34}H_{50}O_{12}$
Molecular Weight: 650.79 g/mol

Appendix F. Permissions

Requests for Permission to Reproduce Previously Published Material.

Permission for Figure 1.3

WOLTERS KLUWER HEALTH, INC. LICENSE TERMS AND CONDITIONS

Jun 26, 2016

This Agreement between Robert A Larson ("You") and Wolters Kluwer Health, Inc. ("Wolters Kluwer Health, Inc.") consists of your license details and the terms and conditions provided by Wolters Kluwer Health, Inc. and Copyright Clearance Center.

License Number	3896761257215
License date	Jun 26, 2016
Licensed Content Publisher	Wolters Kluwer Health, Inc.
Licensed Content Publication	Hypertension
Licensed Content Title	Chronic Low-Dose Angiotensin II Infusion Increases Venomotor Tone by Neurogenic Mechanisms
Licensed Content Author	Andrew J. King, Gregory D. Fink
Licensed Content Date	Nov 1, 2006
Licensed Content Volume Number	48
Licensed Content Issue Number	5
Type of Use	Dissertation/Thesis
Requestor type	Individual
Portion	Figures/table/illustration
Number of figures/tables/illustrations	1
Figures/tables/illustrations used	Figure 1.
Author of this Wolters Kluwer article	No
Title of your thesis / dissertation	Central Neural Mechanisms of Salt-Sensitive Hypertension
Expected completion date	Jul 2016
Estimated size(pages)	150

Permission for Figure 1.4

Title: Whole body norepinephrine kinetics in ANG II-salt hypertension in the rat

Author: Andrew J. King,Martin Novotny,Greg M. Swain,Gregory D. Fink

Publication: Am J Physiol-Regulatory, Integrative and Comparative Physiology

Publisher: The American Physiological Society

Date: Apr 1, 2008

Logged in as:
Robert Larson
Account #:
3001040593

LOGOUT

Permission Not Required

Permission is not required for this type of use.

BACK CLOSE WINDOW

Permission for Figure 1.7

Title: Hypertension Induced by Angiotensin II and a High Salt Diet Involves Reduced SK Current and Increased Excitability of RVLM Projecting PVN Neurons

Author: Qing-Hui Chen,Mary Ann Andrade,Alfredo S. Calderon,Glenn M. Toney

Publication: Journal of Neurophysiology

Publisher: The American Physiological Society

Date: Nov 1, 2010

Logged in as:
Robert Larson
Account #:
3001040593

LOGOUT

Permission Not Required

Permission is not required for this type of use.

BACK CLOSE WINDOW

Permission for Chapter 2.

RightsLink®

Home | Account Info | Help

Title:	Sympathoexcitation in ANG II-salt hypertension involves reduced SK channel function in the hypothalamic paraventricular nucleus
Author:	Robert A. Larson,Le Gui,Michael J. Huber,Andrew D. Chapp,Jianhua Zhu,Lila P. LaGrange,Zhiying Shan,Qing-Hui Chen
Publication:	Am J Physiol- Heart and Circulatory Physiology
Publisher:	The American Physiological Society
Date:	Jun 15, 2015

Logged in as:
Robert Larson
Account #:
3001040593

LOGOUT

Permission Not Required

Permission is not required for this type of use.

BACK | CLOSE WINDOW